

Electronic Theses and Dissertations, 2020-

2020

Compressibility of Fine-Grained Soil in Central Florida

Andre Kruk
University of Central Florida

 Part of the [Geotechnical Engineering Commons](#), and the [Structural Engineering Commons](#)
Find similar works at: <https://stars.library.ucf.edu/etd2020>
University of Central Florida Libraries <http://library.ucf.edu>

This Masters Thesis (Open Access) is brought to you for free and open access by STARS. It has been accepted for inclusion in Electronic Theses and Dissertations, 2020- by an authorized administrator of STARS. For more information, please contact STARS@ucf.edu.

STARS Citation

Kruk, Andre, "Compressibility of Fine-Grained Soil in Central Florida" (2020). *Electronic Theses and Dissertations, 2020-*. 80.
<https://stars.library.ucf.edu/etd2020/80>

COMPRESSIBILITY OF FINE-GRAINED SOIL IN CENTRAL FLORIDA

by

ANDRE KRUK
B.S. University of Central Florida, 2019

A thesis submitted in partial fulfillment of the requirements
for the degree of Master of Sciences
in the Department of Civil, Environmental, and Construction Engineering
at the College of Engineering and Computer Science
at the University of Central Florida
Orlando, Florida

Spring Term
2020

@ 2020 Andre Kruk

ABSTRACT

Settlement is a limiting design aspect in most geotechnical projects. Fine-grained cohesive soils are typically responsible for the majority of site settlements through a time dependent process known as consolidation. For this reason, it is desirable to accurately determine the degree of consolidation, referred to in the report as soil compressibility, of the fine-grained layers impacted by loading. Soil compressibility is commonly determined from the Oedometer test; however, this test is time consuming, expensive, highly susceptible to soil disturbance, and represents a very small zone of the soil layer. An alternative method to estimate the compressibility would be correlations with index properties which can be performed for all soil layers at a low cost and with quick turnover. Other methods include in-situ testing techniques such as Standard Penetration Testing (SPT), Cone Penetration Testing (CPT), Dilatometer Testing (DMT), and Pressuremeter Testing (PMT). The CPT is the most ideal test as it is repeatable, continuous, and commonly used. For this reason, this study utilizes an empirical method to refine correlations to index properties for local soils and estimate the compressibility via CPT. It was found that compressibility can be accurately estimated via CPT for soils with relatively high activity and moisture content. Index test correlations, when refined for the local geology, performed better than the generic correlations. The results for both techniques are not accurate enough to completely replace better in-situ or laboratory tests. However, it is this authors opinion that accurate determination of preconsolidation pressure is more important for accurate settlement estimation than compressibility indices. If the preconsolidation pressure is well defined for the site, the small error in the compressibility indices will have a minimal impact on the overall estimation of settlement. Consequently, this study will recommend a refined model for preconsolidation pressure in the conclusion chapter.

ACKNOWLEDGMENTS

I would like to thank my advisor, Dr. Boo Hyun Nam, for patiently guiding and supporting me throughout this process. I also sincerely appreciate my committee members, Dr. Manoj Chopra, Dr. Arboleda Monslave and Dr. Dingbao Wang for reviewing this work. The following members have not only guided me through this research but have shared their knowledge of Geotechnical Engineering through teaching, office hours, and presentations. The support from my co-workers at Ardaman and Associates and S&ME has made this research possible by providing data points, and technically stronger by fielding questions.

TABLE OF CONTENTS

LIST OF FIGURES.....	vii
LIST OF TABLES.....	x
CHAPTER 1 INTRODUCTION.....	1
1.1 Purpose	4
1.2 Methodology	4
1.3 Thesis Outline	5
CHAPTER 2 LITERATURE REVIEW.....	6
2.1 Introduction	6
2.2 Important Concepts.....	6
2.3 Central Florida Geology	8
2.4 Estimation of Compressibility from Index Properties	8
2.5 Compressibility and Cone Penetration Test	12
2.5.1 Elastic Derivation and Calibration Constant	12
2.5.2 Constrained Modulus	16
2.6 Estimation of Preconsolidation Pressure.....	18
2.7 Literature Review Conclusion	20
CHAPTER 3 INDEX PROPERTIES AND COMPRESSIBILITY.....	22
3.1 Introduction	22
3.2 Methodology	25
3.2.1 Data Base	25
3.2.2 Analysis	25
3.3 Results and Discussion.....	26
3.3.1 Correlations from Charts	26
3.3.2 Recommended Models and Discussion.....	32
3.4 Conclusion.....	34
CHAPTER 4 CONE PENETRATION TEST BASED CORRELATION ANALYSIS	35
4.1 Introduction	35
4.2 Methodology	38
4.2.1 Cone Penetration Test Data Base	38
4.2.2 Data Processing Procedure.....	38

4.2.3	Data Processing Procedure: Example	41
4.2.4	Analysis	50
4.3	Results.....	52
4.3.1	Correlations from Charts	52
4.3.2	Recommended Model and Discussion	57
4.4	Conclusion.....	63
CHAPTER 5	CONE PENETRATION TEST BASED CORRELATIONS – DIVIDED DATA BASE FOR ACTIVITY AND MOISTURE CONTENT	64
5.1	Introduction	64
5.2	Methodology	69
5.3	Results.....	69
5.3.1	Correlations from Charts	70
5.3.2	Recommended Models and Discussion	77
5.4	Conclusion.....	80
CHAPTER 6	CONCLUSION.....	81
6.1	Summary	81
6.2	Recommendations.....	81
6.2.1	Compression Index Recommendation.....	81
6.2.2	OCR Recommendation.....	82
6.3	Limitations and Future Works	83
APPENDIX A – INDEX PROPERTY CORRELATIONS		85
APPENDIX B – CONE PENETRATION TEST BASED CORRELATIONS (UNDIVIDED)		96
APPENDIX C - CONE PENETRATION TEST BASED CORRELATIONS (DIVIDED)		107
APPENDIX D – SNIPPET OF UCF DATA BASE		120
APPENDIX E – SNIPPET OF CPT DATA BASE		122
LIST OF REFERENCES		124

LIST OF FIGURES

Figure 2-1: Typical Consolidation Curve for Clay	7
Figure 2-2: Results of Lyons Research, q_c vs C_c from Sanglerat (1972)	15
Figure 2-3: Laboratory measured constrained modulus, M , compared with CPT predicted.....	17
Figure 2-4: Comparison between Undrained Shear strength from Triaxial compression and measured cone resistance from mechanics and electric cones, taken from Mayne and Kemper 1988	19
Figure 2-5: Trend Between Laboratory OCR and Normalized net cone resistance taken from Mayne and Kemper 1988.....	20
Figure 3-1: Recompression Index vs Moisture Content, W	27
Figure 3-2: Recompression Index vs Initial Void Ratio, e_o	27
Figure 3-3: Recompression Index vs Liquid Limit, LL	28
Figure 3-4: Recompression Index vs Compression Index	28
Figure 3-5: Compression Index vs Moisture Content, W	29
Figure 3-6: Compression Index vs Initial Void Ratio, e_o	29
Figure 3-7: Compression Index vs Liquid Limit, LL	30
Figure 3-8: Compression Index vs Wet Unit Weight, γ	30
Figure 3-9: Compression Index vs Dry Unit Weight, γ_d	31
Figure 3-10: Void Ratio vs Moisture Content	33
Figure 4-1: CPT Soil Failure Surface	37
Figure 4-2: CPT Pore Pressure Distribution	37
Figure 4-3: Data Base Creation and Analysis Logic Chart	40
Figure 4-4: CPT and SPT Location (Example)	42
Figure 4-5: SPT and CPT Profile Matching (Example)	44
Figure 4-6: Oedometer Test Results (Example)	46
Figure 4-7: Recreated Test Results for Calculations	47
Figure 4-8: Recompression Index vs Pore Pressure Ratio, B_q	53
Figure 4-9: Compression Index vs Recompression Index	53
Figure 4-10: Compression Index vs Pore Pressure, u_2	54
Figure 4-11: Compression Index vs Ratio of Pore Pressures, u_N	54
Figure 4-12: Compression Index vs Pore Pressure Ratio, B_q	55
Figure 4-13: Compression Index vs Friction Ratio, R_f	55
Figure 4-14: Ratio of Pore Pressures vs Percent Finer	58
Figure 4-15: Ratio of Pore Pressures vs Activity, A	59
Figure 4-16: Ratio of Pore Pressures vs Preconsolidation Pressure, σ_c'	59
Figure 4-17: Friction Ratio vs Percent Finer	61
Figure 4-18: Friction Ratio vs Plasticity index	61
Figure 4-19: Friction Ratio vs Preconsolidation Pressure, σ_c'	62
Figure 5-1: Moisture Content vs Pore Pressure, u_2	65
Figure 5-2: Moisture Content vs Sleeve Friction, f_s	66
Figure 5-3: Recompression Index vs Ratio of Pore Pressures, u_N	70
Figure 5-4: Compression Index vs Ratio of Pore Pressures, u_N	71

Figure 5-5: Compression Index vs Pore Pressure Ratio, B_q	71
Figure 5-6: Compression Index vs Friction Ratio, R_f	72
Figure 5-7: Compression Index vs Normalized Friction Ratio, f_r	72
Figure 5-8: Recompression Index vs Pore Pressure Ratio, B_q	73
Figure 5-9: Compression Index vs Ratio of Pore Pressures, u_N	74
Figure 5-10: Compression Index vs Pore Pressure Ratio, B_q	74
Figure 5-11: Compression Index vs Friction Ratio, R_f	75
Figure 5-12: Compression Index vs Normalized Friction Ratio, f_r	75
Figure 5-13: Moisture Content vs Percent Finer	78
Figure 5-14: Activity vs Percent Finer	78
Figure 6-1: Over Consolidation Ratio vs Normalized Net Cone Resistance.....	83
Figure A-0-1: Recompression Index vs Moisture Content, W	86
Figure A-0-2: Recompression Index vs Initial Void Ratio, e_o	86
Figure A-0-3: Recompression Index vs Standard Penetration Test Blow Count, N	87
Figure A-0-4: Recompression Index vs Liquid Limit, LL	87
Figure A-0-5: Recompression Index vs Plasticity Index, PI	88
Figure A-0-6: Recompression Index vs Effective Vertical Stress.....	88
Figure A-0-7: Recompression Index vs Wet Density, γ	89
Figure A-0-8: Recompression Index vs Dry Density, γ_d	89
Figure A-0-9: Recompression Index vs Percent Finer, -200	90
Figure A-0-10: Recompression Index vs Activity, A	90
Figure A-0-11: Recompression Index vs Compression Index.....	91
Figure A-0-12: Compression Index vs Moisture Content, W	91
Figure A-0-13: Compression Index vs Initial Void Ratio, e_o	92
Figure A-0-14: Compression Index vs Liquid Limit, LL	92
Figure A-0-15: Compression Index vs Plasticity Index, PI	93
Figure A-0-16: Compression Index vs Effective Vertical Stress, σ'	93
Figure A-0-17: Compression Index vs Wet Unit Weight, γ	94
Figure A-0-18: Compression Index vs Dry Unit Weight, γ_d	94
Figure A-0-19: Compression Index vs Percent Finer.....	95
Figure A-0-20: Compression Index vs Activity, A	95
Figure B-0-1: Recompression Index vs Tip Resistance, q_c	97
Figure B-0-2: Recompression Index vs Corrected Tip Resistance, q_t	97
Figure B-0-3: Recompression Index vs Sleeve Friction, f_s	98
Figure B-0-4: Recompression Index vs Pore Pressure, u_2	98
Figure B-0-5: Recompression Index vs Ratio of Pore Pressures, u_N	99
Figure B-0-6: Recompression Index vs Pore Pressure Ratio, B_q	99
Figure B-0-7: Recompression Index vs Friction Ratio, R_f	100
Figure B-0-8: Recompression Index vs Normalized Friction Ratio, f_r	100
Figure B-0-9: Recompression Index vs Soil Behavior Type Index, I_c	101
Figure B-0-10: Compression Index vs Recompression Index.....	101
Figure B-0-11: Compression Index vs Tip Resistance, q_c	102
Figure B-0-12: Compression Index vs Corrected Tip Resistance, q_t	102

Figure B-0-13: Compression Index vs Sleeve Friction, f_s	103
Figure B-0-14: Compression Index vs Pore Pressure, u_2	103
Figure B-0-15: Compression Index vs Ratio of Pore Pressures, u_N	104
Figure B-0-16: Compression Index vs Pore Pressure Ratio, B_q	104
Figure B-0-17: Compression Index vs Friction Ratio, R_f	105
Figure B-0-18: Compression Index vs Normalized Friction Ratio, f_r	105
Figure B-0-19: Compression Index vs Soil Behavior Type Index, I_c	106
Figure C-0-1: Recompression Index vs Corrected Tip Resistance, q_t	108
Figure C-0-2: Recompression Index vs Sleeve Friction, f_s	108
Figure C-0-3: Recompression Index vs Ratio of Pore Pressures, u_N	109
Figure C-0-4: Recompression Index vs Pore Pressure Ratio, B_q	109
Figure C-0-5: Recompression Index vs Friction Ratio, R_f	110
Figure C-0-6: Recompression Index vs Normalized Friction Ratio, f_r	110
Figure C-0-7: Recompression Index vs Compression Index	111
Figure C-0-8: Compression Index vs Corrected Tip Resistance, q_t	111
Figure C-0-9: Compression Index vs Sleeve Friction, f_s	112
Figure C-0-10: Compression Index vs Ratio of Pore Pressures, u_N	112
Figure C-0-11: Compression Index vs Pore Pressure Ratio, B_q	113
Figure C-0-12: Compression Index vs Friction Ratio, R_f	113
Figure C-0-13: Compression Index vs Normalized Friction Ratio, f_r	114
Figure C-0-14: Recompression Index vs Corrected Tip Resistance, q_t	115
Figure C-0-15: Recompression Index vs Ratio of Pore Pressures, u_N	115
Figure C-0-16: Recompression Index vs Pore Pressure Ratio, B_q	116
Figure C-0-17: Recompression Index vs Friction Ratio, R_f	116
Figure C-0-18: Recompression Index vs Normalized Friction Ratio, f_r	117
Figure C-0-19: Compression Index vs Corrected Tip Resistance, q_t	117
Figure C-0-20: Compression Index vs Ratio of Pore Pressures, u_N	118
Figure C-21: Compression Index vs Pore Pressure Ratio, B_q	118
Figure C-22: Compression Index vs Friction Ratio, R_f	119
Figure C--23: Compression Index vs Normalized Friction Ratio, f_r	119

LIST OF TABLES

Table 2-1: Existing Correlations of Index Properties to Compressibility Indices	9
Table 2-2: Correlations of Index Properties to Compressibility Indices for Florida Soils from Kirtis et al. 2018	11
Table 2-3: Correlations of Index Properties to Compressibility Indices for Florida Soil from Kirtis et al. 2019	11
Table 2-4 Correction Constant, α , from NIASL for Fine Grained Soils from Sanglerat (1972)	14
Table 2-5 Correction Constant, α , from NIASL for Peats and Organic Soils from Sanglerat (1972)	14
Table 2-6 Correction Constant, α , from NIASL for Chalks and Sands from Sanglerat (1972)	14
Table 3-1: Summary of Results, Index Properties	31
Table 3-2: Recommended Models for Index Properties	32
Table 3-3: Recommended Model for Void Ratio	32
Table 4-1: Oedometer Test Quality Rating	49
Table 4-2: Values of Unit Weight of granular soils base on the SPT number	49
Table 4-3: Values of Unit Weight of cohesive soils base on the SPT number	49
Table 4-4: Summary of Results, CPT	56
Table 4-5: Recommended Models for CPT Parameters	62
Table 5-1: Correlation of Activity and the Minerology and Geology of Clay from Skempton 1984	68
Table 5-2: Summary of Results, Activity ($A > 0.5$)	73
Table 5-3: Summary of Results, Moisture Content ($w > 40\%$)	76
Table 5-4: Model Reliability Increase	77
Table 5-5: Recommended Model, Activity	79
Table 5-6: Recommended Model, Moisture Content	79
Table 6-1: Summary of Recommended Models	82
Table 6-2: Void Ratio Model	82

CHAPTER 1 INTRODUCTION

In most Geotechnical projects a major design consideration is settlement. The magnitude of settlement is estimated by defining the soil's compressibility, which is dependent on composition (stress) and structure (void ratio).

The in-situ stress and void ratio define the current compressive state of the soil. The in-situ effective vertical stress consists of the total vertical stress and the pore pressure, implying the effective stress is time-dependent. This time-dependent compression is known as consolidation which is the transfer of stress from the pore pressure to the soil skeleton. Any combination of composition and structure that allows a soil to exist at a high volume of voids, as indicated by a high natural water content or void ratio, results in the potential for large volume changes. The change in stress (change in stress from pre-post construction) results in the reconfiguration of the structure into a decreased void ratio. (Terzaghi et al. 1996). The pre- construction stress state, also known as the preconsolidation pressure, can be defined as the amount of maximum pressure previously experienced by the soil through geologic conditions and marks the stress level at which the soil switches from elastic to plastic behavior.

Volume change within the elastic region is strongly influenced by the natural soil structure, however, once the preconsolidation pressure is exceeded the change in volume is more influenced by the loading. Within the elastic region the soil skeleton accommodates the stress with little interparticle displacements, which are recoverable, resulting from minor slips at interparticle contacts. Within the plastic region major particle rearrangement, which is not recoverable, is required to develop interparticle resistance to the increased effective stress. This resistance must accommodate the stress applied as well as compensate for the destroyed interparticle bond resistance. (Terzaghi et al. 1996)

The elastic region is occupied by over consolidated (OC) soils, a soil which has experienced a stress greater than the current stress and is commonly referred to as the over consolidation line (OCL). These soils could be overconsolidated due to natural causes such as erosion and groundwater fluctuation, or unnatural causes such as surcharging and previous construction. The plastic response occurs in normally consolidated (NC) soil, a soil which has never experienced the current magnitude of stress and is referred to as the virgin or normally consolidated line (NCL) of the compression response curve.

The stress path (change in stress from pre to post construction loading) determines which equation to utilize to estimate the magnitude of consolidation (Das 2002). Equation (1) is used for an OC soil that remains on the OCL after loading (i.e. never exceeds its past maximum pressure). Equation (2) is used for an OC soil that exceeds the past-maximum pressure and now acts on the NCL. Equation (3) is for a NC soil. The stress history of the soil can be changed with unloading; however, this is not within the scope of the current research.

$$S_C = \frac{C_r H_C}{1+e_0} \log \left(\frac{\sigma'_0 + \Delta\sigma'}{\sigma_{o'}} \right) \quad (1)$$

$$S_C = \frac{C_r H_C}{1+e_0} \log \left(\frac{\sigma_{c'}}{\sigma_{o'}} \right) + \frac{C_c H_C}{1+e_0} \log \left(\frac{\sigma'_0 + \Delta\sigma'}{\sigma_{o'}} \right) \quad (2)$$

$$S_C = \frac{C_c H_C}{1+e_0} \log \left(\frac{\sigma'_0 + \Delta\sigma'}{\sigma_{o'}} \right) \quad (3)$$

These equations state that settlement is a direct function of compressibility, stress states, and the drainage path. Where S_c is the settlement from loading, C_r is the recompression index (slope of OCL), C_c is the compression index (slope of NCL), e_0 is the soils initial ratio of voids to solids in terms of volume of the soil, H_c is the thickness of soil layer between drainage paths, σ'_0 is the initial vertical effective stress at the midpoint of the soil layer, $\Delta\sigma'$ is the change in vertical effective stress due to

loading, and σ_c' is the past maximum pressure. From here on, the soils compressibility is referring to the recompression and compression indices, C_r and C_c .

The parameters describing the soil's stress deformation response within the equations are the recompression and compression indices. The pre-consolidation pressure indicates which of these parameter(s) to use when estimating the magnitude of settlement. These values (C_c , C_r , σ_c') are most accurately obtained from the oedometer test creating a 1-D compression curve. However, it is often favorable to estimate these parameters through other means. This paper will recommend correlations to utilize index properties and the Cone penetration test (CPT) as an accurate and efficient means to estimate the compressibility indices, as well as check the reliability of pre-existing preconsolidation pressure correlations to the CPT. Please note that the term compressibility indices, is referring to the recompression and compression indices in void ratio-stress space unless otherwise stated.

Assuming the compressibility indices and preconsolidation pressure are empirically estimated, the only parameters left to determine are the thickness of the soil layer, initial vertical effective stress, the change of effective stress due to loading, and the void ratio. The soil layer thickness can be determined via CPT or SPT soil profiling. The initial effective stress can be determined by correlations to unit weights and proper soil profiling. The change of effective vertical stress is dependent on the force exerted from the structure onto the soil and is typically assumed or provided by the structural engineer.

The point being that these parameters can all be relatively well defined without extensive field or laboratory testing. However, the void ratio would require its own correlation or to be determined via lab testing. It is possible to completely avoid the void ratio by utilizing the compression and recompression indices in strain-stress space, referred to as C_c' and C_r' , respectively. These parameters are the slope of the elastic and plastic region in strain-stress space and are equal to C_c and C_r divided by

($1+e_0$). This transformation equation from void ratio- to strain – stress space is utilized in equations 1 through 3. The correlations to compressibility indices provided in this study will be presented in strain-stress space where applicable or in void- stress space with an accompanying correlation to void ratio. With void ratio now accounted for, everything needed to estimate settlement in Central Florida can be determined cost effectively and accurately via CPT and/or index testing techniques.

1.1 Purpose

The purpose of this research is to estimate the compressibility of fine-grained cohesive soils via index properties and the Cone penetration test (CPT) in the Central Florida region. Strong correlations between certain index properties and compressibility have been previously defined. This study will refine these correlations to the local geology. Correlations between compressibility and CPT for elastic soil behavior have also been well defined, however, correlations for plastic behavior have not. This study will refine elastic compressibility (recompression index) correlations and propose a model for estimation of plastic compressibility (compression index). The yielding point at which soil behavior transitions from elastic to plastic, also known as preconsolidation pressure, is required to estimate settlement. As a result, a pre-existing model from Mayne and Kemper (1988) will be refined for the local soil.

1.2 Methodology

Two data bases will be utilized to recommend a model for index properties and CPT parameters. The first data base, created for the CPT correlations, consists of 24 coupled Oedometer and Cone penetration tests. The first step in creating this data base is to locate projects in the Central Florida area in which both CPT and Oedometer tests have been performed. Next, the CPT and Oedometer test results will be checked for reliability and then, if deemed to be of good quality, the couple is added to the data base. Once enough data has been collected to produce statistically reliable correlations, each

parameter will be plotted against the compressibility coefficients to recommend a model. This data set will be utilized to recommend models for CPT and compressibility for the entire data base in Chapter 4, as well as CPT outputs and compressibility for the specific soil categories. The second data base consists of 393 coupled Oedometer and Index test results. This data base is a combined set of the first data set, discussed above, and the University of Central Florida's data set created by Scott Kirtis. This data set will be used to recommend a model to estimate compressibility from index properties. Since this study utilizes an empirical method, it is important to provide a theoretical justification for each model.

1.3 Thesis Outline

Chapter 2 will review relevant studies; including two papers regarding empirical analysis of index properties, three works regarding the CPT for both elastic and plastic compressibility, one paper summarizing the preconsolidation equation refined in the conclusion, and one work explaining the Central Florida geology. Chapter 3 will relate the recompression and compression indices to index properties via regression analysis from the combined data set. Chapter 4 will recommend a model to estimate compressibility via CPT parameters and provide an in-depth explanation of the CPT data base creation. Chapter 5 will be similar to chapter 4 but it will recommend a model for soils with relatively high activity and high moisture content to give insight into the effect of varying index properties. Chapter 6 will summarize all the findings, recommend a refined preconsolidation pressure equation, provide insight to future studies, and discuss possible sources of error within the data base.

CHAPTER 2 LITERATURE REVIEW

2.1 Introduction

This chapter will discuss important concepts, summarize previous research on index properties and CPT correlations to compressibility and preconsolidation pressure. Section 2.2 will review information about the Cone penetration test, Soil Behavior, and the Oedometer Test. Section 2.3 will explain the relative aspects of the local geology. Section 2.4 will cover previous research relative to index properties and soil compressibility. Section 2.5 will discuss previous research relative to CPT and compressibility correlations and section 2.6 will summarize the derivation of the correlation between CPT and preconsolidation pressure. The purpose of this section is to inform the reader on the current state of the practice and provide insight into the methods previously utilized as they will be emulated in this study.

2.2 Important Concepts

The Cone penetration test is an in-situ test which pushes a penetrometer into the earth at a constant rate as it records the tip resistance (q_c), sleeve friction (f_s), and pore pressure (u_2). These readings are continuous, repeatable, and efficient. For this reason, many correlations arise relating CPT readings to soil parameters such as soil behavior type, elastic compressibility, overconsolidation ratio, undrained shear strength, friction angle, and many more.

The soil being studied consists primarily of clayey soils. These soil types exhibit a non-linear stress strain relationship, recoverable and unrecoverable deformation, and a memory of previous stress states. Therefore, the compression curve this study aims to approximate displays elastic-plastic behavior as well as a yield value dependent on the past maximum stress. The primary cause of compression is consolidation, the process of stress transfer from pore pressure to the soil skeleton via the dissipation of

water from the voids, and results in a denser configuration. The magnitude and rate of consolidation vary for each soil type, soil stratigraphy, and stress path, and is best determined via oedometer testing.

The oedometer test is performed by incrementally loading a soil sample with a 75mm diameter and 15mm height and recording the deformation after 24 hours at each load. The oedometer test results produce a load-deformation curve, typically in stress- void ratio space. This curve, known as a consolidation curve as seen in Figure 2-1, depicts elastic behavior followed by yielding then plastic behavior. These three components are defined as the slope of the elastic and plastic region, known as the recompression and compression indices, respectively, and the yielding of the curve is defined as the past-maximum pressure.

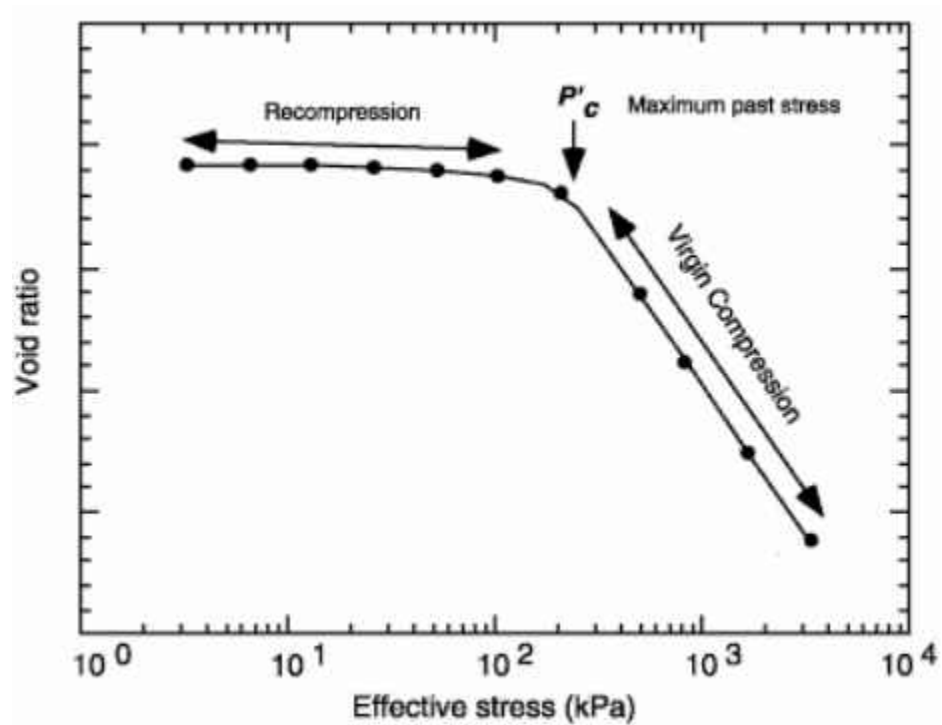


Figure 2-1: Typical Consolidation Curve for Clay

2.3 Central Florida Geology

The Florida Peninsula is a 2- to 6- kilometer porous plateau of carbonate rock (limestone) sitting atop the Florida Platform of Paleozoic to Mesozoic age igneous and metasedimentary rocks. In geotechnical practice the limestone is commonly referred to as the bedding layer. Atop this limestone is a thin 1- to 150- meter layer of mostly quartz sands on the surface and siliciclastic below (Hine 2009). Mixed into these sands are silts and clays. The clay layer typically referred to as the Hawthorne formation sits atop the limestone and, in some areas, mixes with the sand. The typical Florida profile looks like a sandy and clayey overburden atop limestone. Most of the soils analyzed for settlement are sandy clays due to the compressive nature of the clays and redistributive nature of sands (Kirts, Scott, et al. 2018).

2.4 Estimation of Compressibility from Index Properties

The following discussion references “Soil-Compressibility Prediction Models Using Machine Learning” from Kirtis et al. 2018. The data base briefly mentioned in the introduction, and to be utilized in chapter 3, was taken from this study. The objective is to estimate the compressibility coefficients for different soil types from moisture content, void ratio, dry and wet unit weight, SPT blow counts, and fines content. A machine learning approach was followed to achieve this goal. Machine learning classification is the process of estimating the category of a previously unknown object out of a finite set of predefined categories based on a set of objects whose category is known (Bishop C.M. 2006).

Many single and multi-variable correlations have been previously defined to estimate compressibility coefficients via index properties. The existing correlations along with their statistical reliability for use in Florida soils are displayed in Table 2-1.

Table 2-1: Existing Correlations of Index Properties to Compressibility Indices

Equation	Reference	Notes	R ²	RMSE
$C_c = 0.01w - 0.05$	Azzouz et al. (1976)	All soils	0.7448	0.8359
$C_c = 0.01w$	Koppula (1981)	Clays	0.5202	0.4191
$C_c = 0.01w - 0.075$	Herrero (1983)	Clays	0.5189	0.4336
$C_c = 0.013w - 0.115$	Park and Lee (2011)	Clays	0.6729	0.3953
$C_c = 0.0075w$	Miyakawa (1960)	Peat	0.5784	1.5194
$C_c = 0.011w$	Cook (1956)	Peat	0.6611	1.9601
$C_c = 0.54e - 0.19$	Nishida (1956)	Clays	0.7236	0.3945
$C_c = 0.43e - 0.11$	Cozzolino (1961)	Clays	0.6120	0.4046
$C_c = 0.75e - 0.38$	Sowers (1970)	Clays	0.7362	0.5552
$C_c = 0.49e - 0.11$	Park and Lee (2011)	Clays	0.6847	0.3924
$C_c = 0.4(e - 0.25)$	Azzouz et al. (1976)	All soils	0.5676	0.7501
$C_c = 0.15e + 0.01077$	Bowles (1989)	Clays	0.3157	0.7536
$C_c = 0.287e - 0.015$	Ahadiyan et al. (2008)	Clays	0.3847	0.7692
$C_c = 0.6e$	Sowers (1970)	Peat	0.6715	1.7876
$C_c = 0.3(e - 0.27)$	Hough (1957)	Clays	0.4081	0.5425
$C_c = 0.006(LL - 9)$	Azzouz et al. (1976)	Clays	0.2857	0.6213
$C_c = (LL - 13)/109$	Mayne (1980)	Clays	0.4323	0.5638
$C_c = 0.009(LL - 10)$	Terzaghi and Peck (1967)	Clays	0.4236	0.5641
$C_c = 0.014LL - 0.168$	Park and Lee (2011)	Clays	0.5569	0.7921
$C_c = 0.0046(LL - 9)$	Bowles (1989)	Clays	0.2780	0.6989
$C_c = 0.011(LL - 16)$	McClelland (1967)	Clays	0.5094	0.5991
$C_c = 0.009w + 0.005LL$	Koppula (1981)	Clays	0.5701	0.5518
$C_c = 0.009w + 0.002LL - 0.01$	Azzouz et al. (1976)	Clays	0.5866	0.4875
$C_c = 0.4(e + 0.001w - 0.25)$	Azzouz et al. (1976)	All soils	0.7057	0.7414
$C_c = -0.156 + 0.411e - 0.00058LL$	Al-Khafaji and Andersland (1992)	Clays	0.5276	0.3881
$C_c = -0.023 + 0.271e + 0.001LL$	Ahadiyan et al. (2008)	Clays	0.3400	0.4597
$C_c = 0.37(e + 0.003LL + 0.0004w - 0.34)$	Azzouz et al. (1976)	Clays	0.5014	0.3888
$C_c = -0.404 + 0.341e + 0.006w + 0.004LL$	Yoon and Kim (2006)	Clays	0.6805	0.4991
$C_c = 0.1597(w^{-0.0187})(1 + e)^{1.592}(LL^{-0.0638})(\gamma_{dry}^{-0.8276})$	Ozer et al. (2008)	Clays	0.6824	0.5886
$C_c = 0.151 + 0.001225w + 0.193e - 0.000258LL - 0.0699\gamma_{dry}$	Ozer et al. (2008)	Clays	0.3006	0.5204
$C_r = 0.156e + 0.0107$	Elnaggar and Krizek (1970)	Clays	0.5330	0.2536
$C_r = 0.208e + 0.0083$	Peck and Reed (1954)	Clays	0.5419	0.3643
$C_r = 0.14(e + 0.007)$	Azzouz et al. (1976)	All soils	0.6016	0.3369
$C_r = 0.003(w + 7)$	Azzouz et al. (1976)	All soils	0.5780	0.4415
$C_r = 0.002(LL + 9)$	Azzouz et al. (1976)	All soils	0.5485	0.1682
$C_r = 0.142(e - 0.009w + 0.006)$	Azzouz et al. (1976)	All soils	0.6089	0.1802
$C_r = 0.003w + 0.0006LL + 0.004$	Azzouz et al. (1976)	All soils	0.5674	0.2344
$C_r = 0.126(e + 0.003LL - 0.06)$	Azzouz et al. (1976)	All soils	0.5808	0.2109
$C_r = 0.135(e + 0.1LL - 0.002w - 0.06)$	Azzouz et al. (1976)	All soils	0.5548	0.3131

Machine learning is discussed in detail, however, this is not the focus of this study, so no further comments on this method will be made. It is important to note the impressive data base utilized, consisting of 623 data points of coupled oedometer test results and the parameters of interest from locations throughout the state of Florida. The results of this analysis can be found in Table 2-2 and show that a strong correlation between index properties and compressibility for Florida soils exists. It is clear the author's initial assumption that the data base must be separated into groups was accurate. The finding that different soils with similar index properties may exhibit drastically different behaviors is

useful. This supports hypothesis' utilized within Chapter 5 stating that one soil type must be utilized (cohesive, fine-grained) and should be further categorized by some specific soil property. Three distinct soil classes were suggested within this study, coarse grained, fine grained and organic peat. It should be noted that both coarse-grained and organic peat performed exceptionally well, while the fine-grained model was on par with existing correlations. Highly compressible organics and predominately sandy soils are plentiful in Florida, so this was a useful finding for local practitioners. Another important note is that plasticity indices were not utilized in this study but were added in for future research. As seen in Table 2-2 and 2-3, there was no major increase in the reliability of this correlation when plasticity indices were introduced. This does not agree with the correlations shown in Table 2-1. Further investigation is needed to determine the effects of plasticity indices on compressibility. The reference discussed below expands upon these correlations.

The purpose of this study, "Settlement Prediction Using Support Vector Machine (SVM)-Based Compressibility Models: A Case Study." From Kirts, Scott, et al 2019, is to compare estimated site settlement from machine learning correlations and from oedometer test results to the measured site settlement. The results show good predictive capabilities of the proposed correlations presented in Table 2-2. It is also shown that the prediction of C_r via machine learning is poor, and suggests it is more accurate to use a base rule of thumb to assume C_r as one fifth of C_c . The results presented in Chapter 3 agree with this author's recommendation, for this reason, this technique will be utilized in this thesis to estimate C_r by refining the one fifth fraction.

Table 2-2: Correlations of Index Properties to Compressibility Indices for Florida Soils from Kirtis et al. 2018

Equation	Notes	R^2	R^2_{adj}	RMSE
$C_c = -0.146 + 0.001 \times \gamma_{wet} - 0.003 \times \gamma_{dry} + 0.007 \times N + 0.005 \times \text{Fines} + 0.373 \times e_o - 0.0006 \times [(\gamma_{wet} - 115.484) \times (N - 6.493)] + 0.001 \times [(\gamma_{wet} - 115.484) \times (\text{Fines} - 31.584)] + 0.032 \times [(\text{Fines} - 31.584) \times (e_o - 1.028)] + 0.001 \times [(\gamma_{wet} - 115.484) \times (\gamma_{wet} - 115.484)] - 0.0003 \times [(\gamma_{dry} - 86.024) \times (\gamma_{dry} - 86.024)] - 0.0005 \times [(N - 6.493) \times (N - 6.493)]$	Coarse grained	0.9079	0.8888	0.1108
$C_c = 0.759 + 0.0048 \times \gamma_{wet} - 0.012 \times \gamma_{dry} - 0.002 \times N - 0.0012 \times e_o - 0.0006 \times [(\gamma_{wet} - 115.484) \times (\gamma_{wet} - 115.484)]$	Simplified model	0.8308	0.8133	0.1436
$C_c = -0.217 + 0.006 \times w + 0.287 \times e_o$	Fine grained	0.6487	0.6462	0.3906
$C_c = 1.272 + 0.006 \times w - 0.021 \times \text{Fines} + 0.121 \times e_o - 0.000009 \times [(w - 359.133) \times (\text{Fines} - 65.666)] - 0.000985 \times [(w - 359.133) \times (e_o - 5.543)] + 0.0521 \times [(e_o - 5.543) \times (e_o - 5.543)]$	Organic peat	0.7724	0.7480	1.0904
$C_r = 0.0607 + 0.0004 \times w - 0.0024 \times \text{Fines} + 0.0303 \times e_o - 0.00001 \times [(w - 359.133) \times (\text{Fines} - 65.666)] + 0.00549 \times [(e_o - 5.543) \times (e_o - 5.543)]$	Organic peat	0.8101	0.7935	0.1387

Table 2-3: Correlations of Index Properties to Compressibility Indices for Florida Soil from Kirtis et al. 2019

Equations	Notes	R^2	R^2_{adj}	RMSE
$C_c = -0.146 + 0.001 \times \gamma_{wet} - 0.003 \times \gamma_{dry} + 0.007 \times N + 0.005 \times \text{fines} + 0.373 \times e_o - 0.0006 \times [(\gamma_{wet} - 115.484) \times (N - 6.493)] + 0.001 \times [(\gamma_{wet} - 115.484) \times (\text{fines} - 31.584)] + 0.032 \times [(\text{fines} - 31.584) \times (e_o - 1.028)] + 0.001 \times [(\gamma_{wet} - 115.484) \times (\gamma_{wet} - 115.484)] - 0.0003 \times [(\gamma_{dry} - 86.024) \times (\gamma_{dry} - 86.024)] - 0.0005 \times [(N - 6.493) \times (N - 6.493)]$	Coarse grained	0.9079	0.8888	0.1108
$C_r = 0.071 + 0.006 \times \sigma - 0.0005 \times \gamma_{wet} + 0.0004 \times N + 0.0002 \times \text{fines} - 0.0001 \times \text{LL} - 0.0006 \times [(\sigma - 1.966) \times (\text{fines} - 32.934)] - 0.00005 \times [(\gamma_{wet} - 117.148) \times (N - 6.439)] - 0.00003 \times [(\gamma_{wet} - 117.148) \times (\text{LL} - 50.943)] - 0.00001 \times [(\gamma_{wet} - 117.148) \times (\gamma_{wet} - 117.148)]$		0.695	0.666	0.013
$C_c = -0.296 + 0.001 \times \text{PI} + 0.485 \times e_o + 0.001 \times [(\text{PI} - 65.685) \times (e_o - 1.859)]$	Fine grained	0.6740	0.6700	0.3600
$C_r = -0.276 + 0.003 \times \gamma_{dry} + 0.002 \times w - 0.0003 \times \text{fines} + 0.0002 \times \text{LL} - 0.005 \times G_s + 0.00005 \times [(\gamma_{dry} - 61.171) \times (w - 71.207)] + 0.000007 \times [(w - 71.207) \times (\text{LL} - 98.843)] - 0.002 \times [(w - 71.207) \times (G_s - 2.595)] + 0.004 \times [(\text{fines} - 80.226) \times (G_s - 2.595)]$		0.532	0.516	0.058
$C_c = 1.272 + 0.006 \times w - 0.021 \times \text{fines} + 0.121 \times e_o - 0.000009 \times [(w - 359.133) \times (\text{fines} - 65.666)] - 0.000985 \times [(w - 359.133) \times (e_o - 5.543)] + 0.0521 \times [(e_o - 5.543) \times (e_o - 5.543)]$	Organic peat	0.7724	0.7480	1.0904
$C_r = 0.0607 + 0.0004 \times w - 0.0024 \times \text{fines} + 0.0303 \times e_o - 0.00001 \times [(w - 359.133) \times (\text{fines} - 65.666)] + 0.00549 \times [(e_o - 5.543) \times (e_o - 5.543)]$		0.8101	0.7935	0.1387

2.5 Compressibility and Cone Penetration Test

Research that estimates the compressibility of soils via cone penetration testing is presented within this section. Correlations for granular soils, idealized as an elastic material, have been mathematically, empirically, and theoretically justified. An attempt is made to relate elastic correlations to elastic-plastic soil behaviors. The error with this approach is that the assumptions made for the elastic material cannot be applied to plastic material, which makes it difficult to defend mathematically. For this reason, all research referenced in this section utilizes empirical methods to determine a soil type specific parameter to estimate compressibility. This parameter, referred from here on as the calibration constant, is multiplied by tip resistance to estimate the stiffness of the soil. This approach allows the originally derived correlation for elastic material to be applied to an elastic-plastic material.

2.5.1 Elastic Derivation and Calibration Constant

The method discussed in this section references “The Static Penetrometer and the Prediction of Settlements” from Sanglerat, G. (1972) and is based on a mathematical derivation of an equation to estimate compressibility from cone tip resistance. Keverling Buisman derived an equation in 1940 to estimate compressibility of elastic materials. The derivation is founded upon the assumption that the volume decrease occurs at the point of the penetrometer, implying tip resistance is only a function of soil compression and the constrained modulus is constant due to the small loading area. Since the constrained modulus is assumed constant, it is implied very small levels of strain occur as well as an elastic response. Boussinesq’s solution (Boussinesq 1885) were utilized to determine stress at any point from the cone tip. These assumptions were utilized for the solution shown in (4). When this solution was tested against actual parameters specifically for sandy soils, it was shown to be the upper bounds of settlement and a conservative estimation.

$$C = \frac{3}{2} \left(\frac{q_c}{\sigma_{v0}} \right) \quad (4)$$

Sangleret and others proposed altering Buisman's solution to work for cohesive soils by replacing 3/2 shown above in (4) with a constant dependent on soil classification, α , as seen below in (5). The theoretical error in the application of this derivation to soft soils is that Buisman originally assumed an elastic response. Implying that for clays the correlation is theoretically only applicable to estimate the recompression index.

$$C = \alpha \left(\frac{q_c}{\sigma_{v0}} \right) \quad (5)$$

The National Institute of Applied Sciences of Lyons (NIASL) determined the values of α for different soil types through extensive data collection. The process used by the NIASL was to acquire the compressibility constant from oedometer testing and the tip resistance from cone penetration testing. Since the compressibility constant C , tip resistance (q_c), and vertical stress (σ_{v0}) are known, α can be assigned. The NIASL utilized 600 comparative couples for fine grained soils (>50% fines) to create tables of α for different soil behavior types shown in Table 2-4, which also includes information on water content.

Table 2-4 Correction Constant, α , from NIASL for Fine Grained Soils from Sanglerat (1972)

	q_c (bar)	α
Low Plasticity Clay	< 7	3 to 8
	7 to 20	1 to 5
	> 20	1 to 2.5
Low Plasticity Loam	< 20	3 to 6
	> 20	1 to 2.5
Very Plastic Clay and Loam	< 20	2 to 6
	> 20	1 to 2

Table 2-5 Correction Constant, α , from NIASL for Peats and Organic Soils from Sanglerat (1972)

	q_c (bar)	α
Very Organic Loam	< 12	2 to 8
Peat and Very Organic Clay	< 7	
	50 < w < 100	1.5 to 4
	100 < w < 200	1 to 1.5
	w > 300	<.4

Table 2-6 Correction Constant, α , from NIASL for Chalks and Sands from Sanglerat (1972)

	q_c (bar)	α
Chalks	20 to 30	2 to 4
	> 30	1.5 to 3
Sands	< 50	2
	> 100	1.5

The NIASL used this data base for further research to plot tip resistance versus compressibility index, found below in Figure 2-2. This graph shows an upper and lower hyperbolic bound, but no regression function to accurately describe a relationship can be recommended. The results indicate when tip resistance is low (<12 bar), the compression index is highly dependent on moisture content. This was not the main purpose of the research by the NIASL, and therefore does not receive an extensive analysis of results.

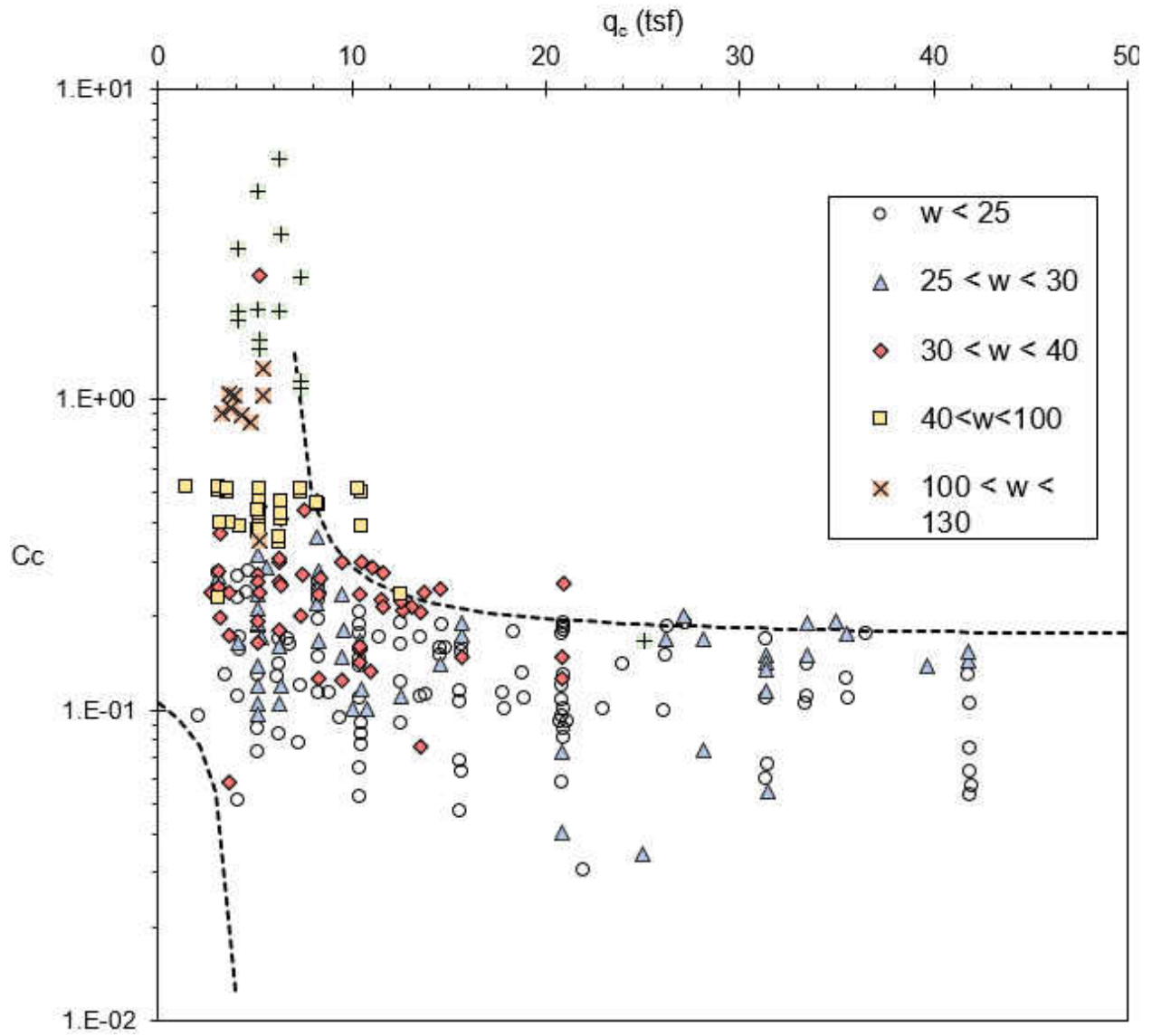


Figure 2-2: Results of Lyons Research, q_c vs C_c from Sanglerat (1972)

2.5.2 Constrained Modulus

The following section references “Interpretation of cone penetration tests - a unified approach” from Robertson, P. K. (2009). This study presents a method to estimate the constrained modulus (stress: strain response with no net lateral displacement) via the Cone penetration test. This modulus can be analogous to the compressibility indices as it is a means to describe soil deformation due to loading. Robertson’s previous research into Normalized Soil Behavior Type (SBTn) enables one to create a soil profile and identify transition zones from the CPT. The SBTn graph is also useful as a tool to better relate CPT parameters to soil parameters, in this case to the constrained modulus.

In short, Robertson accomplished this correlation via multiple empirical relationships. First, the CPT is correlated to the shear wave velocity, which is directly related to the small shear modulus. The small shear modulus is then correlated to the constrained modulus.

Initially, a set of normalized shear wave velocity (V_{s1}) contours are plotted on the SBTn chart from over 100 SCPT profiles. Then, a function that best approximates the V_{s1} contours is used to relate shear wave velocity to cone tip resistance and soil behavior type. This relationship is theoretically justified since both of these parameters are dependent on the soil’s relative density, effective stress state, age, and cementation.

Small strain shear modulus (G_0) is a soil stiffness parameter that describes the material’s deformation response to shear stress in the linear elastic zone (shear levels less than 10^{-4} %). Since G_0 is a direct function of shear velocity it can be contoured on the SBTn chart and become a function of tip resistance, sleeve friction ratio, and soil type. This step is controversial as the small shear strain modulus describes the stiffness in the elastic zone. However, there is a small error in the results, shown below in Figure 2-3, when these contours were extended into the plastic region of the SBTn chart.

Paul Mayne suggests the small strain shear modulus is directly related to constrained modulus as a ratio. Using a similar method as above, the constrained modulus can be contoured on the SBTn chart and written as a function of tip resistance, sleeve friction ratio, and soil type.

$$M = \alpha_M(q_t - \sigma_{v0}) \quad (6)$$

The estimated constrained modulus from equation (6) has a strong correlation to the actual constrained modulus measured directly from oedometer testing. The results in Figure 2-3 were especially accurate in soft soils with a normalized tip resistance less than 14. The main source of error is from double correlations and the use of an elastic parameter during the derivation.

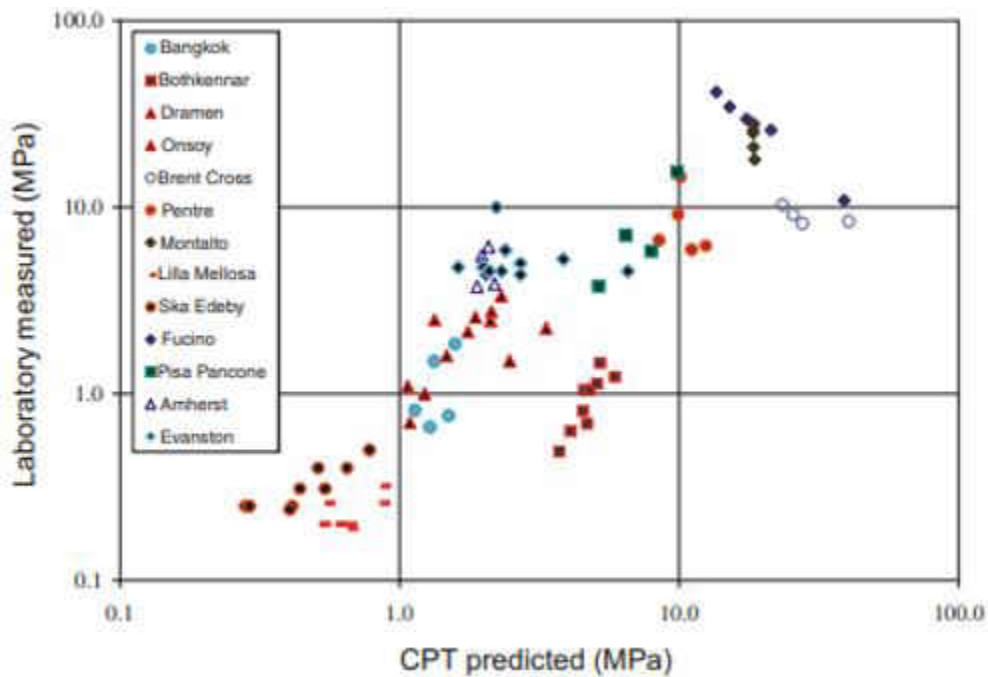


Figure 2-3: Laboratory measured constrained modulus, M , compared with CPT predicted

2.6 Estimation of Preconsolidation Pressure

This section presents a reliable semi-empirical model to estimate the preconsolidation pressure from the CPT. This compressibility parameter is required to define the soils compressibility and estimate settlements. A model will not be proposed within the analysis of this thesis as more reliable correlations already exist.

The reference discussed below, “Profiling OCR in stiff clays by CPT and SPT” by Mayne & Kemper (1988), utilizes a semi - empirical methodology to estimate OCR from the CPT. In short, the cone penetration test is commonly used to estimate undrained shear strength which is dependent on the soils stress history. Relating undrained shear strength to stress history allows continuous profiling of overconsolidation ratio from tip resistance.

The data base utilized consists of CPT data from 40 different clays with a plasticity index ranging from 3 to 9 and an OCR ranging from normally consolidated to heavily overconsolidated. These clays have been deposited in a variety of geologic environments including terrestrial, marine, glacial and alluvial, implying this correlation is generic and not refined to a specific geology. Since the data is from different sites the CPT and oedometer test equipment and technician likely vary, which makes it difficult to control the quality and consistency of each point.

This data base was first used to correlate undrained shear strength to cone tip resistance as shown in Figure 2-4 and equation 7. Stress history and normalized soil engineering properties (SHANSEP) method relates undrained shear strength and OCR, as shown in equation 8. Now, Undrained shear strength has been correlated to tip resistance and OCR, which implies that OCR is a function of tip resistance. This correlation is shown graphically in Figure 2-5 and mathematically in equation 9. The

calibration parameter in equation (10), k_c , is dependent on soil type and stress path. This parameters makes it possible to refine the model to the local geology.

$$\frac{Su}{\sigma_0'} = \frac{q_c - \gamma Z}{N_k \sigma_0'} \quad (7)$$

$$OCR = \left(\frac{\frac{Su}{\sigma_0'}}{\frac{Su}{\sigma_c'}} \right)^{\frac{1}{\lambda}} \quad (8)$$

$$OCR = 0.37 \left(\frac{q_c - \gamma Z}{\sigma_0'} \right)^{1.01} \quad (9)$$

$$OCR = k_c \left(\frac{q_c - \gamma Z}{\sigma_0'} \right) \quad (10)$$

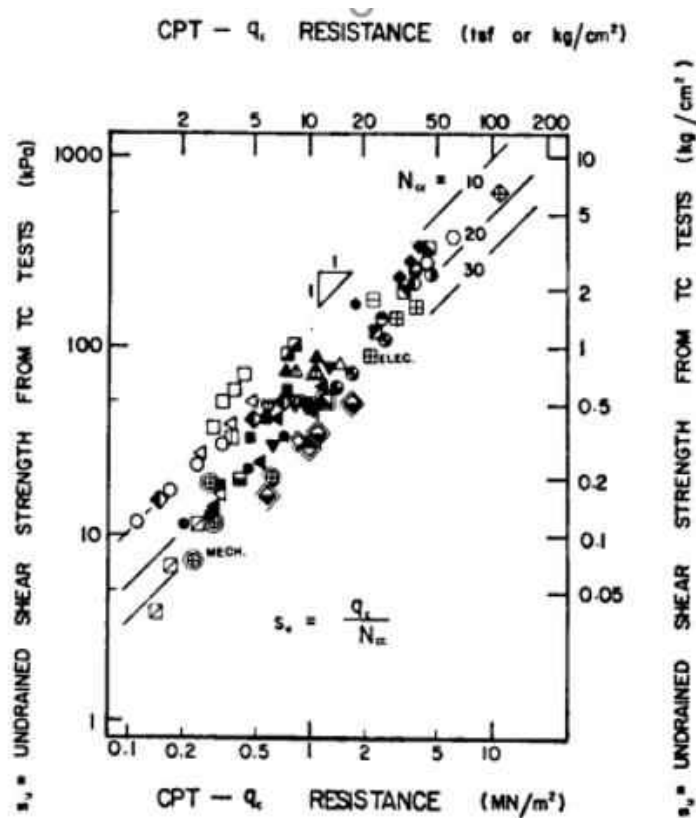


Figure 2-4: Comparison between Undrained Shear strength from Triaxial compression and measured cone resistance from mechanics and electric cones, taken from Mayne and Kemper 1988

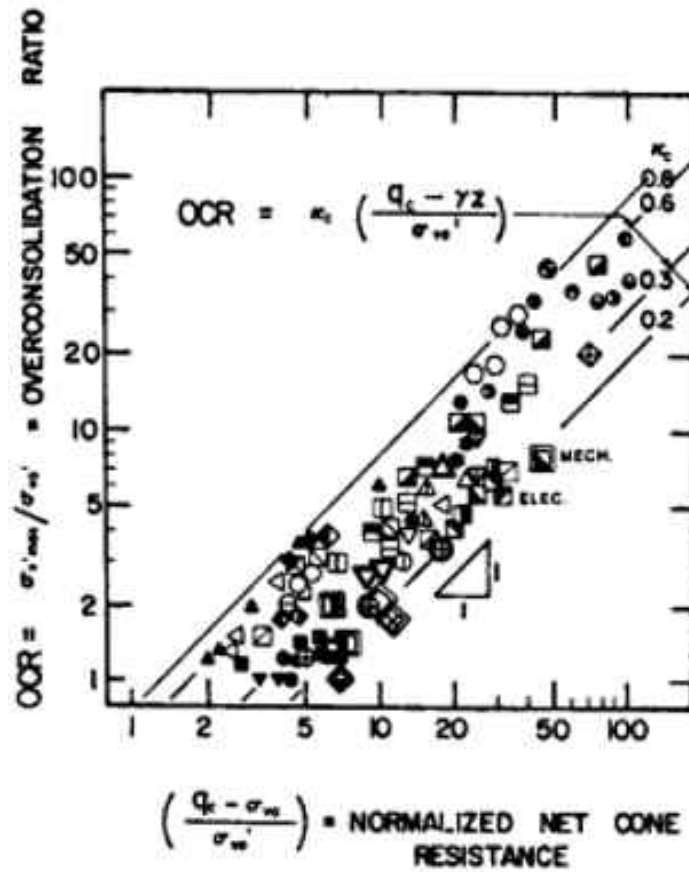


Figure 2-5: Trend Between Laboratory OCR and Normalized net cone resistance taken from Mayne and Kemper 1988

2.7 Literature Review Conclusion

Index properties have been shown empirically to have a strong correlation to the compression index and a poor correlation to the recompression index. It was then suggested a ratio from the compression index to estimate the recompression index may be more accurate. It was also shown that different soil types require different correlations.

Robertson and Buisman's derivation of the coefficient of compressibility utilizes elastic theory and therefore is not theoretically sound for prediction of elastic-plastic soil behavior. However, Robertson's correlation compared very well to estimated values and Buisman's equation can be applied to clays after receiving a correction constant, α , dependent on the soil behavior type. A derivation using elastic and plastic theory would be ideal, but properly selected calibration parameters determined via empirical methods have proven accurate.

The derivation and justification of the CPT correlation to past maximum pressure is sound. There is no need to propose a new model in this paper. Instead, the accuracy of the model will be checked and the proper correction factor, K_c , for Central Florida soils will be recommended.

CHAPTER 3 INDEX PROPERTIES AND COMPRESSIBILITY

3.1 Introduction

The objective of this chapter is to provide a model to estimate the compressibility of fine-grained soils in the Central Florida region via index properties. Previous researchers have demonstrated that index properties can accurately estimate the compressibility of the soil, however, most of these models are generic and not refined for specific geologies. This section will differ from Kirtis et al., which studied Central Florida Soils, by building upon their data base and by recommending a single variable model. Since this is an empirical method, any firm with adequate data can create a data base and perform the following analysis, allowing more accurate estimation of compressibility via index properties in their specific area.

The specific index properties compared with compressibility include moisture content (W), Liquid Limit (LL), Plasticity index (PI), Liquidity Index (LI), Percent Finer (-200), Activity (A), moist unit weight (γ), dry unit weight (γ_d), and Initial Void Ratio (e_0). Moisture content describes the ratio by weight of water to solids. The Liquid and Plastic limits are defined as the moisture content required to change the behavior to a liquid and to a solid state, respectively. The Plasticity index is the range between the plastic and liquid limit and describes the soil's ability to hold water as well as its susceptibility to volume change via shrinking and swelling. The Liquidity Index scales the Atterberg limits to the moisture content. Percent Finer is the percentage of particles less than $75\mu\text{m}$, which are referred to as fine-grained soil and are typically clays and silts. Activity is the ratio of plasticity index to percent finer. This parameter "normalizes" the plasticity index and describes the colloidal properties of the soil providing information into the soil behavior, geology and strength (Skempton 1988). The moist unit weight is measured from the Shelby tube before sample extraction by measuring the volume and total weight minus weight of Shelby tube then multiplying this density by gravity. The dry unit weight is equal to the

moist unit weight divided by one plus the average moisture content. And finally, the void ratio is the ratio by volume of voids and solids.

$$w_n = \frac{W_w}{W_s} \quad (11)$$

$$PI = LL - PL \quad (12)$$

$$LI = \frac{W - PL}{PI} \quad (13)$$

$$A = \frac{PI}{\% \text{ finer}} \quad (14)$$

$$\gamma = \frac{W}{V} \quad (15)$$

$$\gamma_d = \frac{\gamma}{1+W} \quad (16)$$

It can be assumed from fundamental soil mechanics and supported by other researcher's work that moisture content, plasticity indices, unit weight, and void ratio will be the dominating index parameters for estimating soil compressibility.

Moisture content, void ratio, and unit weights are likely to be strongly correlated to compressibility. This is attributed to the process of consolidation, in which the outflow of water relieves the excess pore pressure and the soil skeleton then densifies to accommodate the new stresses. Therefore, more voids present in the initial structure may indicate the amount of volume change the sample will undergo and vice versa. Assuming the sample is saturated, both the void ratio and moisture content indicate the amount of void space present in the soil sample. This implies that the moisture content and void ratio should be a direct indication of the soil's susceptibility to volume change. The unit weights are direct measurements of the soil's density.

Plasticity index is the range between liquid limit and plasticity limit, in other words, the range of moisture in which the soil behaves plasticly as neither a liquid nor a solid. The greater the plasticity index, the more susceptible the material is to volume change, commonly seen as high shrinking and

swelling potential. Since this index provides insight into the soil's ability to change volume with moisture, it is likely that it will be strongly correlated to compressibility indices. By association, the liquid limit and plastic limit may also show strong correlations.

3.2 Methodology

3.2.1 Data Base

The data base utilized in this chapter is a combination of UCF's data base and the CPT data base created for use in Chapters 4 and 5. UCF's data base consists of 350 oedometer test and index test results for fine-grained soil. All the data is from Florida soils and majority is from FDOT district five. The CPT data base was created from scratch. It originally consisted of thirty-five data points, of which twenty-three were accepted. The removal of data points was in accordance with the filters discussed in Chapter 4 which was done to ensure a high quality, reliable data base. Of the twenty-three accepted points twenty-one are clays with more than 50 % fines and two are clayey sands with 40 to 50 % fines. The combination of the two data bases total 375 couples of index properties and compressibility parameters.

3.2.2 Analysis

A regression analysis is utilized in which each index property is plotted against the recompression and compression indices. Then, the parameters indicating a strong correlation indicated by statistical quantifiers (R^2 and RMSE) will be interpreted and presented as a viable model. The correlation with the highest statistical reliability that is also theoretically justifiable will be recommended as the final model to estimate compressibility. All correlations are in Appendix A, the reliable correlations are presented in section 3.3.1, and the final recommended model is in section 3.3.2

This analysis will recommend compressibility indices in void ratio – stress space and a correlation to estimate void ratio will be provided. The analysis in strain – stress space yielded weaker correlations, so it has been deemed more accurate to utilize a double correlation.

3.3 Results and Discussion

The strong correlations will be discussed and summarized within this section. A strong correlation was an R^2 greater than 0.3 for the recompression index and 0.4 for the compression index. The R^2 value is the initial statistical parameter utilized to quantify the correlations strength. For the relatively strong correlations, the root mean squares error (RMSE) is also determined to further quantify the correlations reliability. The R^2 parameter represents the portion of observed values which can be captured using the proposed model. The RMSE describes how concentrated the data is around the line of best fit with 0 being a perfect fit. It is important to note that R^2 is a dimensionless parameter while RMSE is dependent on the dimension of the parameter. Therefore, RMSE will have the dimensions of compression or recompression index, where deemed applicable. The equation for the line of best fit and the statistical parameters are found within each graph and summarized in Table 3-2. The subsections will display each correlation, discuss the results and recommend the best model to estimate the compressibility of cohesive soil in the Central Florida area.

3.3.1 Correlations from Charts

This section presents the strongest correlations between index properties and compressibility indices. The weaker correlations not shown in this section are in Appendix A. The parameters which correlated well are moisture content, void ratio, liquid limit and dry unit weight. Moisture content, void ratio and dry unit weight provide insight into the in-situ soil structure, and liquid limit indicates the soil behavior. The correlations are presented and summarized below in figures 3-1 to 3-9 and table 3-1, respectively, and further discussed in section 3.3.2.

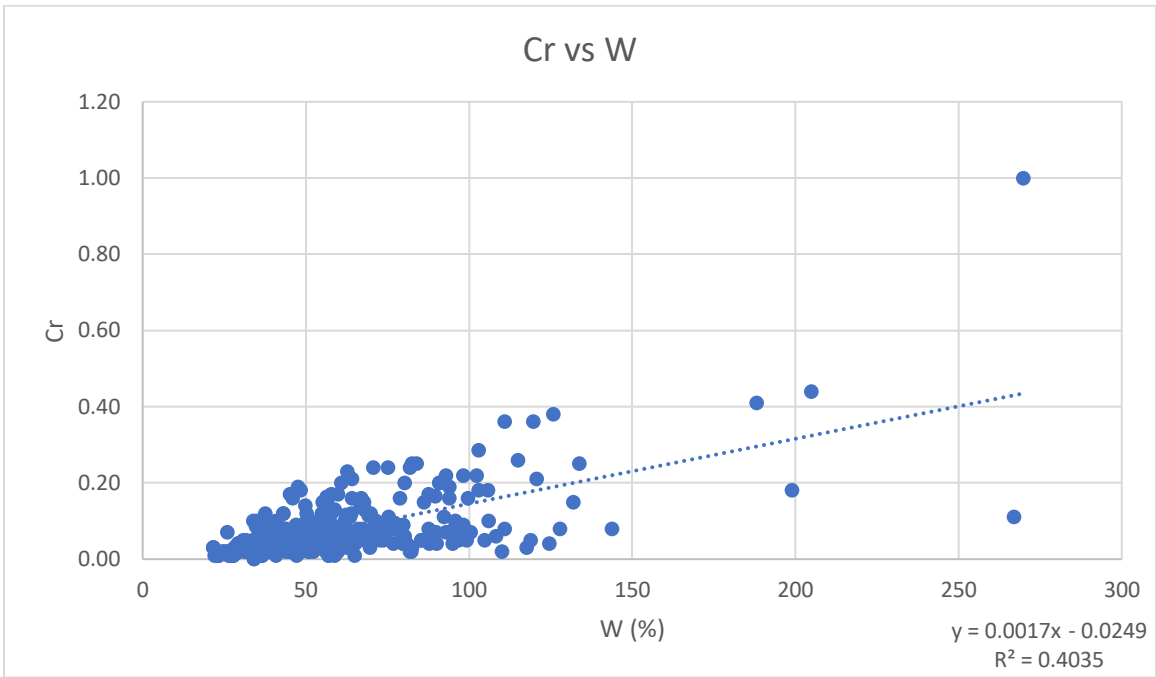


Figure 3-1: Recompression Index vs Moisture Content, W

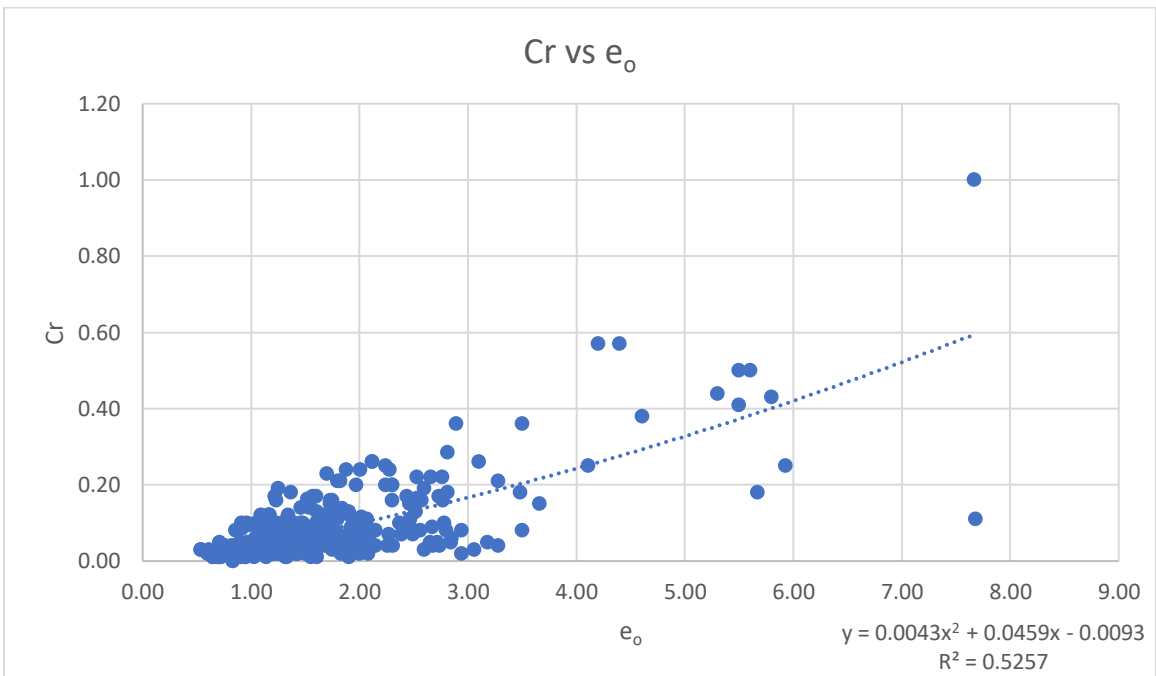


Figure 3-2: Recompression Index vs Initial Void Ratio, e_o

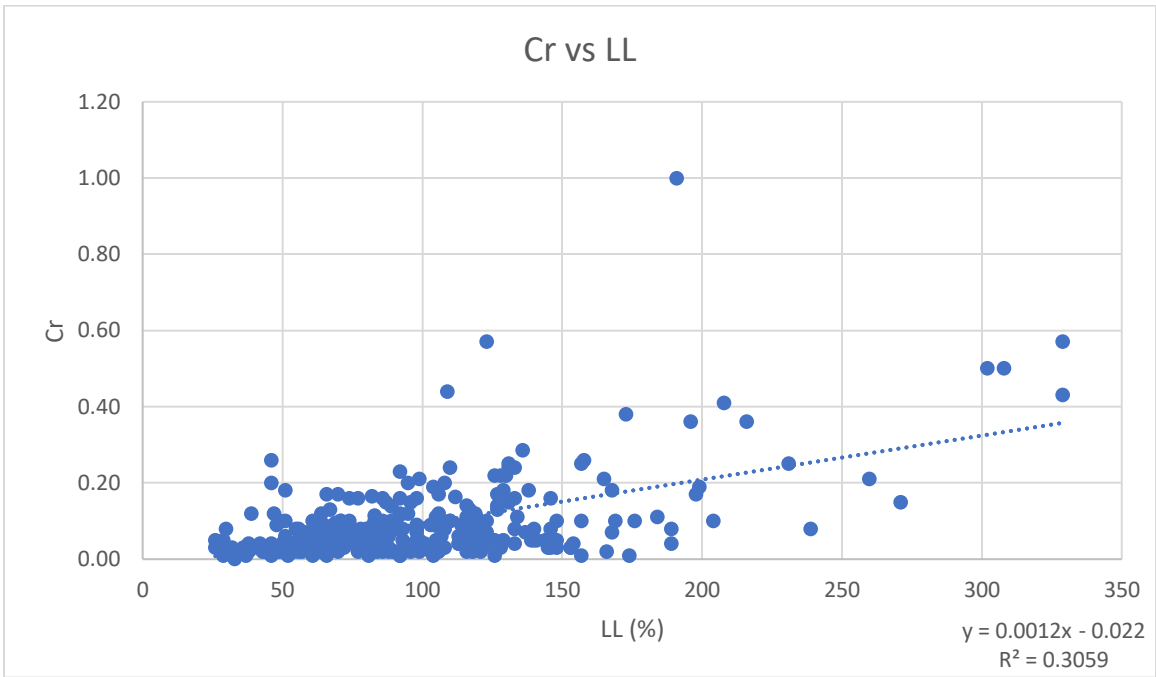


Figure 3-3: Recompression Index vs Liquid Limit, LL

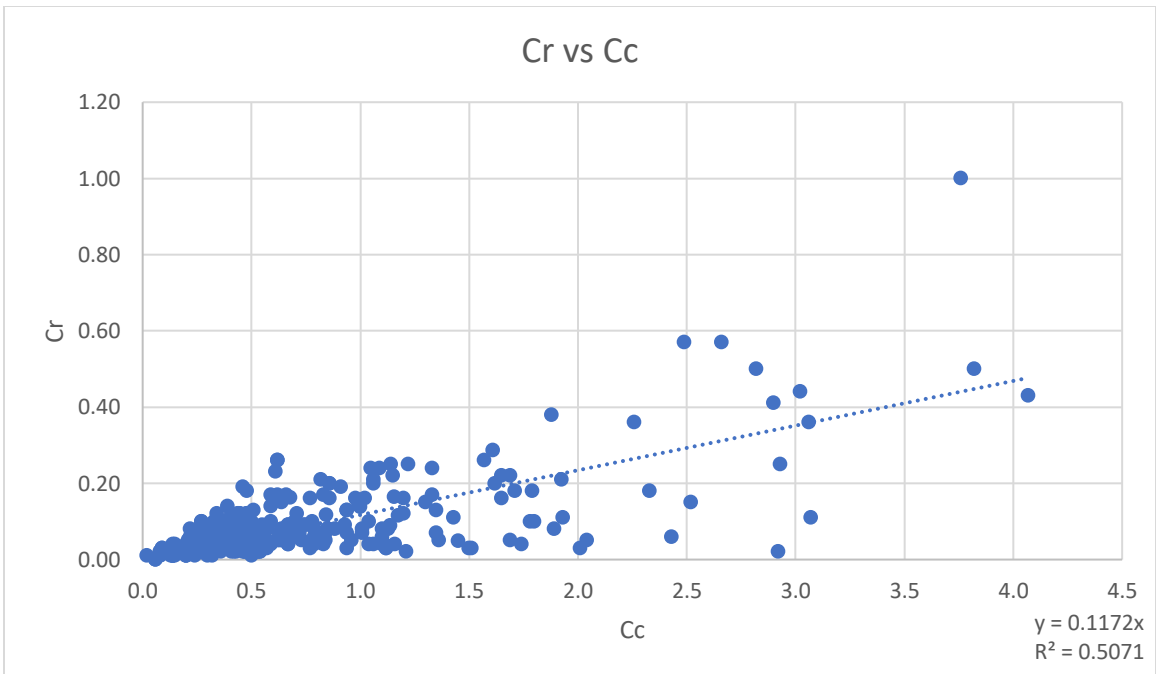


Figure 3-4: Recompression Index vs Compression Index

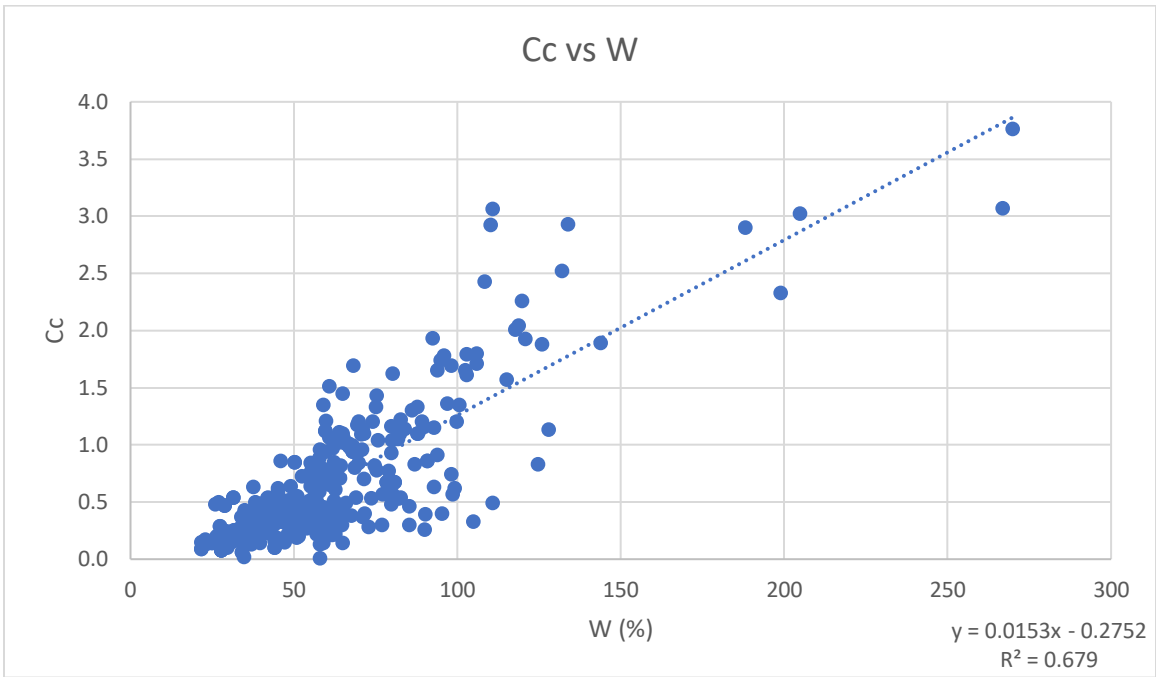


Figure 3-5: Compression Index vs Moisture Content, W

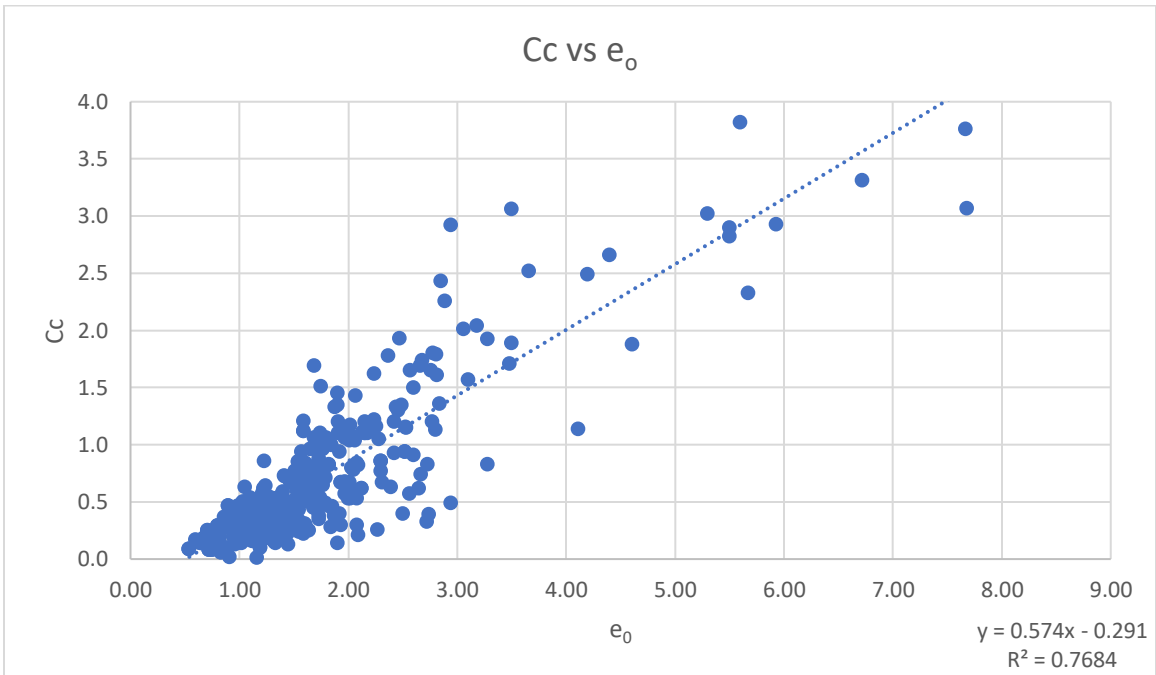


Figure 3-6: Compression Index vs Initial Void Ratio, e_0

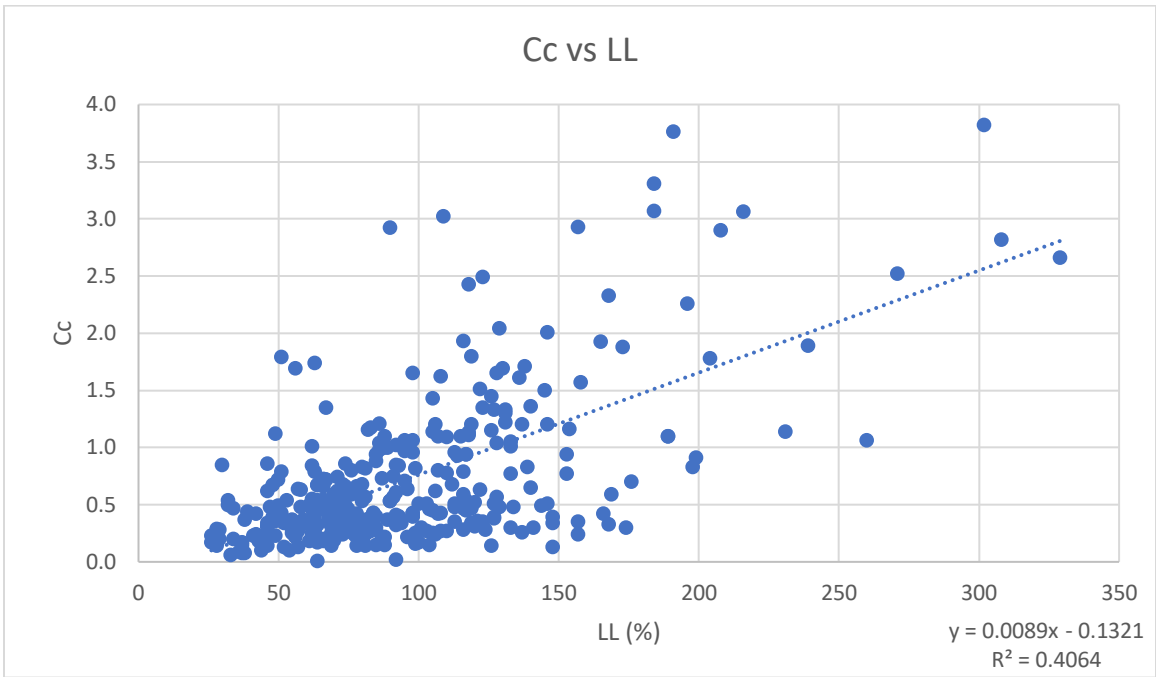


Figure 3-7: Compression Index vs Liquid Limit, LL

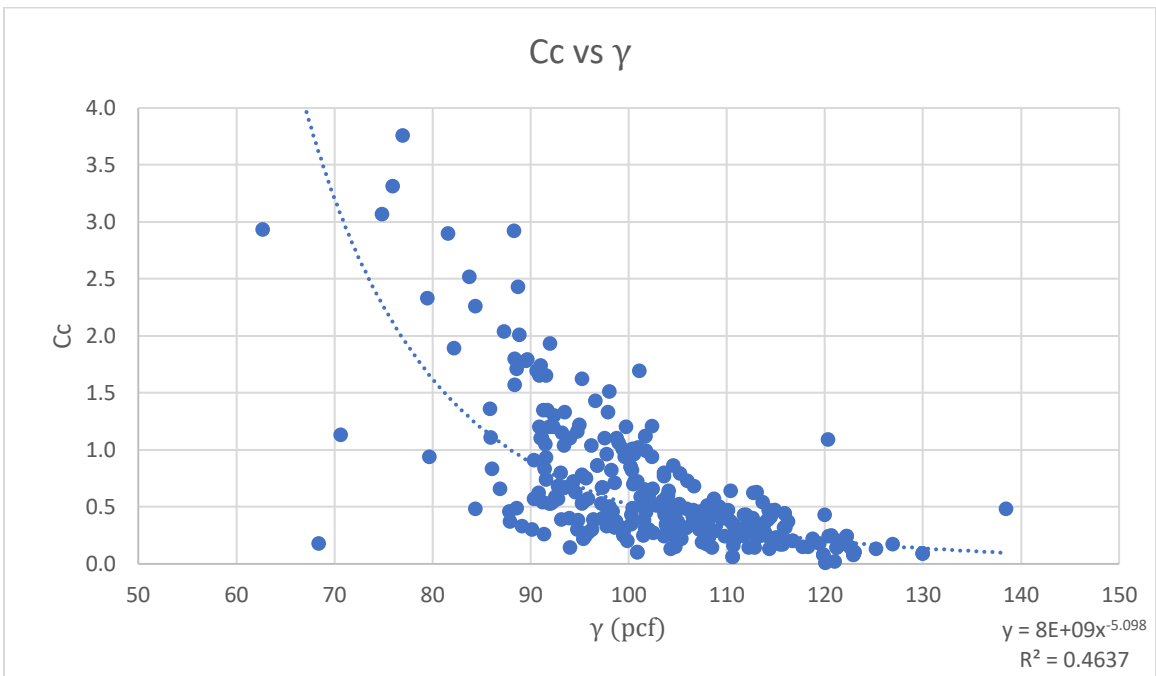


Figure 3-8: Compression Index vs Wet Unit Weight, γ

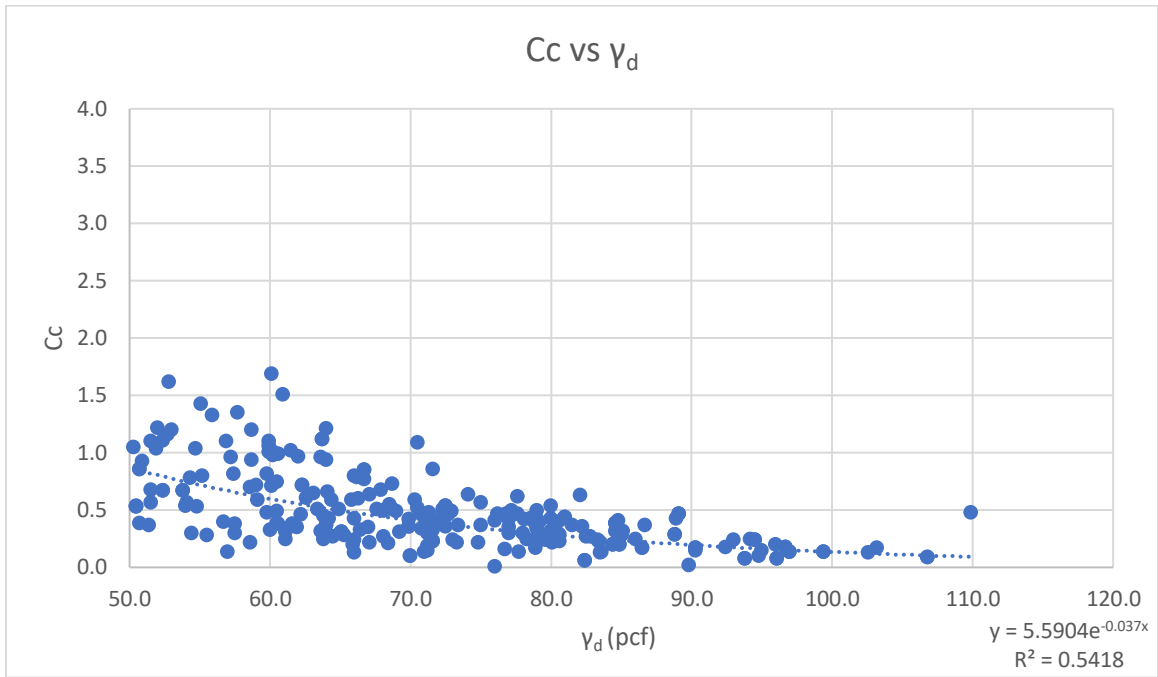


Figure 3-9: Compression Index vs Dry Unit Weight, γ_d

Table 3-1: Summary of Results, Index Properties

Recompression Index	Equation	R ²	RMSE
Moisture Content	$Cr = 0.0017W - 0.0249$	0.404	0.066
Void Ratio	$Cr = 0.0043(e_0)^2 + 0.0459(e_0) - 0.0093$	0.526	0.073
Liquid Limit	$Cr = 0.0012LL - 0.022$	0.306	0.086
Compression Index	$Cr = 0.1087Cc + 0.011$	0.513	0.073
Compression Index			
Moisture Content	$Cc = 0.015W - 0.275$	0.679	0.329
Void Ratio	$Cc = 0.574(e_0) - 0.291$	0.768	0.317
Liquid Limit	$Cc = 0.009LL - 0.132$	0.406	0.501
Dry Density	$Cc = 5.5904e^{-0.037x}$	0.542	0.351

3.3.2 Recommended Models and Discussion

Moisture Content, Liquid Limit, and Void Ratio demonstrate strong correlation to compressibility and are summarized in Table 3-1. As previously discussed, the moisture content and void ratio provide insight into the amount of void space (structure) and therefore, the amount of potential volume change. The plasticity indices show the soil's colloidal properties by quantifying its ability to shrink and swell.

Void Ratio will be removed from the recommended models for both compression and recompression indices because it is not a common index test. Moisture content and plasticity indices are supported by theory and previous researchers and provide strong correlations. For this reason, they will be considered as final models. However, since moisture content shows a stronger correlation and is a simpler, less expensive lab test it will be recommended as the final model. The equation and statistical parameters for the moisture content correlations to the recompression and compression indices, as well as to void ratio is summarized in Table 3-2 and 3-3, respectively. According to the fundamental phase relation ($G_s w = S e$) and supported by figure 3-21 it may be recommended, with a very high degree of reliability, that moisture content be used to estimate void ratio.

Table 3-2: Recommended Models for Index Properties

Recompression Index	Equation	R²	RMSE
Moisture Content	$Cr = 0.0017W - 0.0249$	0.404	.066
Compression Index	$Cr = 0.1087Cc + 0.011$	0.513	.073
Compression Index			
Moisture Content	$Cc = 0.015W - 0.275$	0.679	.329

Table 3-3: Recommended Model for Void Ratio

Void Ratio	Equation	R²	RMSE
Moisture Content	$e_0 = 0.0271W - 0.0247$	0.953	.188

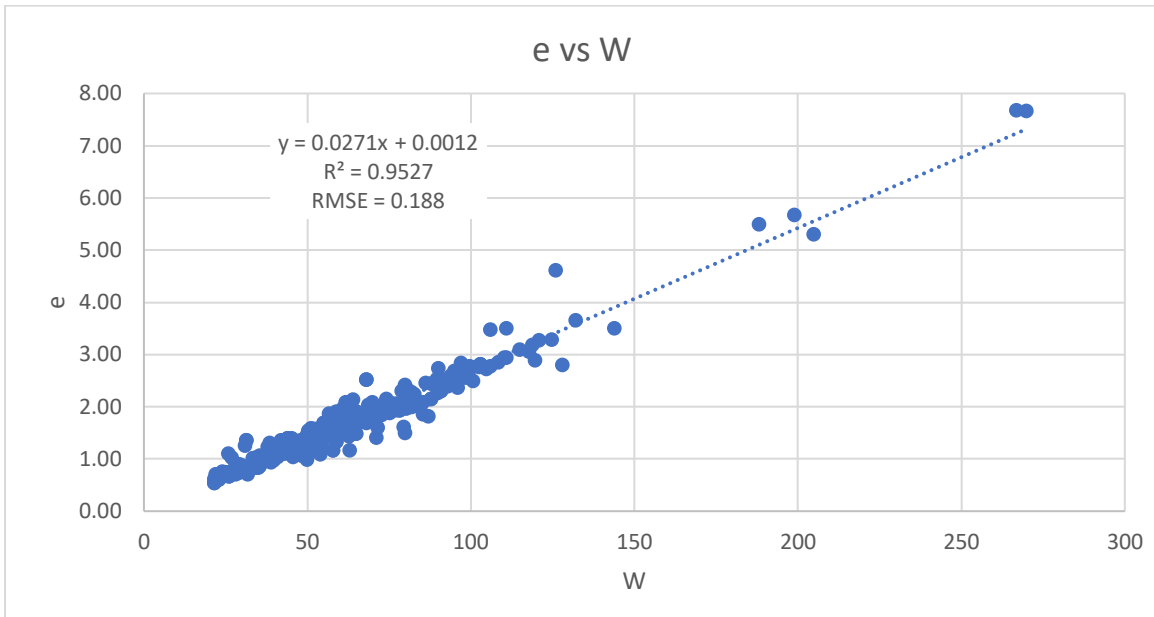


Figure 3-10: Void Ratio vs Moisture Content

Other parameters correlated to the compression index with weaker reliability (R^2 values between 0.2 and 0.3) are plastic limit, percent finer, and activity. Correlations to the recompression index with an R^2 between 0.2 and 0.3 are percent finer and activity. Activity is a function of Percent Finer and Plasticity and provides insight to the colloidal behavior. Since this parameter defines the behavior of the soil well for an index property, it will be used in Chapter 5 to segregate the data base, regardless of its relatively poor correlations.

3.4 Conclusion

This study has provided strong correlation to moisture content and Atterberg limits for cohesive soil in Central Florida. The soil index properties have been proven by previous researchers and supported by this study to accurately estimate the compressibility. The recommended correlations between moisture content and compressibility are more accurate than the correlations utilizing moisture content summarized in Table 2-1.

These models, although accurate, are still a crude way to determine the compressibility of soil. For sites where settlement needs to be well defined it is best to use a combination of Oedometer testing, experience, as well as these correlations. It is also important to note that the definition of OCR is as important as the definition of compressibility. Misjudging the range of the stress levels for the recompression and compression index will be responsible for much more error than a slightly inaccurate definition of compressibility indices. For this reason, if the OCR is well defined from other correlations (see Mayne & Kemper 1988), then the usage of crude estimations of compressibility is acceptable. An OCR model is recommended for the local soil in Chapter 6.

CHAPTER 4 CONE PENETRATION TEST BASED CORRELATION ANALYSIS

4.1 Introduction

The objective of this chapter is to recommend a model to estimate the compressibility of fine-grained cohesive soils in the Central Florida region via the Cone Penetration Test. Previous researchers, as mentioned in the literature review, have shown that it is difficult and not theoretically sound to estimate the compressibility of an elastic-plastic material from the CPT. For this reason, the CPT has been primarily used to estimate elastic stiffness moduli (recompression index, elastic modulus, small shear strain modulus, etc.) which applies to granular material and the elastic zone of clays. Two things will be done differently from previous researchers to present new findings: the pore pressure will be incorporated into the analysis and each data point will be carefully filtered. Previously, only tip resistance has been correlated, and massive data bases were created making it difficult to perform quality control.

Since this is an empirical method, any firm with an adequate quantity of reliable data can recreate this analysis to define correlations refined to their location. These results may be useful for firms in the Central Florida region, or areas with similar geology, but will mainly show how the CPT can be used to estimate compressibility of soft, elastic-plastic materials.

Based on previous findings and soil mechanics it is expected that the tip and sleeve friction will accurately estimate the compressibility in the elastic zone, known as the recompression index. It is also expected that the pore pressure reading in the u_2 position will be the controlling parameter for estimating the compression index. This hypothesis is made because the deformation pre yielding is due to soil structure while the deformation post-yielding is due to composition (stress). Therefore, the

process of consolidation, transfer of stress from the pore water to the soil skeleton, will be the main mechanism occurring in the compression index.

It is important to first discuss the mechanisms causing the CPT readings of tip resistance, sleeve friction, and pore pressure. The penetrometer is shearing the soil to failure to maintain the constant rate of push; therefore, the tip and sleeve resistance is the amount of force the penetrometer must exert to maintain that constant rate. Following this logic, it is reasonable that tip and sleeve resistance would provide strong correlations to soil strength parameters. The pore pressure reading is the pore pressure developed from the shearing of the soil layer and at time zero should be equal to the load exerted on the soil (some combination of tip resistance and sleeve friction). The rate at which this pressure dissipates determines the pore pressure value reported at the u_2 position. Meaning, if the soil cannot dissipate any pressure, it should be equal to the force required to fail the soil, indicating very low permeability and potentially high compressibility. If the soil can dissipate the pressure instantaneously, it will read hydrostatic pressure indicating the material has a high permeability and low compressibility. Most cohesive soils will lay somewhere in between these two extremes. Following this logic, it is assumed that the U_2 pore pressure reading will provide a strong correlation to the compression indices. The figures below support this logic and show the failure surface of the soil and pore pressure distribution around the penetrometer.

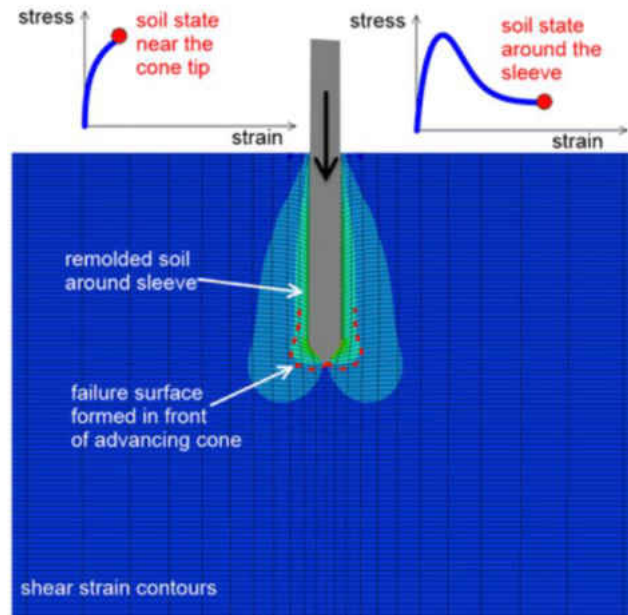


Figure 4-1: CPT Soil Failure Surface

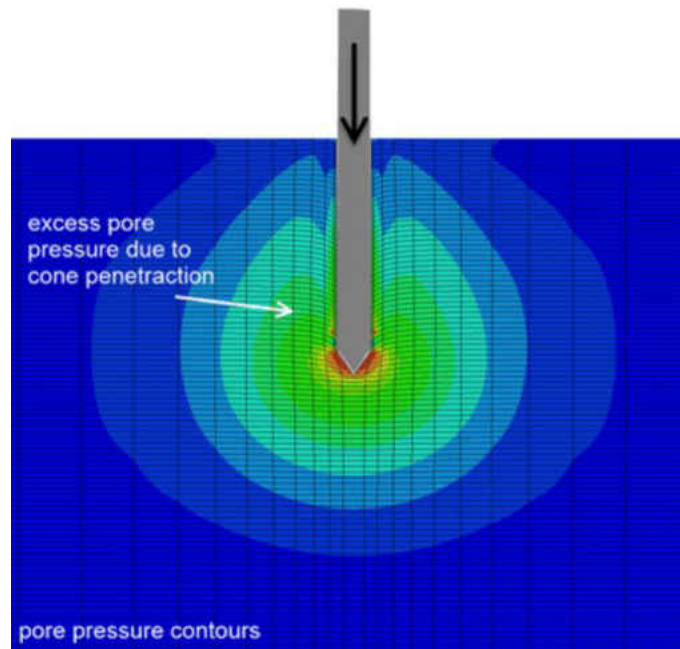


Figure 4-2: CPT Pore Pressure Distribution

4.2 Methodology

4.2.1 Cone Penetration Test Data Base

The following section describes, in detail, the creation of the CPT data base, followed by an example of data selection, and the analysis process performed in this chapter. In order to create the data base, information from local projects with Oedometer testing and CPTs performed must be acquired. The data is then filtered and a data base with adequate points is created. A description of each test, the filtering process, and the CPT analysis process is covered in the following section. A logic chart (Figure 4-3) summarizing the methodology can be found at the end of this section.

4.2.2 Data Processing Procedure

The data utilized for this data base include oedometer test results, CPT results, and index properties (moisture content, void ratio, liquid and plastic limits, and percent finer). All test results must be interpreted and if deemed unreliable, removed.

The correlations are aimed to estimate the compressibility of soil, specifically the recompression and compression indices obtained from the oedometer test. This test is utilized to determine the response of soil in 1-D compression. For soft soils this response is non-linear, elastic-plastic and dependent on the material's past maximum pressure. Soils of this nature deform due to a time dependent process known as consolidation. Defining parameters from this test are the slopes of elastic response or OCL (swelling index), the slope of the plastic response or NCL (compression index), and the vertical stress at yielding (preconsolidation pressure). The elastic response turns into a plastic response at the preconsolidation pressure. This is important because simple elastic analysis may be performed up to this point while a more complex definition is required after this point. The oedometer test is highly

sensitive to soil sample disturbance, therefore, quality rating suggested by Terzaghi et al (1996) and Lunne et al (1997a) is utilized to check for disturbance and help attain a reliable data base (Table 3-1).

The Cone Penetration Test is performed near the Shelby tube borehole to capture the soil layer in which the oedometer sample is taken. Checks implemented for the CPT results are to confirm that the rate of push is around 2 cm/s, the inclination of push is less than 2 degrees, and that all readings agree. This last part is important as a highly plastic clay with no nearby drainage should indicate low tip, relatively high friction, and some pore pressure. If there is a contradiction with what is expected, a more detailed check of the profile is performed and justifications made. Robertson's normalized soil behavior type is then used to compare the CPT soil behavior type profile with the Shelby tube boring visually classified soil profile to confirm the soil stratum is similar within the couple. This step is crucial as soil in this geology can be highly variable, meaning a CPT and SPT boring performed nearby can display different soil profiles and fail to capture the oedometer sample layer.

If the oedometer and cone penetration tests are acceptable and agree with one another, the couple is added to the data base. Next, the depth of representative values of cone tip resistance, sleeve friction and pore water pressure are designated with extreme care as selection of the proper values is key to the success of the research. The depth of CPT readings is ideally at or near the depth of the Shelby tube. The exact location of the sample extraction within the Shelby tube has not been provided with the oedometer results, limiting the precision of the representative readings. However, from experience working at Ardaman and Associates' Soil Testing Laboratory the sample is not extracted from the bottom 3 in. or top 9 in. as the sample is disturbed in these zones. Minimizing the zone of the sample location is important as the CPT outputs can experience a high range of values over the length of the Shelby tube. On top of refining the sample extraction zone to 1 ft., an arbitrary filter requiring all data points to have a range of less than half the average value for each CPT output will be applied.

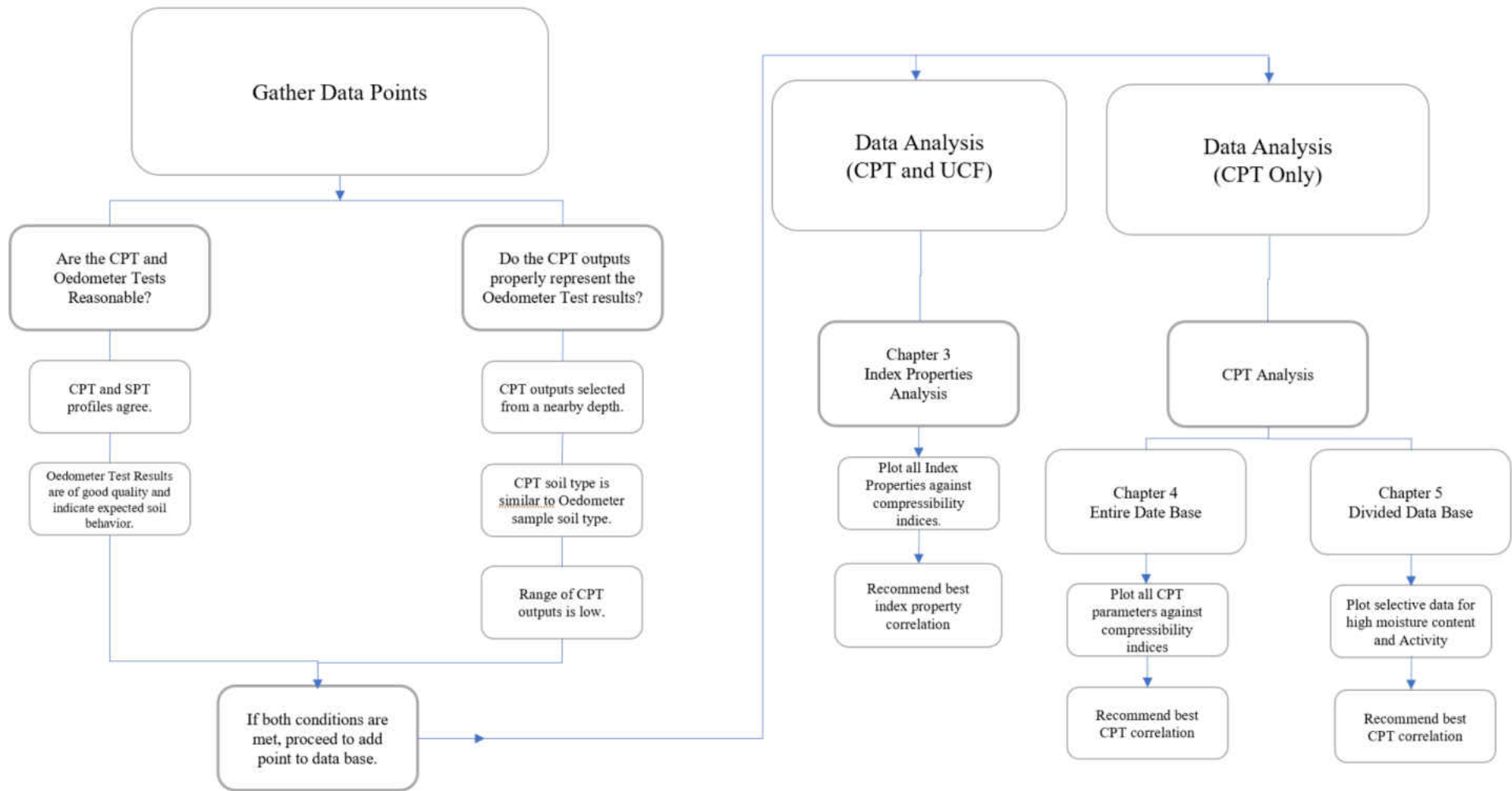


Figure 4-3: Data Base Creation and Analysis Logic Chart

4.2.3 Data Processing Procedure: Example

This section will provide an example of the process described above for one accepted data point located in Seminole County, Florida. Extra comments providing insight to the process at each step are also provided. The procedure is as follows:

1. A local firm shared a project, for research purposes only, in Seminole County, Florida with CPT and Oedometer Testing.
2. This step checks that CPT and SPT are performed nearby and at similar elevations. Figure 3-2 shows that the borings were performed near one another at similar elevations. The boring logs indicate the two tests were performed within 1 month of each other, therefore, it is fair to assume no modification to the soil stratigraphy occurs between tests.

Two potential problems in this step can cause the removal of a few data points. The SPT and CPT may be performed too far apart, making it unlikely the tests represent the same soil profile, or fill has been placed offsetting the soil layers. Initially, the time in between testing was of concern as the site conditions may change and affect the soil layer of interest. A prime example of this is surcharging. Oedometer testing may be used to assess the compressibility of a soft soil and if the soil is deemed too soft, surcharging programs may be utilized to increase the past maximum pressure and minimize post-construction settlements. A CPT is then used to confirm the profile has been strengthened, which will cause the soil at time of CPT to be stiffer than at the time of oedometer testing. This changes the CPT outputs but does not call for removal of the point because the recompression and compression indices will not be affected, only the past maximum pressure and the position of the soil on the over-consolidation line will be modified.

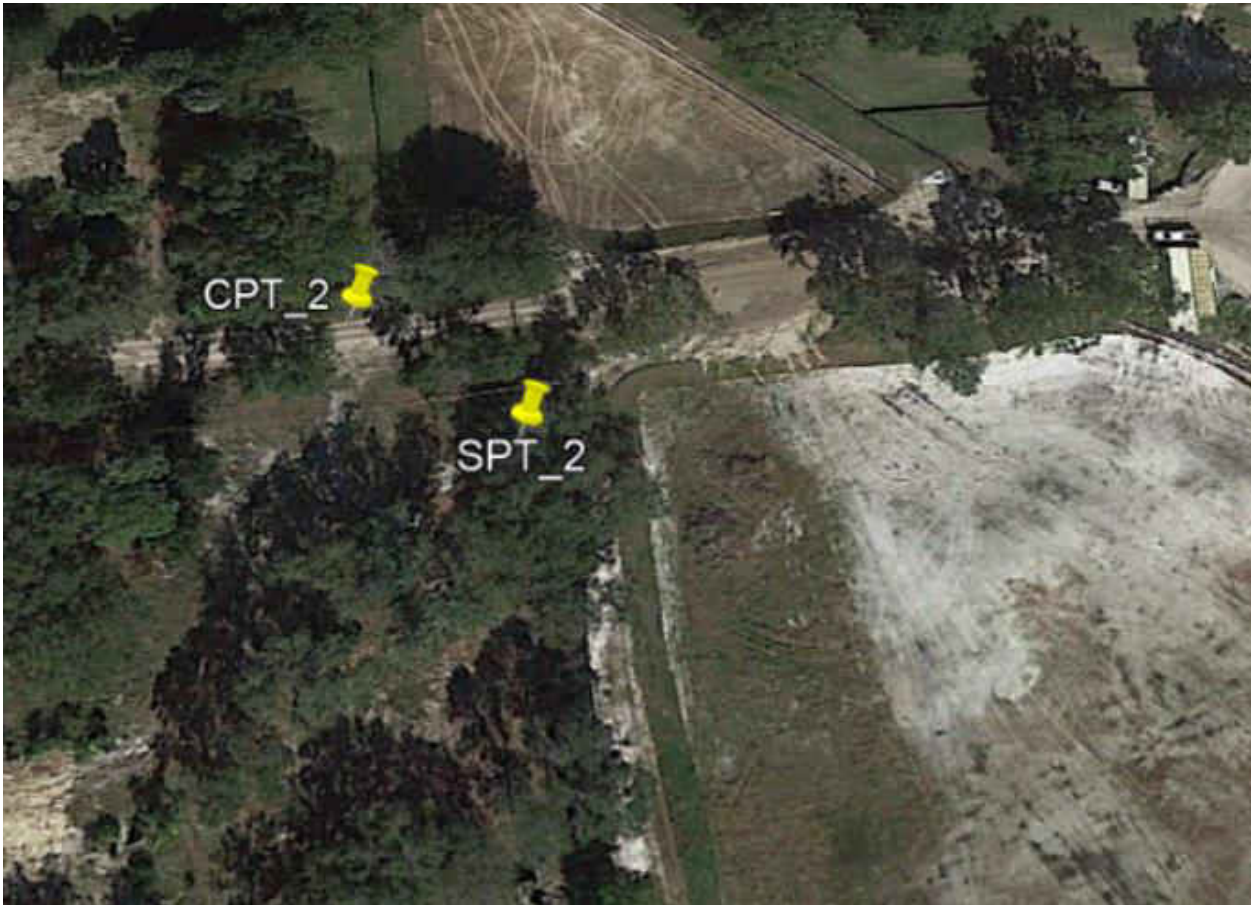


Figure 4-4: CPT and SPT Location (Example)

3. Next, the CPT and SPT profiles are compared to ensure there is not much variability in the soil strata between borings. As seen in figure 3-3, the majority of the soil profiles from each test agree and both indicate clayey soils at the Shelby tube depth. However, the top of Shelby tube depth is a transition zone, so the data point was taken to be in the middle to lower portion of the Shelby tube requiring a small shift down of about 3 inches. This matching still provides a high degree of reliability that the selected CPT output depth represents the oedometer test sample.

In the scenario in which the profile has been offset due to fill or simply different soil stratum thicknesses, judgment must be used to best match these profiles and select the representative

CPT depth. However, the process of moving CPT depths has potential to create bias in the results. This shifting of depths is done when the matching soil type in the CPT profile is very close to the SPT soil type and the current matching is clearly incorrect. For example, if the SPT indicated a weight of hammer blow count and a fat clay soil description at oedometer depth but the CPT indicates a dense granular material with a very soft cohesive material two feet below, it may be acceptable to shift the CPT representative depth up to a few feet to capture that clay layer. The data point fails this check if it is not clear where the matching soil layer is located or too much movement from the Shelby tube depth is required.

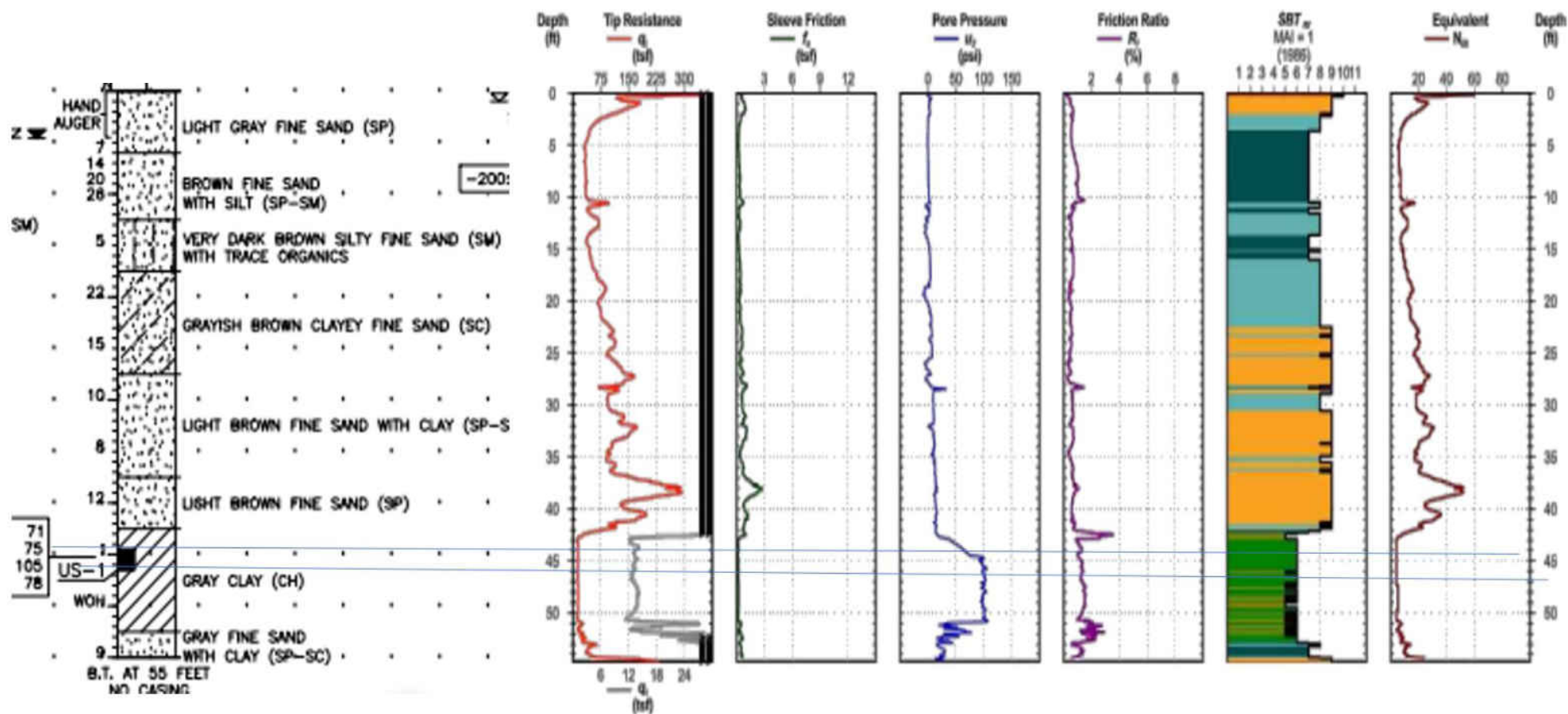


Figure 4-5: SPT and CPT Profile Matching (Example)

4. The final step performed before adding the point to the data base is to analyze the oedometer test results. This involves selecting the recompression and compression indices, as well as checking the overall quality of the test. The first check is that the sample represents the soil type labeled in the SPT profile log. If not, any adjustments made to the CPT depth to match the Oedometer sample depth may have been presumptuous and incorrect, requiring the previous step to be redone. This test always depicts a gentle slope defined as the recompression index, a preconsolidation pressure, and a steep slope defined as the compression index, as well as displayed hysteresis behavior during unloading and reloading cycles. These responses, as well as the high moisture content, plasticity index, percent passing and void ratio, confirm that the sample matches the SPT profile as a high plasticity clay (CH).

EPTH: 44.0 - 46.0 ft, m
 LAB IDENTIFICATION NO.: 186444/1120R
 IATE SAMPLE RECEIVED: 11/06/18 SAMPLE DESCRIPTION.: Gray fat clay with sand
 IATE SAMPLE SET-UP: 11/09/18 (CH), friable
 IATE REPORTED: 01/22/19

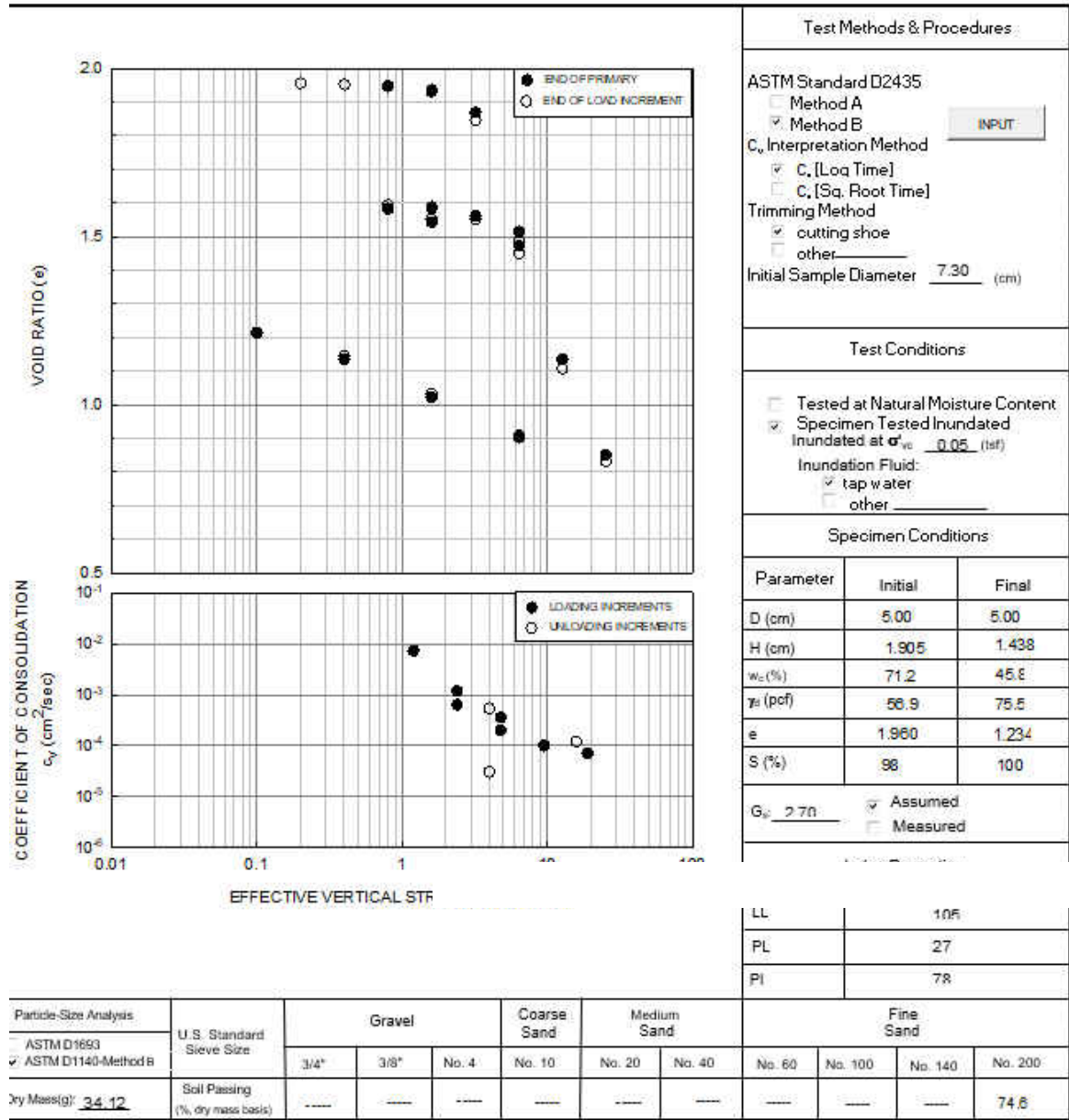


Figure 4-6: Oedometer Test Results (Example)

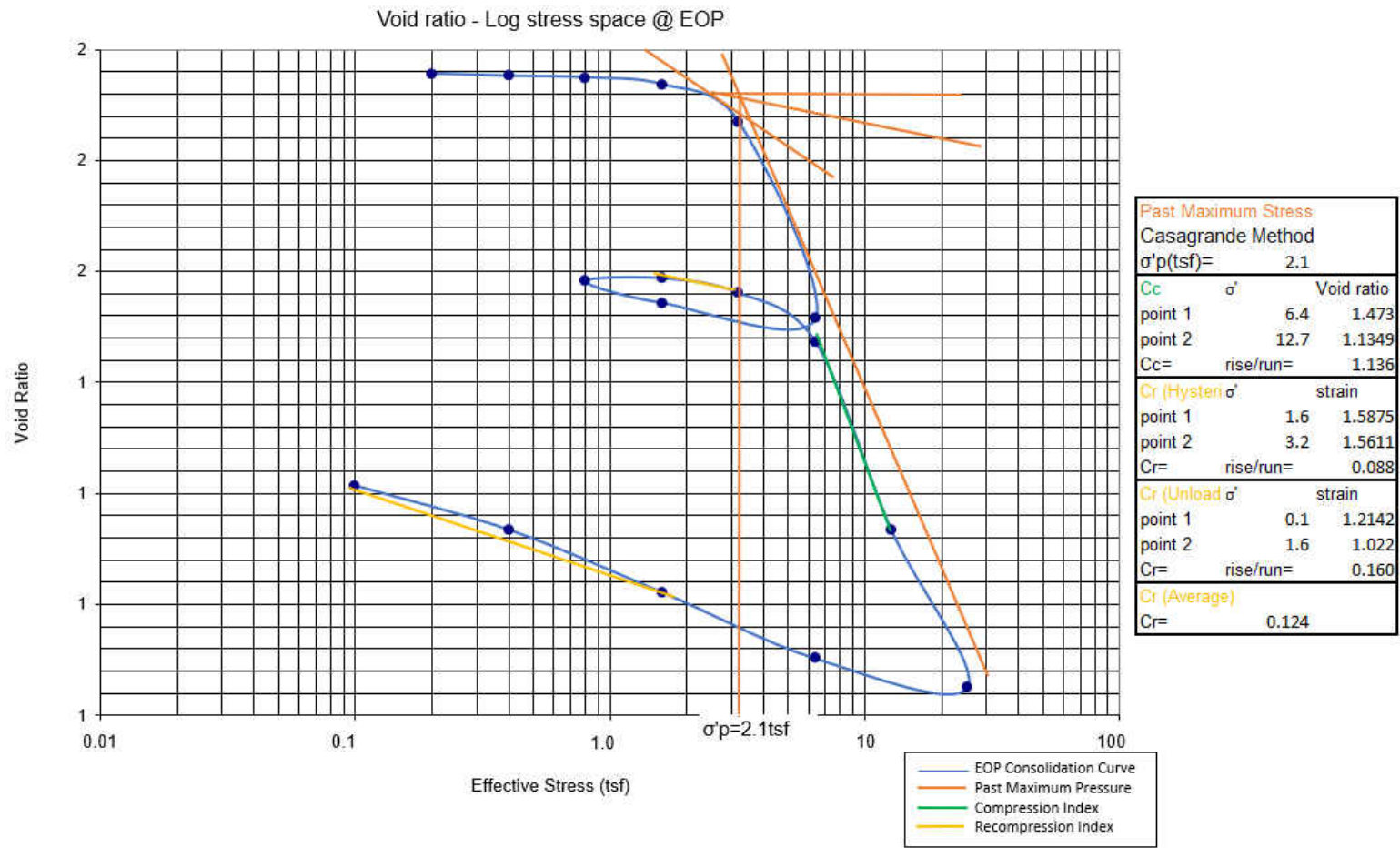


Figure 4-7: Recreated Test Results for Calculations

Next, the degree of sample disturbance is checked using the quality rating technique shown in table 4-1. This is done by checking the amount of volume change (in terms of strain or void ratio) that occurs between the start of loading and the in-situ effective stress conditions. In order to be enter into this table, the in-situ effective stress must be calculated. This is done by estimating the unit weight of each soil layer using soil type and number of blows from the SPT (correlations found in table 4-2 and 4-3) to calculate the total stress then subtracting the hydrostatic pressure to obtain the effective stress. The quality rating table also considers over consolidation ratio (OCR), therefore the past maximum pressure must be determined. This was done by the Casagrande Method as this charts range allows for a crude estimation. The casagrande method is a simple visual method with a relatively low degree of accuracy, however, since the preconsolidation pressure is only being used to check sample quaility this method is acceptable. This sample has an OCR of 1.6, effective stress of 1.35 tsf, and a void ratio at the effective stress of approximately 1.945, indicating an excellent quality sample with minimal sample disturbance. This research requires high quality data as the purpose is to estimate compression indices. For this reason any data point with a quality rating less than poor (Iunne) or D (Terizaghi) from Table 4-1 will be removed.

Table 4-1: Oedometer Test Quality Rating

Terzaghi et al. (1996)		Lunne et al. (1997a)		
ϵ_{v0} (%)	SQD	$\frac{\Delta e}{e_0}$ OCR = 1-2	$\frac{\Delta e}{e_0}$ OCR = 2-4	Rating
<1	A	<0.04	<0.03	Very Good to excellent
1-2	B	0.04-0.07	0.03-0.05	Good to fair
2-4	C	0.07-0.14	0.05-0.10	Poor
4-8	D	>0.14	>0.10	Very poor
>8	E			

Table 4-2: Values of Unit Weight of granular soils base on the SPT number

SPT Penetration, N-Value (blows/ foot)	γ (lb/ft ³)
< 4	70 - 100
4 to 10	90 - 115
10 to 30	110 - 130
30 to 50	110 - 140
>50	130 - 150

Table 4-3: Values of Unit Weight of cohesive soils base on the SPT number

SPT Penetration, N-Value (blows/ foot)	γ_{sat} (lb/ft ³)
< 4	100 - 120
4 to 8	110 - 130
8 to 32	120 - 140

- At this step the data point has either been accepted or rejected. Due to the fact that there are not many data points in this data base, attempts are made to recover filtered points without creating bias, and if that is not possible they are disposed of. Once the data base has enough reliable points, the analysis begins. The complete data base and all accepted data points can be found in Appendix I.

4.2.4 Analysis

The analysis of compressibility and CPT were performed from the data base described in section 3.2. The recompression and compression indices were each plotted against tip resistance (q_c), corrected tip resistance (q_t), sleeve friction (f_s), pore pressure (u_2), ratio of pore pressures (u_N), pore pressure ratio (B_q), friction ratio (R_f), normalized friction ratio (f_r), Net pore pressure (Δu), and the soil behavior type index (I_c). In summary, the compression indices will be plotted against raw and corrected outputs as well as calculated parameters. A brief explanation and the equations of each parameter are found below.

$$q_t = q_c + u(1 - \alpha) \quad (17)$$

$$R_f = \left(\frac{f_s}{q_t} \right) \times 100\% \quad (18)$$

$$R_f^{-1} = \frac{q_t}{f_s} \quad (19)$$

$$\sigma_v = \sigma_z \quad (20)$$

$$u_o = \gamma_w(z - z_w) \quad (21)$$

$$\sigma'_v = \sigma_v - u_o \quad (22)$$

$$Q_t = \left(\frac{q_t - \sigma_v}{\sigma'_v} \right) \quad (23)$$

$$F_r = \left(\frac{f_s}{q_t - \sigma_v} \right) \times 100\% \quad (24)$$

$$B_q = \frac{u - u_o}{q_t - \sigma_v} \quad (25)$$

$$I_c = ((3.47 - \log Q_t)^2 + (\log F_r + 1.22)^2)^{.5} \quad (26)$$

$$u_N = \frac{u_2}{u_o} \quad (27)$$

$$\Delta u = u_2 - u_o \quad (28)$$

Water pressure acts on the shoulder behind the cone and on the ends of the friction sleeve. For this reason, in soft clays and silts, the recorded tip resistance must be corrected for pore water pressures acting on the cone, a parameter referred to as corrected cone resistance, q_t (Robertson, P. K.,

& Robertson, K. L. (2006)). The ratio of pore pressures, U_N , was created for this research to give relativity to the pore pressure readings by making a ratio of the excess pressure reading and hydrostatic water pressure. The net pore pressure, Δu , is the measured pore pressure minus the in-situ hydrostatic water pressure, indicating the excess pore water pressure developed. The pore pressure ratio, B_q , is the ratio of net pore pressure to net cone resistance and is typically used to define the soil type. The friction ratio, R_f , is the ratio of sleeve friction to the corrected tip resistance expressed as a percentage, which is useful for interpreting soil type and is typically low in sands and high in clays. The inverse friction ratio is the ratio of corrected tip resistance to sleeve friction. The soil behavior type index, I_c , defines the radius of circles that represent the boundaries of SBTn zones as a function of normalized cone penetration resistance, Q_t , and normalized friction ratio, F_r (Robertson, P. K., & Robertson, K. L. (2006)).

The regression analysis will be performed utilizing each parameter to determine the best correlation. The only parameter not previously documented is the Ratio of Pore Pressures. This parameter was added to narrow down the exact parameter responsible for creating a strong correlation, while combinations of parameters may make it unclear and difficult to interpret. Fortunately, all parameters meet this standard by having corrected or normalized form which will make interpretation and determination of influential parameters distinct. Each chart will then be analyzed and displayed in section 4.3.1. The strongest correlations will be discussed and presented in section 4.3.2. The model with the strongest correlation and theoretical justification will be recommended in section 4.3.3.

4.3 Results

The goal of this section is to recommend a model to estimate recompression and compression indices from CPT parameters. This chapter follows an elimination approach to achieve this goal by first reviewing all correlations (Appendix B), then presenting and discussing the strongest correlations (section 4.3.1), and finally recommending the strongest model (section 4.3.2). Table 4-4 lists the equation for the line of best fit and the associated R^2 and RMSE values for strong correlations. Table 4-5 lists the equation and statistical parameters for the recommended model. The line of best fit and R^2 for every correlation can be found in the bottom right corner of each graph. It is also important to note that this chapter's analysis is performed in strain – stress space, unlike chapter 3 which is performed in void ratio – stress space.

4.3.1 Correlations from Charts

This section presents the strongest correlations between CPT parameters and Compressibility Indices. The correlations must have a R^2 greater than 0.01 and 0.1 for recompression and compression indices, respectively. All correlations may be found in Appendix B.

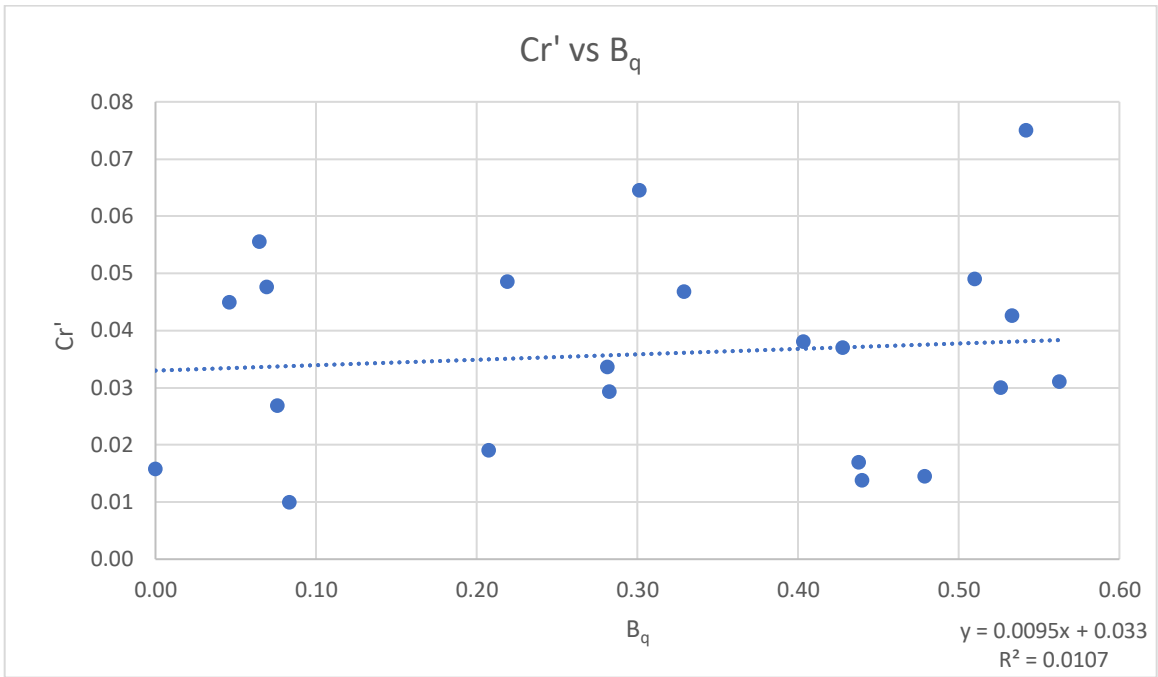


Figure 4-8: Recompression Index vs Pore Pressure Ratio, B_q

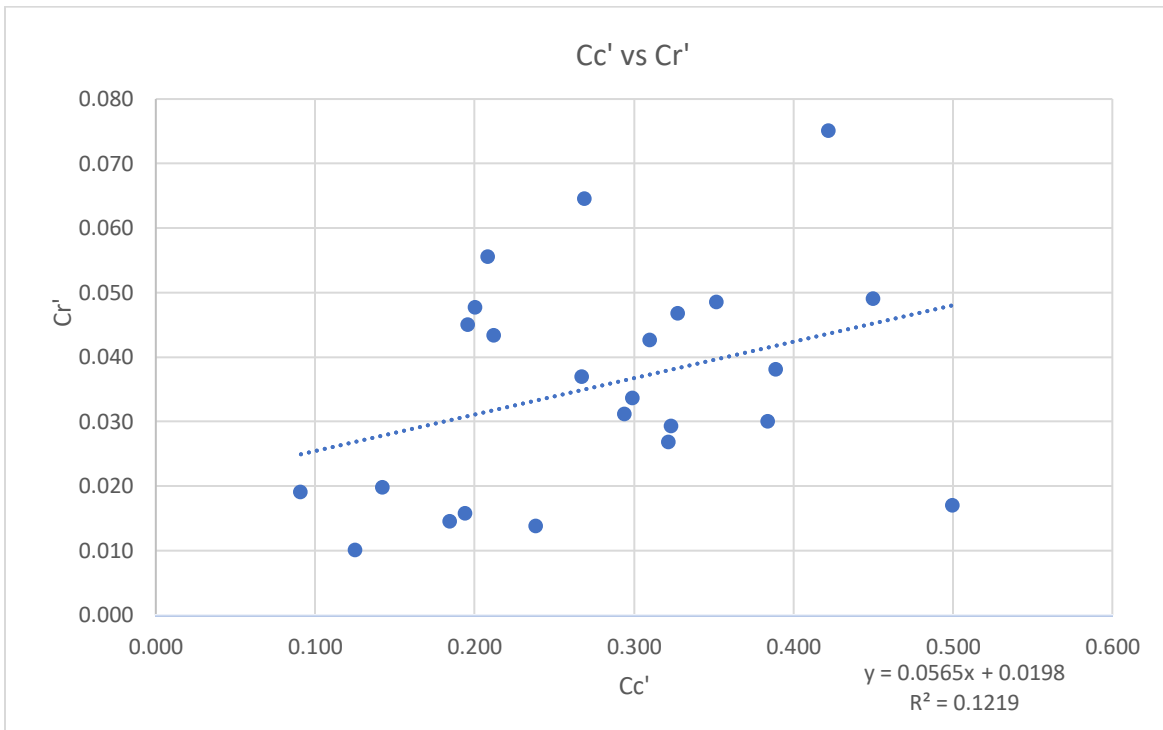


Figure 4-9: Compression Index vs Recompression Index

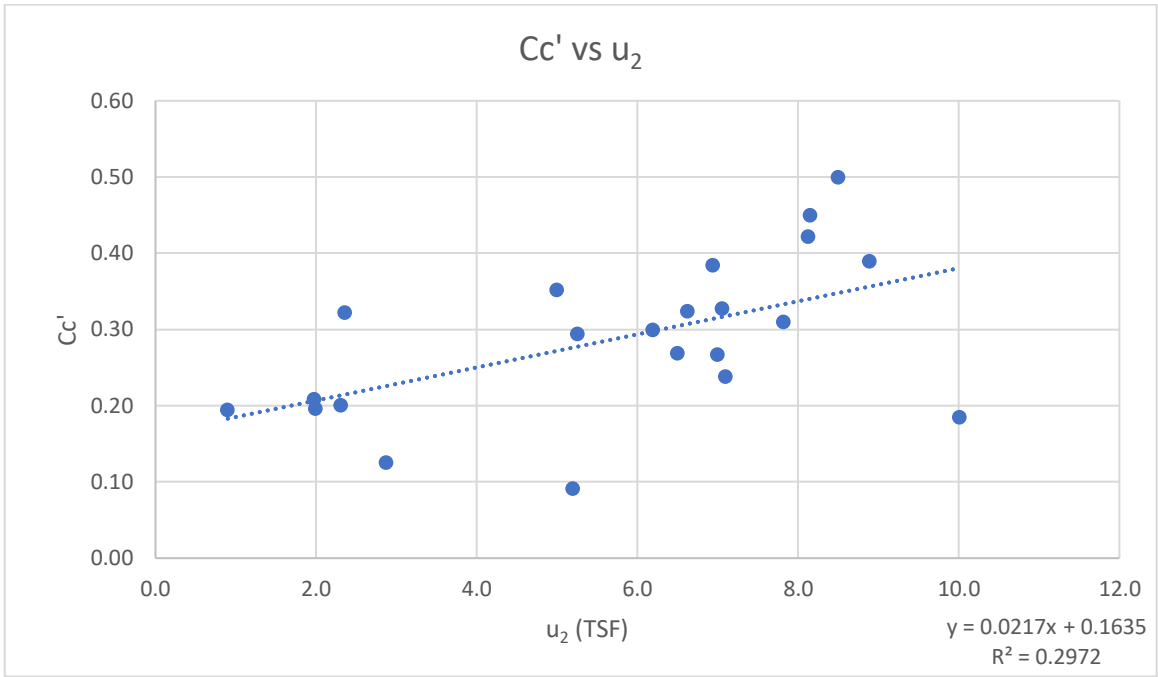


Figure 4-10: Compression Index vs Pore Pressure, u_2

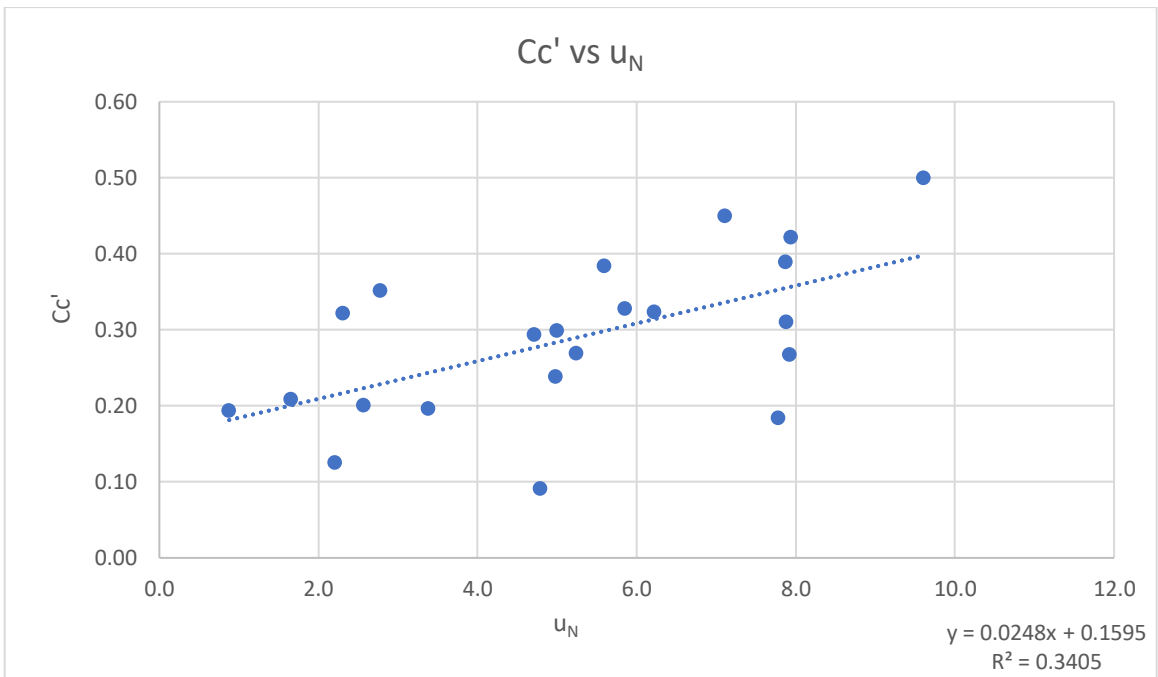


Figure 4-11: Compression Index vs Ratio of Pore Pressures, u_N

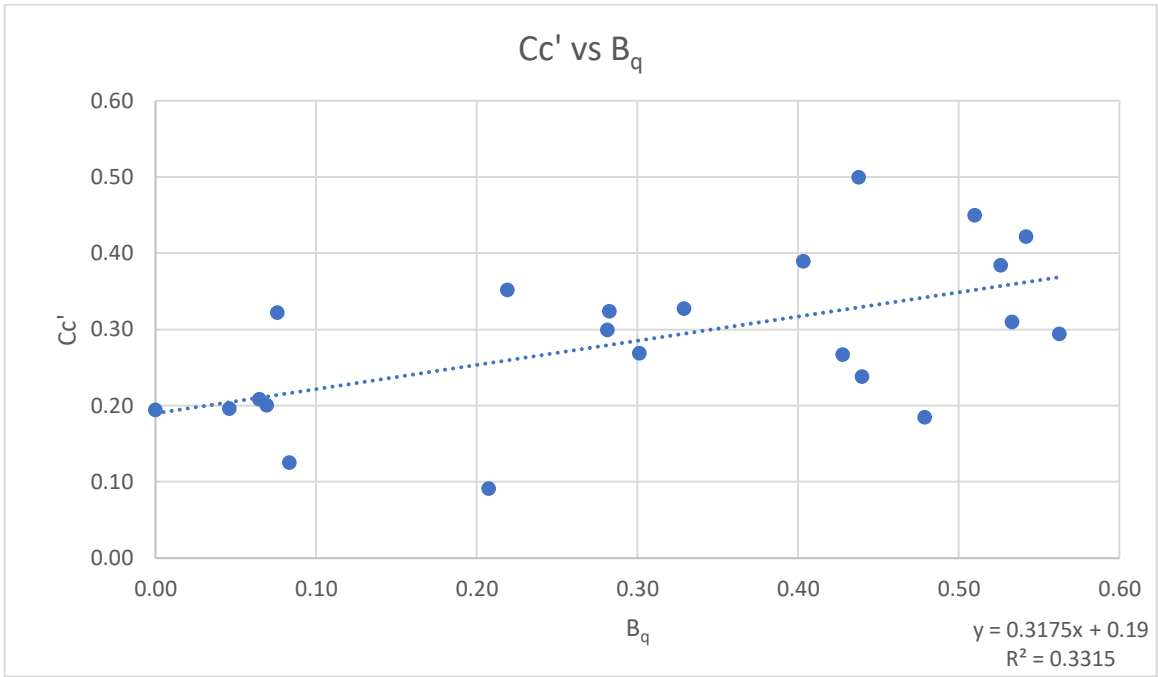


Figure 4-12: Compression Index vs Pore Pressure Ratio, B_q

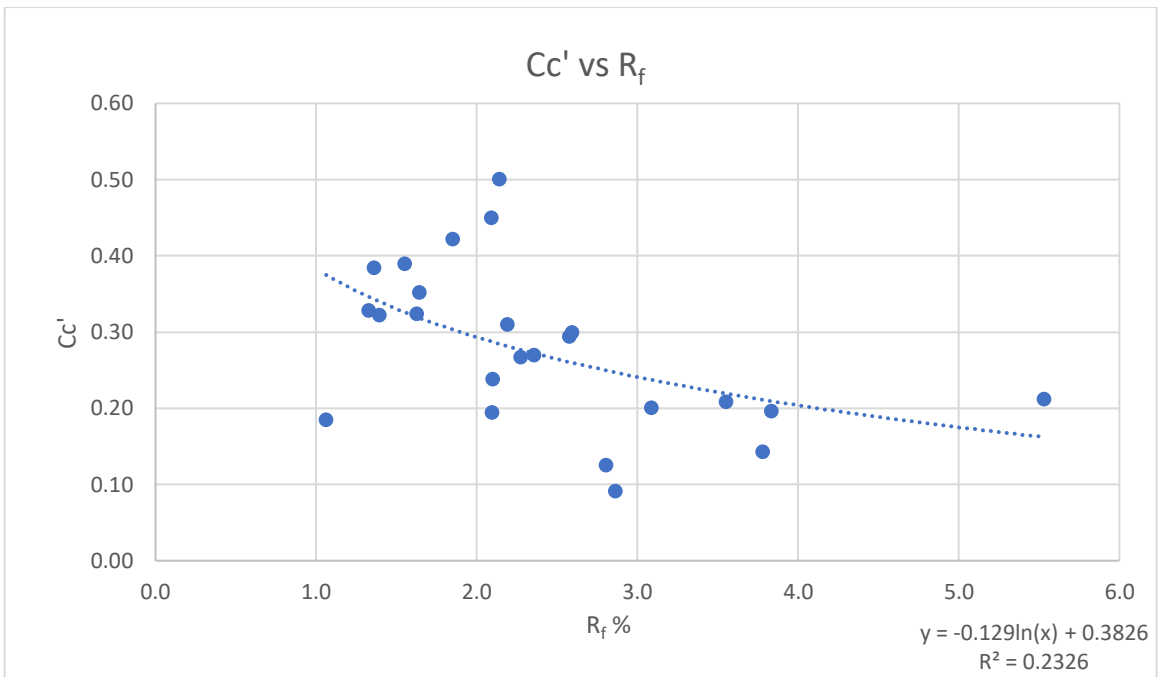


Figure 4-13: Compression Index vs Friction Ratio, R_f

Table 4-4: Summary of Results, CPT

Recompression Index	Equation	R²	RMSE
Pore Pressure Ratio	$Cr' = 0.0095(Bq) + 0.033$	0.011	0.017
Compression Index	$Cr' = 0.0565(Cc') + 0.0198$	0.122	0.018
Compression Index			
Pore Pressure	$Cc' = 0.0217(u_2) + 0.1635$	0.297	0.085
Ratio of Pore Pressures	$Cc' = 0.0248(u_N) + 0.1595$	0.341	0.083
Pore Pressure Ratio	$Cc' = 0.3175(Bq) + 0.190$	0.332	0.083
Friction Ratio	$Cc' = -0.129\ln(Rf) + 0.3826$	0.233	0.090

4.3.2 Recommended Model and Discussion

The findings of this study show relatively good correlations of the compression index to friction and pore pressure parameters. These findings will be condensed to avoid redundancy by defining all pore pressure correlations using only the Ratio of Pore Pressures (u_N) and all friction correlations using the Friction Ratio (R_f).

Of these correlations the ratio of pore pressures is the strongest. This relationship is positive, indicating as the ratio of excess pore water pressure (PWP) to hydrostatic PWP increases, the compressibility increases.

It was mentioned in the introduction that the pore pressure reading (u_2) is dependent on the rate of dissipation. In the extreme example, clays will dissipate pore pressure much slower than sands, which is why sands record hydrostatic pressures and clays record some net pore pressure. It is also understood that sands have a lower compressibility than clays. There are varying dissipation rates for clays as the drainage behavior is heavily influenced by stress history, sand content, and mineral type. The effects of each factors are further examined in figures 4-14 to 4-16. Figure 4-14 shows a strong positive correlation between percent finer and pore pressure. This indicates that the sand content decreases the pore pressures by increasing the drainage rate. Figure 4-15 shows a strong correlation between Plasticity index and pore pressure. This shows that as the colloidal properties become more pronounced that soil's dissipation rate decreases. Figure 4-16 shows a weak positive correlation to preconsolidation pressure. This parameter is influential for stress-strain response; however, the mechanism of the CPT is that the penetrometer is quickly failing the soil not slowly straining it. Due to this violent loading scenario, the preconsolidation pressure is likely quickly surpassed and does not heavily impact the CPT outputs. This is not to say the CPT cannot estimate preconsolidation pressure but

instead states the primary soil behavior captured by the CPT outputs are not controlled by the soil's preconsolidation pressure. Based on these figures, it can be argued that the positive correlation between pore pressure and compressibility is owed to the low compressibility and quick dissipation rates of the sand content and the low intensity of colloidal properties present in the soil. The soil's lowered compressibility from these factors is also due to the subsequently increased density and decreased shrinking and swelling potential. Following this logic, the positive trend between compressibility and ratio of pore pressures, shown in Figure 4-11, is justifiable.

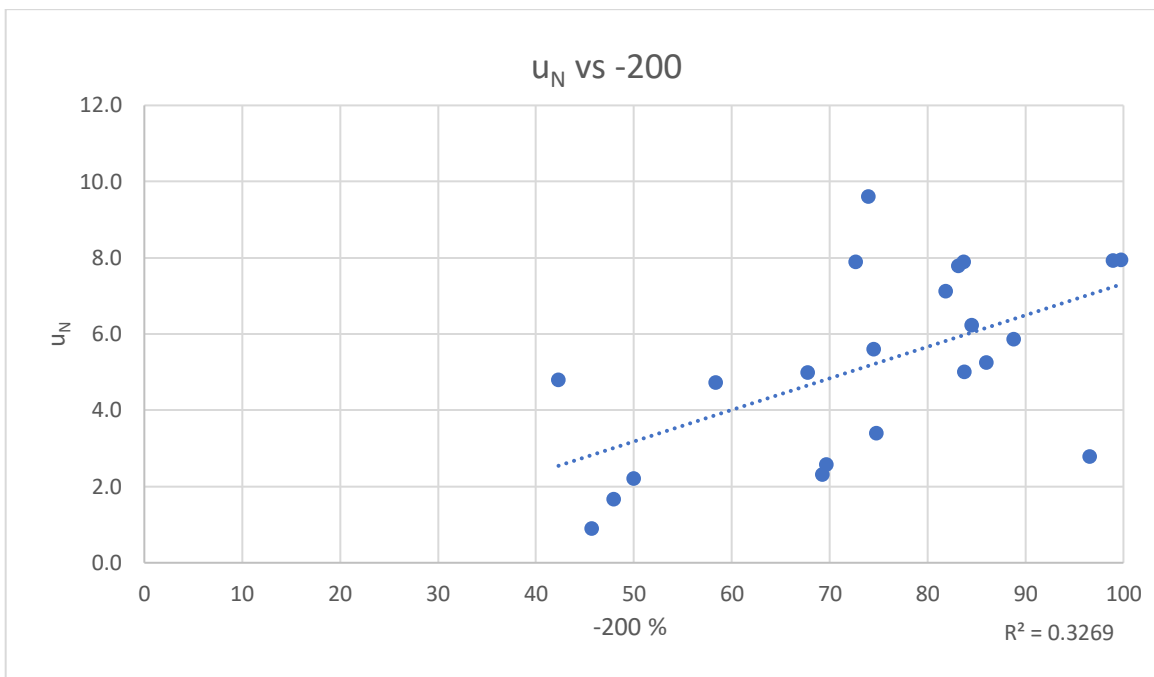


Figure 4-14: Ratio of Pore Pressures vs Percent Finer

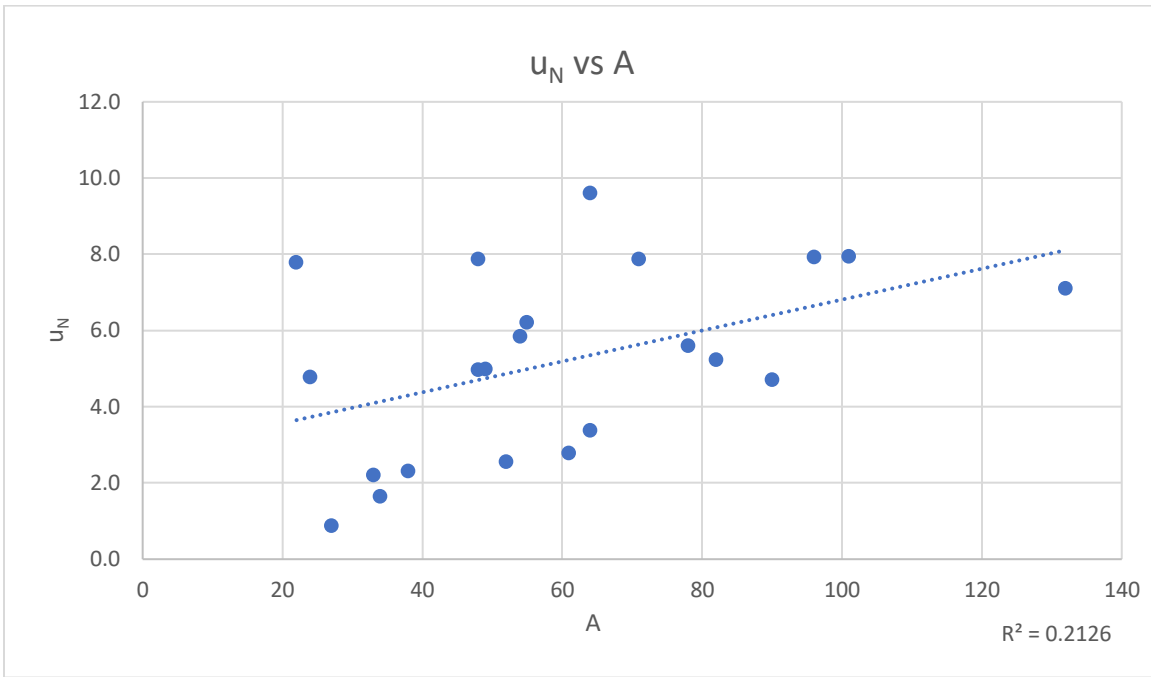


Figure 4-15: Ratio of Pore Pressures vs Activity, A

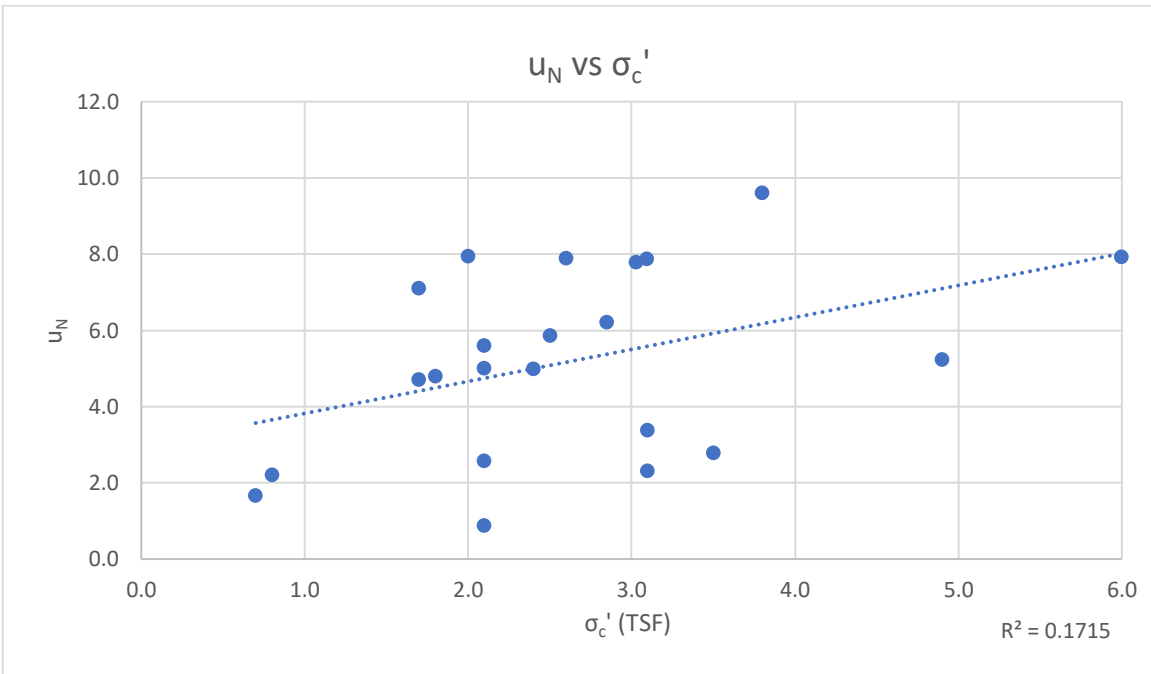


Figure 4-16: Ratio of Pore Pressures vs Preconsolidation Pressure, σ_c¹

The correlation between Friction ratio and compressibility is negative and relatively strong. This means that as the ratio of sleeve friction to tip resistance decreases, the compressibility increases. In order to justify this model, the correlation of sleeve friction and tip resistance to compressibility must first be discussed. Sleeve friction shows a relatively strong negative correlation and tip resistance shows a weak correlation to compressibility. These trends indicate that as strength decreases, the compressibility increases. Sleeve friction correlations will dominate the friction ratio correlations. Therefore, as sleeve friction increases, the friction ratio will increase, and the compressibility will decrease.

This above justification is relatively weak as it relies on an empirical justification. The CPT mechanism would indicate that high friction ratio is an indicator of a soft squeezing clay. However, the trend line indicates the opposite of what one would expect. This indicates the soil type being analyzed is not a squeezing or swelling clay and this common reasoning is not applicable. A justification similar to the ratio of pore pressures is attempted in Figures 4-17 to 4-19 but it is unclear which soil properties are dominating the friction ratio reading. For this reason, the above empirical justification will be utilized.

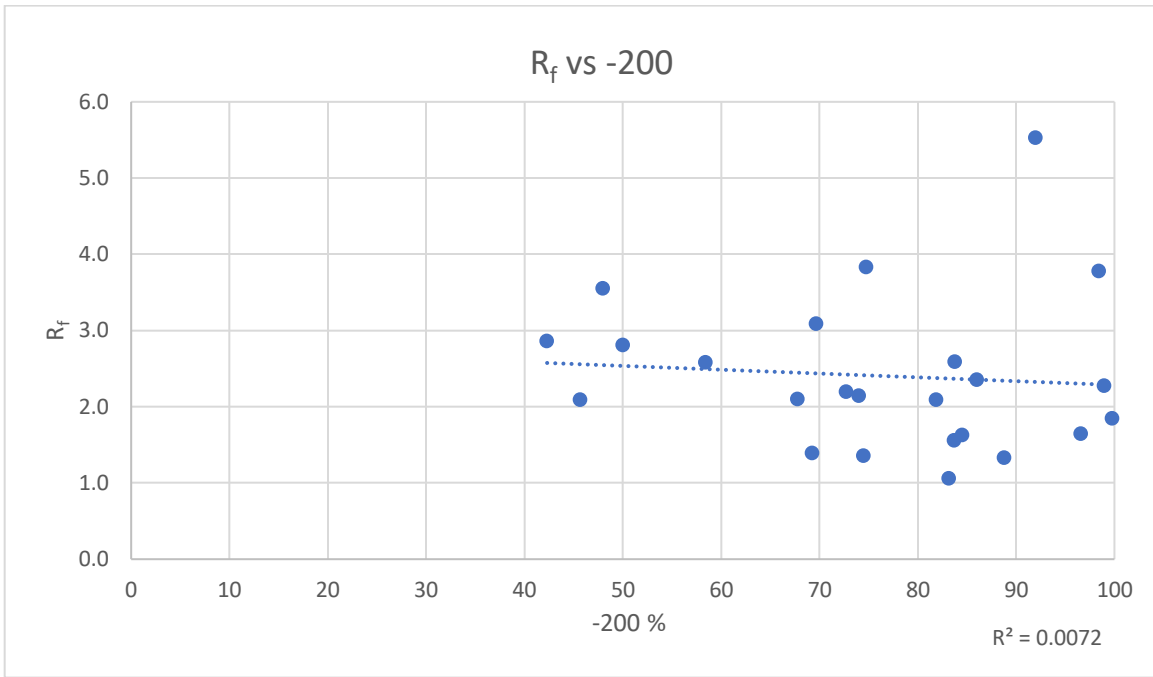


Figure 4-17: Friction Ratio vs Percent Finer

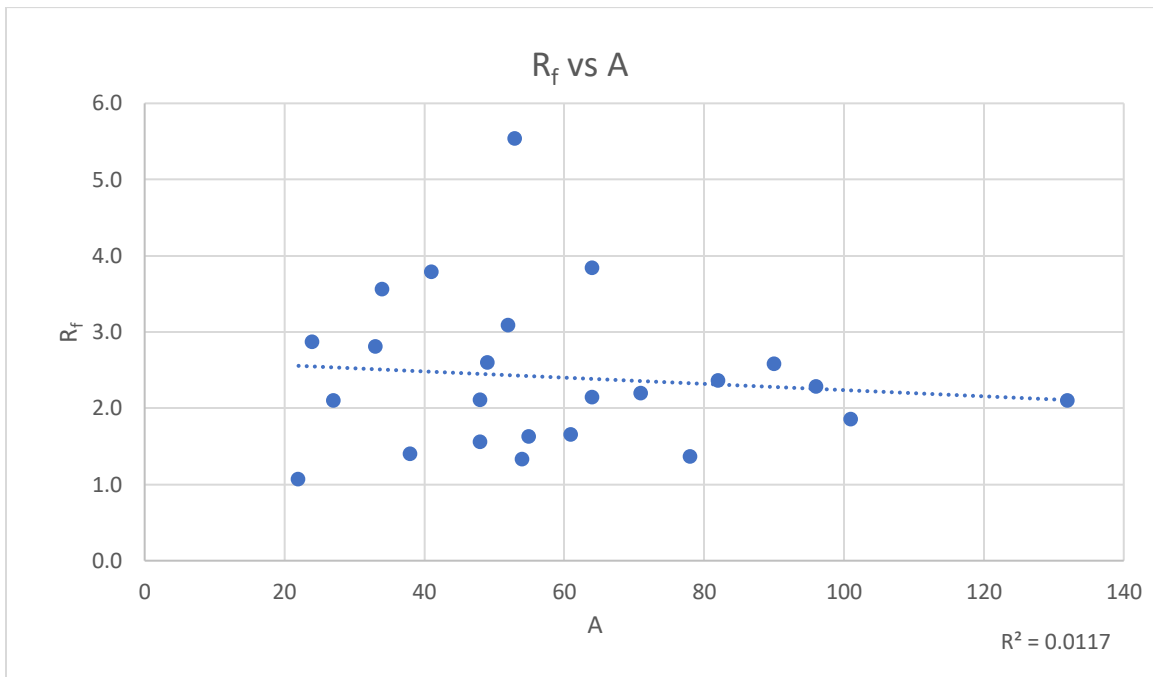


Figure 4-18: Friction Ratio vs Plasticity index

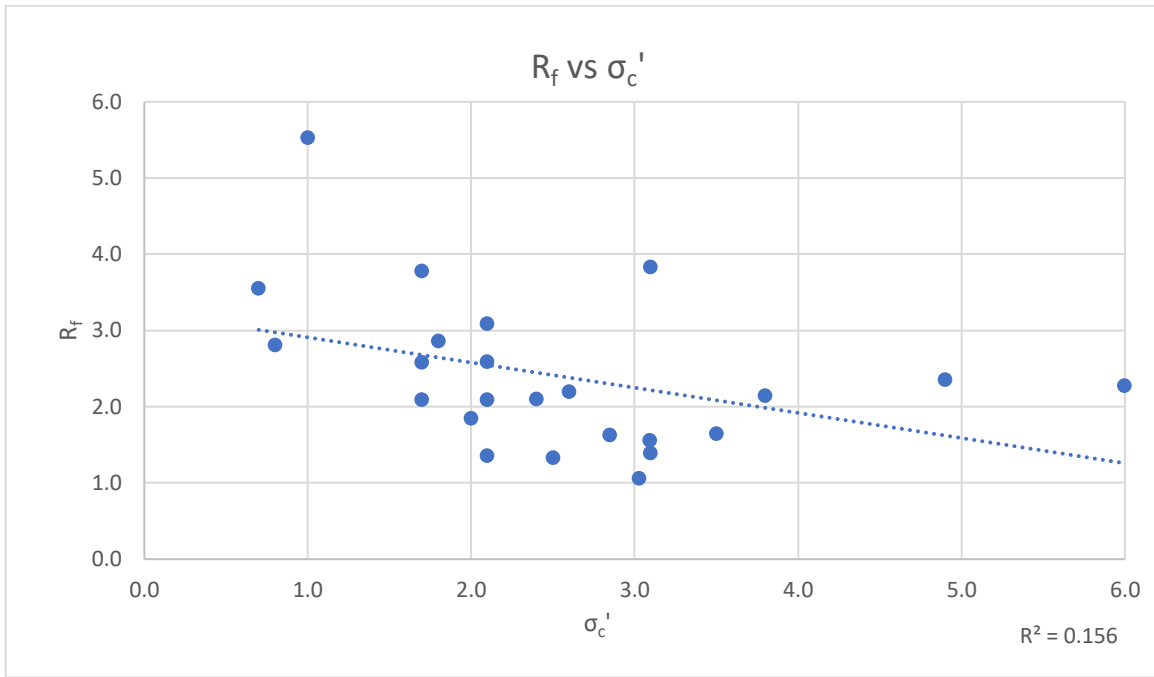


Figure 4-19: Friction Ratio vs Preconsolidation Pressure, σ_c'

Table 4-5: Recommended Models for CPT Parameters

Recompression Index	Equation	R ²	RMSE
Compression Index	$Cr' = 1/7 Cc'$	0	0.019
Compression Index			
Ratio of Pore Pressures	$Cc' = 0.0248(u_N) + 0.1595$	0.341	0.083

4.4 Conclusion

The recommended model to estimate the compressibility of fine-grained soils via CPT is shown below in Table 4.5. The model and discussion above demonstrate a relationship between CPT pore pressure reading and compression index exists. The correlations to the recompression index were poor, indicating the recompression index cannot be estimated from the CPT parameters. This finding is contradicting to the literature review which show elastic correlations from the CPT to compressibility for elastic behavior. The reason for this finding is that some error within the recompression index value exists within the data base. Another possible reason could be owed to the mechanism of the CPT failing the soil column in shear and quickly exceeding the preconsolidation pressure. This process would likely cause the CPT outputs to correlate better to the compression index than the recompression index. For this reason, the “one-fifth rule” discussed in the literature review and utilized in chapter 3 will also be utilized in this chapter. A refined ratio for the CPT data base is recommended in Table 4-5.

These findings indicate it is possible to create a continuous compressibility profile from a commonly utilized field test. However, the data base would have to be expanded and more rigorous filters applied in order to produce any reliable models for use in practice. The purpose of the filter applied in the following section is to support the findings of this chapter and determine the effectiveness of the CPT on soils at varying levels of index properties.

CHAPTER 5

CONE PENETRATION TEST BASED CORRELATIONS – DIVIDED DATA BASE FOR ACTIVITY AND MOISTURE CONTENT

5.1 Introduction

Sangleret (1972) divided the NIASL data base into soil type groups by assigning an α value for different ranges of I_c . The divided data base performed well, producing accurate and conservative estimations of settlement when compared to actual site settlement. However, the studies undivided data base (Figure 2-2) performed poorly, with no model officially recommended. This finding implies that no generic correlation exists, and that in order to suggest a model the data base must be divided into categories of soil behavior.

The objective of this chapter is to recommend a model to estimate the compressibility of fine-grained cohesive soils in Central Florida via the Cone Penetration Test for a specific soil category. This will be achieved by filtering out samples that do not meet the limits defined for each category. These categories will be analyzed separately and consist of relatively high activity soil and relatively high moisture content soils. The purpose of this approach is to filter the data base into groups of high degrees of influential index properties to show the effects these parameters have on the CPT correlations. This will also allow the user to select a more appropriate model.

Chapter 3 demonstrated that the level of activity (A) and moisture content (w) influence the soil's compressibility and Chapter 4 showed that soil compressibility can be estimated via Cone Penetration Testing. It can then be logically assumed that varying degrees of activity and moisture content will affect the CPT estimations. This conclusion is also supported in *The Static Penetrometer and the Prediction of Settlements* by Sangleret (1972).

Looking at high moisture content soils, this category is more likely to correlate well with pore pressure because high moisture content soils are less granular. The lower sand content implies a slower dissipation rate and higher pore pressure. This logic is supported by the positive correlation between moisture content and pore pressure in Figure 5-1. The effect of a high pore pressure on the correlation is that the parameter will carry a greater influence on the correlation and the error in the reading will be less pronounced. It is not expected that sleeve friction correlates well with high moisture content soils. This is assumed because as moisture content increases, the resistance to shearing decreases as water has no shear strength as seen in Figure 5-2. It may also be assumed that the higher moisture content soils are more likely to squeeze and therefore increase the sleeve friction. However, this mechanism has been ruled out as the soils in the data base did not demonstrate squeezing or swelling behavior.

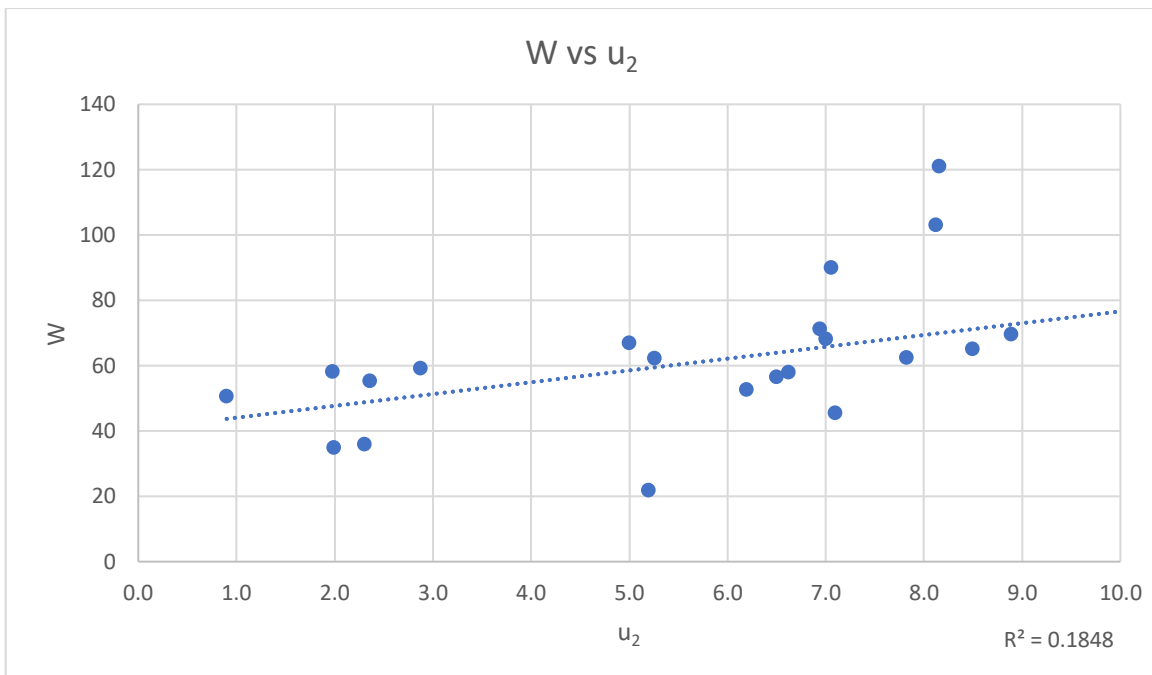


Figure 5-1: Moisture Content vs Pore Pressure, u_2

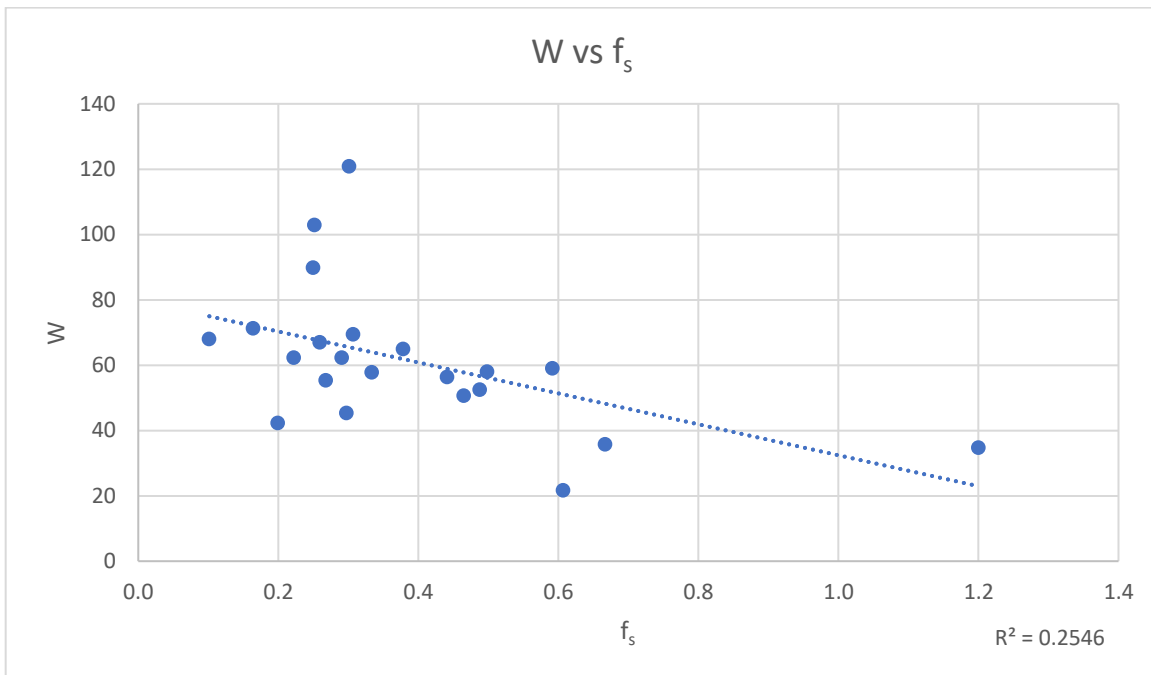


Figure 5-2: Moisture Content vs Sleeve Friction, f_s

Activity is the ratio of plasticity index and percent finer. The plasticity index indicates the range between liquid and solid consistencies. In more relative words, the plasticity index indicates the soils ability to change volume with varying moisture contents. Percent finer represents the number of fines present in the soil mixture. These fines could be kaolinite, illite, montmorillonite, and/or silt. Therefore, the percent finer, when used alone, does not quantify the soil behavior. This implied test is most valuable when used in conjunction with more testing. In the case for the Activity parameter, the plasticity index is combined with the percent finer to describe the soils mineralogy (Skempton 1988). Table 5-1 from Skempton (1988) states that soils with activity less than 0.75 are inactive and predominately kaolinite and illite. Clays with activity from 0.75 to 1.25 are normal and predominately illite. Clays greater than 1.25 are active illite and clays greater than 2 are active montmorillonite.

From Skempton's findings and an understanding of the plasticity and percent finer tests it is assumed that Activity will be a strong indicator of soil behavior. Soils with relatively high Activity ($A > 0.5$) will have a strong correlation to pore pressure and friction parameters. This hypothesis is made because high activity soils are likely to squeeze and develop higher pore pressures, making the sleeve friction and pore pressure readings more pronounced. Neither of these hypotheses are supported through correlation such as the ones utilized within the moisture content discussion. Since Activity has not been seen to correlate well with any parameters within this study, the theoretical hypothesis will be accepted over the graphical hypothesis.

The filters applied to the data base were briefly mentioned above but will formally be summarized within this paragraph. Samples with activity less than 0.5 are removed. As mentioned above the ideal filter would be for soils with activity less than 0.75, however, the limited data points made this filter impractical. This applied limit of 0.5 resulted in the removal of only two data points. For the next analysis samples with moisture content less than 40% are removed, resulting in the removal of three data points. The method used to select the limits is discussed in the following section.

Table 5-1: Correlation of Activity and the Mineralogy and Geology of Clay from Skempton 1984

Group	Range of Activity	Location	Geology	Mineralogy of Clay Fraction		Activity	Authority
				Major	Minor		
Inactive 1	less than 0.5	St. Thuribe, near Quebec	Post Glacial marine or estuarine, leached	Q	Mi	0.33	Peck et al., Grim
		Cornwall, England	Formed in situ by pneumatolysis (kaolin)	k	—	0.39	Northey
		Chicago, U.S.A.	Late Glacial, lacustrine	---	---	0.41	Rutledge
		Boston, U.S.A.	Late Glacial, marine	---	---	0.42	Taylor
		Horten, Norway	Post Glacial, marine, leached	Q Mi i	mo k	0.42	Hansen, Northey, Grim
Inactive 2	0.5 to 0.75	Detroit, U.S.A.	Late Glacial, lacustrine	Mi i C	Q mo	0.49	Peck, Grim
		Wrexham, Wales	Late Glacial, probably lacustrine	---	---	0.54	B.R.S.
		R. Lidan, Sweden	Post Glacial, probably as Horten	---	---	0.58	Cadling
		Weald (various sites), England	Weald Clay, Cretaceous, lacustrine	i k	vermiculite	0.63	B.R.S., A.O.R.G.
		Reading, England	Reading Clay, Eocene, fresh-water	---	---	0.72	B.R.S.
		Seagrove Bay, I.O.W., Engl.	Oligocene, fresh-water	---	---	0.73	Skempton
Normal 3	0.75 to 1.25	Grangemouth, Scotland	Late Glacial, Estuarine	---	---	0.74	Skempton
		Peterborough, England	Oxford Clay, Jurassic, marine	---	---	0.86	B.R.S.
		Gosport, England	Post Glacial, marine	i	h	0.88	Skempton, Nagelschmit
		Grundy County, Ill., U.S.A.	Upper Carboniferous (illite.)	i	—	0.90	Northey, Grim
		Aylesbury, England	Kimmeridge Clay, Jurassic, marine	---	---	0.93	B.R.S.
		London (various sites)	London Clay, Eocene, marine	i	k mo	0.95	Cooling, Skempton, Grim
		Various sites, S.E. England	Gault Clay, Cretaceous, marine	i k	mo	0.96	B.R.S., A.O.R.G.
		Norfolk Fens, England	Post Glacial, marine and estuarine	---	---	1.06	B.R.S.
		Vienna, Austria	Wiener Tegel, Miocene, marine	---	---	1.08	Hvorslev
		Klein-Belt, Denmark	Klein-Belt-Ton, Eocene, marine	---	---	1.18	Hvorslev
Active 4	1.25 to 2.0	Shellhaven, England	Post Glacial, organic and estuarine	i	k	1.33	Skempton, Grim
		La Guardia Airport, New York	Post Glacial, organic, marine	---	---	1.45	Harris et al.
		R. Shannon, Eire	Recent river alluvium, organic	---	---	1.5	B.R.S.
		Belfast, N. Ireland	Post Glacial, organic, estuarine	---	---	1.6	B.R.S.
		Chingford, England	Recent river alluvium, organic	---	---	1.7	B.R.S.
		Panama, Central America	Recent organic, marine	---	---	1.75	Casagrande
Active 5	more than 2.0	Mexico City	Bentonite Clay	mo	---	4.3	Marsal et al.
		Wyoming, U.S.A.	Bentonite	mo	—	6.3	Samuels, Northey

C = Calcite	h = Halloysite	} clay minerals	— negligible
Mi = Mica	i = Illite		---
Q = Quartz	k = Kaolinite		---
	mo = Montmorillonite		---

5.2 Methodology

The CPT data base described in detail within Chapter 4 will be utilized to recommend a model for soils with relatively high activity and for soils of high moisture content. The first step is to filter the data base. The limiting value was selected as the value which, when exceeded, begins to decrease the statistical reliability of the model. This process started at the 50th percentile and continued until the R² began to decrease. There was no bias in this approach as the points for each analysis followed the order of descending activity and moisture content, respectively. Once the data was filtered, the analysis performed in chapter 4, in which all CPT parameters were plotted against Compression and Recompression Indices in strain-stress space, was repeated. All parameters mentioned in Chapter 4 are checked to avoid the “interference” from soils with different behavior types. For example, a correlation may indicate a very low R² when all data points are used but a very high R² once separated into categories. Each correlation is displayed in section 5.1, with an interpretation and summary of models in section 5.3.2. The model with the strongest correlation and theoretical justification will be recommended in section 5.3.3.

5.3 Results

This section will present the correlations between CPT and Compressibility for soils of high activity and high moisture content. This section will follow an identical process as chapter 4 in which the strongest correlations are presented and discussed in section 5.3.1, and the best is interpreted and recommended in section 5.3.1. Again, this chapter will perform two analyses and recommend two models: one for soils of high activity and one for soils of high moisture content.

5.3.1 Correlations from Charts

This section presents the strongest correlations between CPT parameters and Compressibility Indices for the divided data base. Subsection 5.3.1.1 and 5.3.1.2 show the correlations when divided for high activity and high moisture content, respectively. The correlations must have a R^2 greater than 0.02 and 0.2 for recompression and compression indices. The equation and statistical parameters for each subsection are summarized in table 5.2 and 5.3. All correlations are presented in Appendix C.

5.3.1.1 Activity

This subsection includes the strong correlations between CPT parameters and compressibility indices for soil samples with activity greater than 0.5.

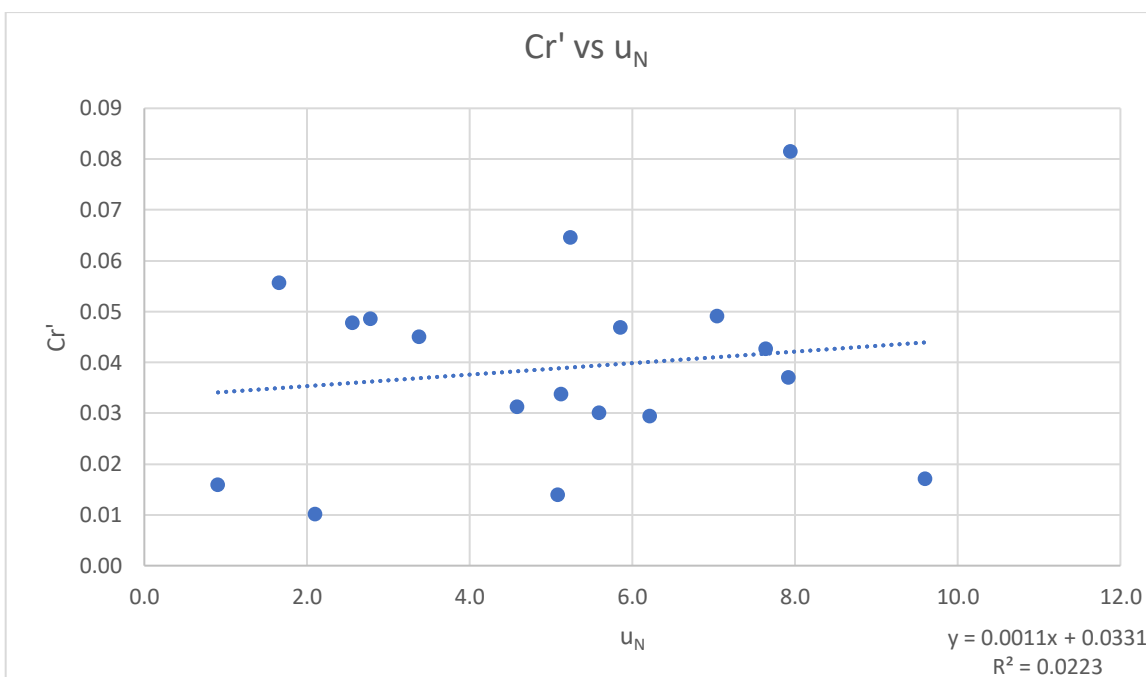


Figure 5-3: Recompression Index vs Ratio of Pore Pressures, u_N

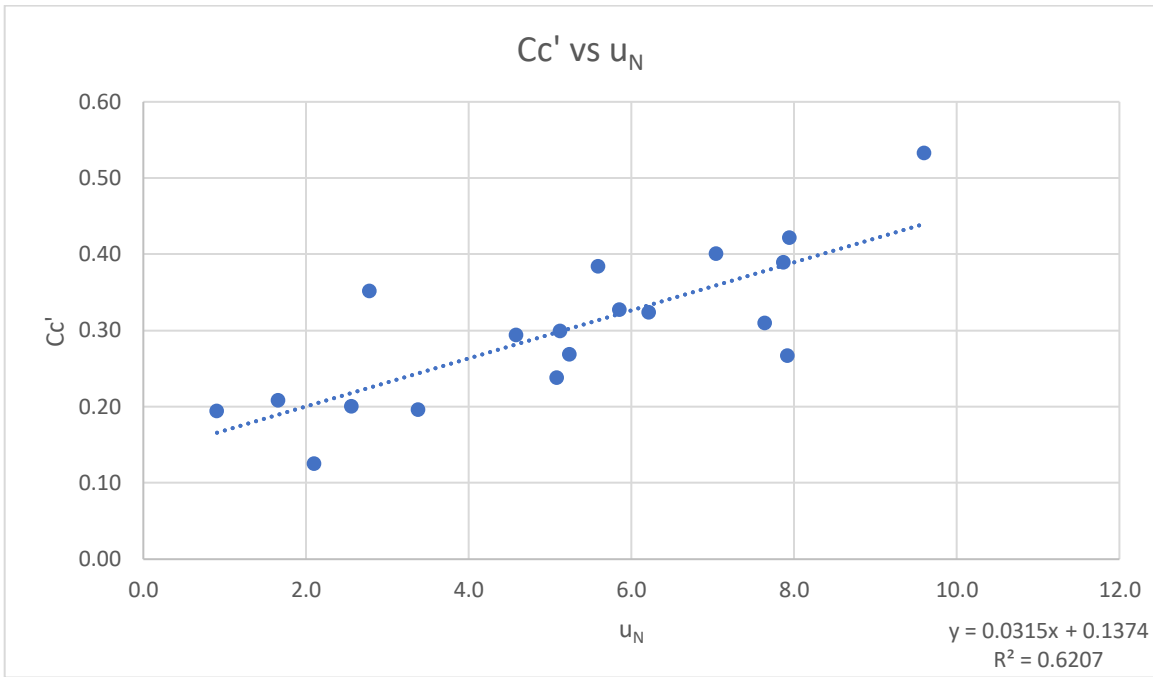


Figure 5-4: Compression Index vs Ratio of Pore Pressures, u_N

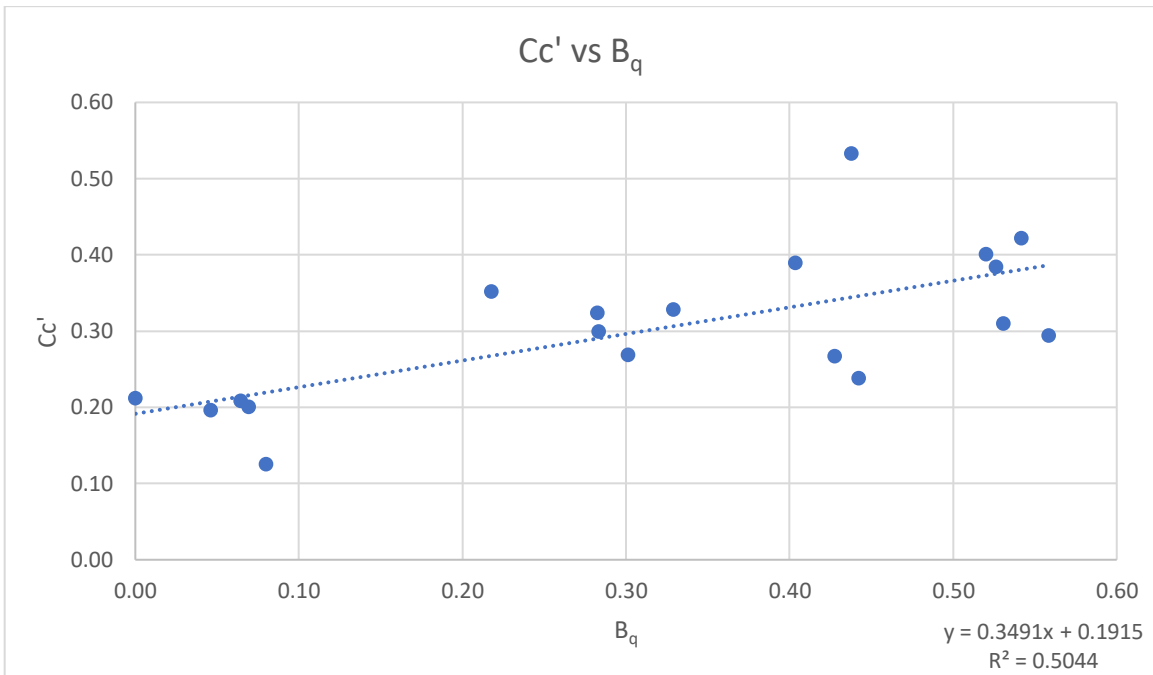


Figure 5-5: Compression Index vs Pore Pressure Ratio, B_q

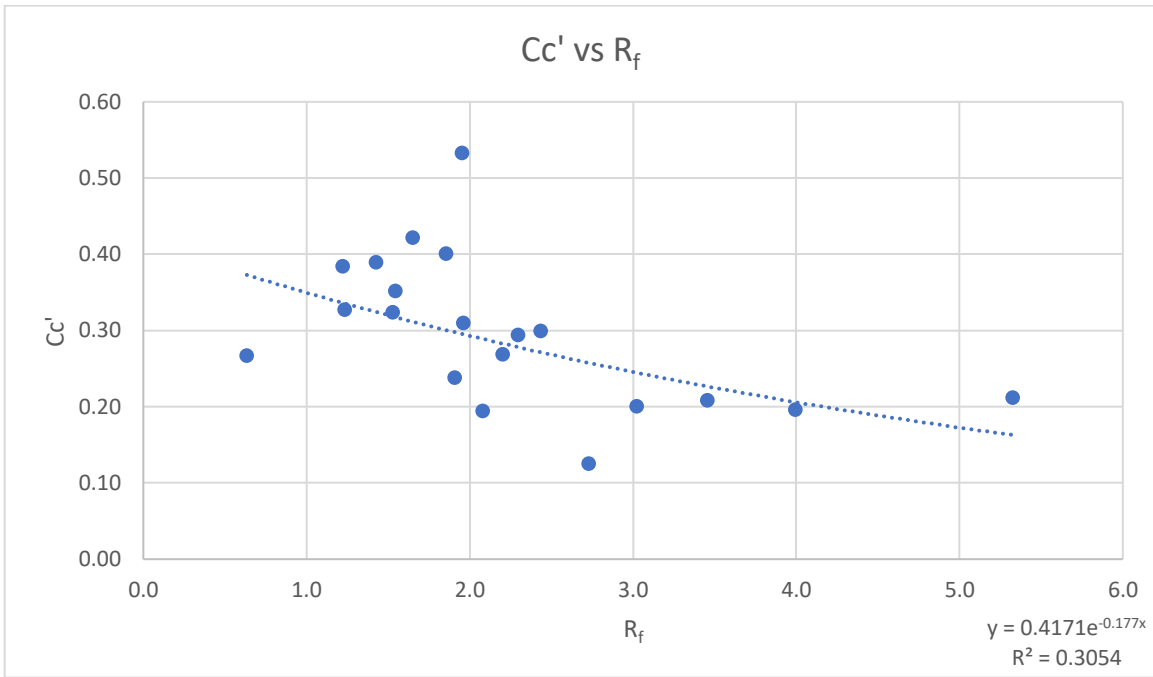


Figure 5-6: Compression Index vs Friction Ratio, R_f

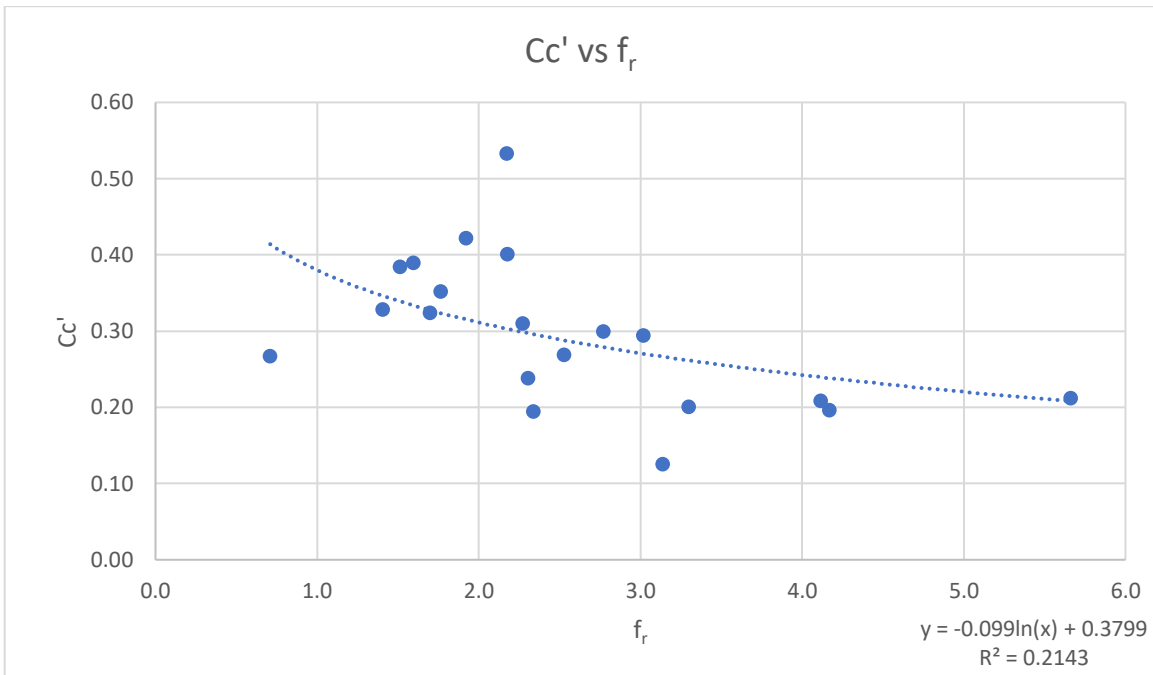


Figure 5-7: Compression Index vs Normalized Friction Ratio, f_r

Table 5-2: Summary of Results, Activity ($A > 0.5$)

Recompression Index	Equation	R ²	RMSE
Ratio of Pore Pressure	$Cr' = 0.0011(u_N) + 0.033$	0.022	0.017
Compression Index			
Ratio of Pore Pressure	$Cc' = 0.0315(u_N) + 0.137$	0.621	0.075
Pore Pressure Ratio	$Cc' = 0.3491(Bq) + 0.192$	0.504	0.079
Friction Ratio	$Cc' = 0.4171e^{-0.177(Rf)}$	0.305	0.086
Normalized Friction Ratio	$Cc' = -0.099\ln(Fr) + 0.380$	0.214	0.089

5.3.1.2 Moisture Content

This subsection includes the strong correlations between CPT parameters and compressibility indices for soil samples with moisture content greater than 40%.

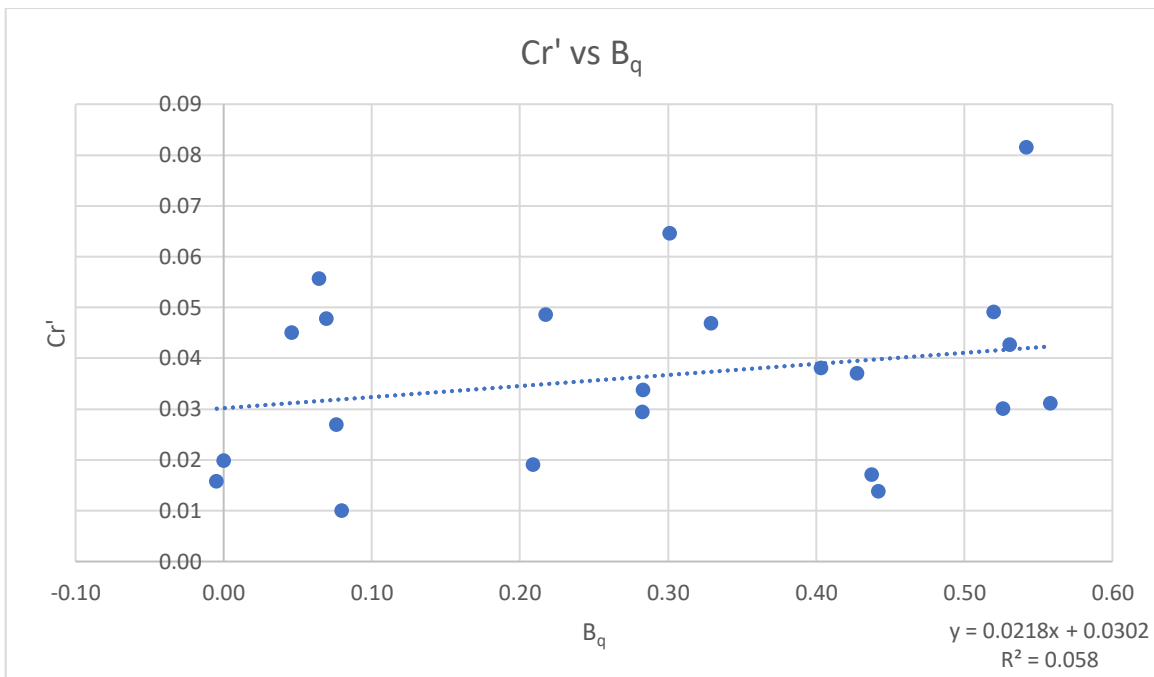


Figure 5-8: Recompression Index vs Pore Pressure Ratio, B_q

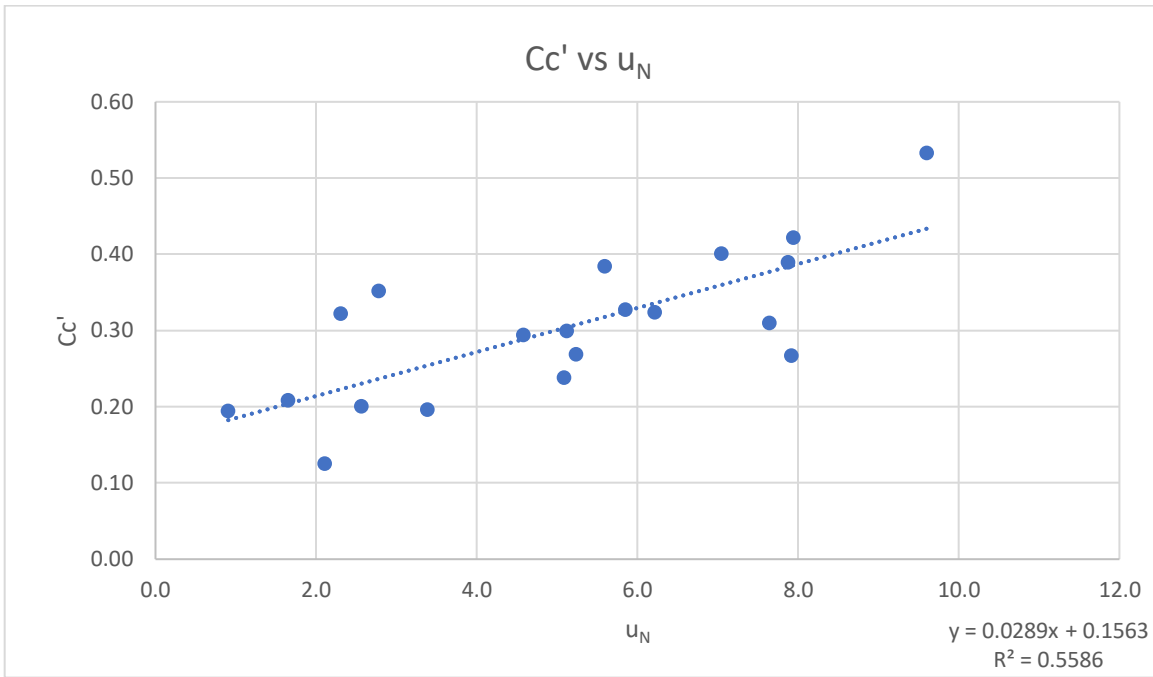


Figure 5-9: Compression Index vs Ratio of Pore Pressures, u_N

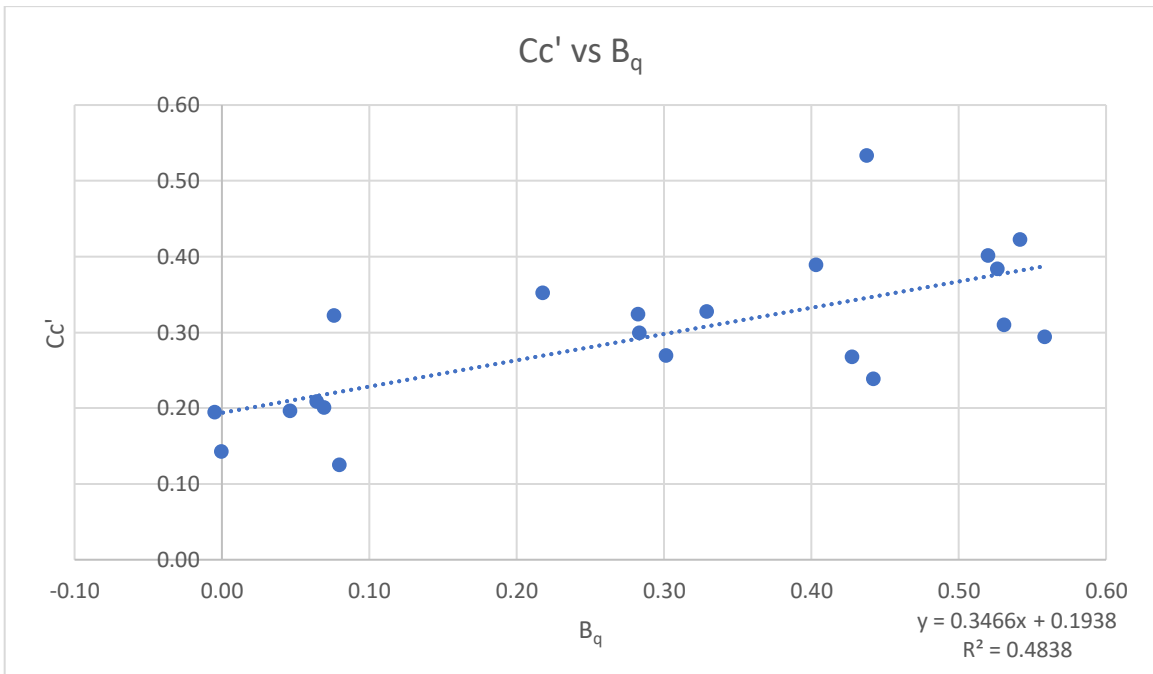


Figure 5-10: Compression Index vs Pore Pressure Ratio, B_q

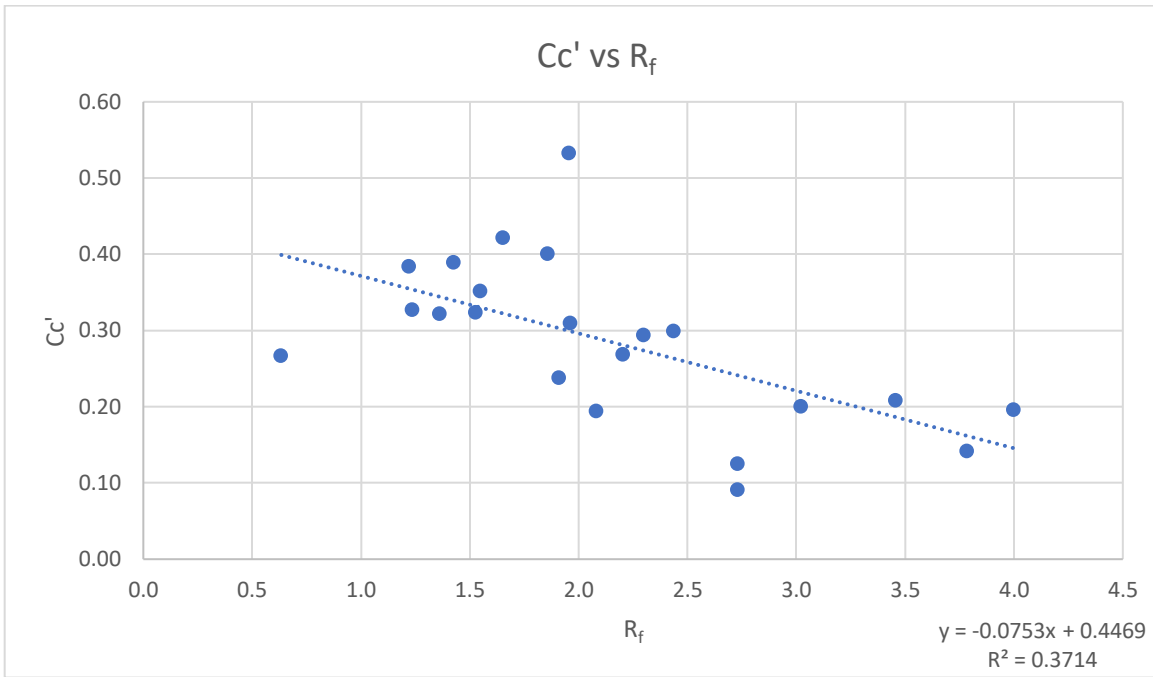


Figure 5-11: Compression Index vs Friction Ratio, R_f

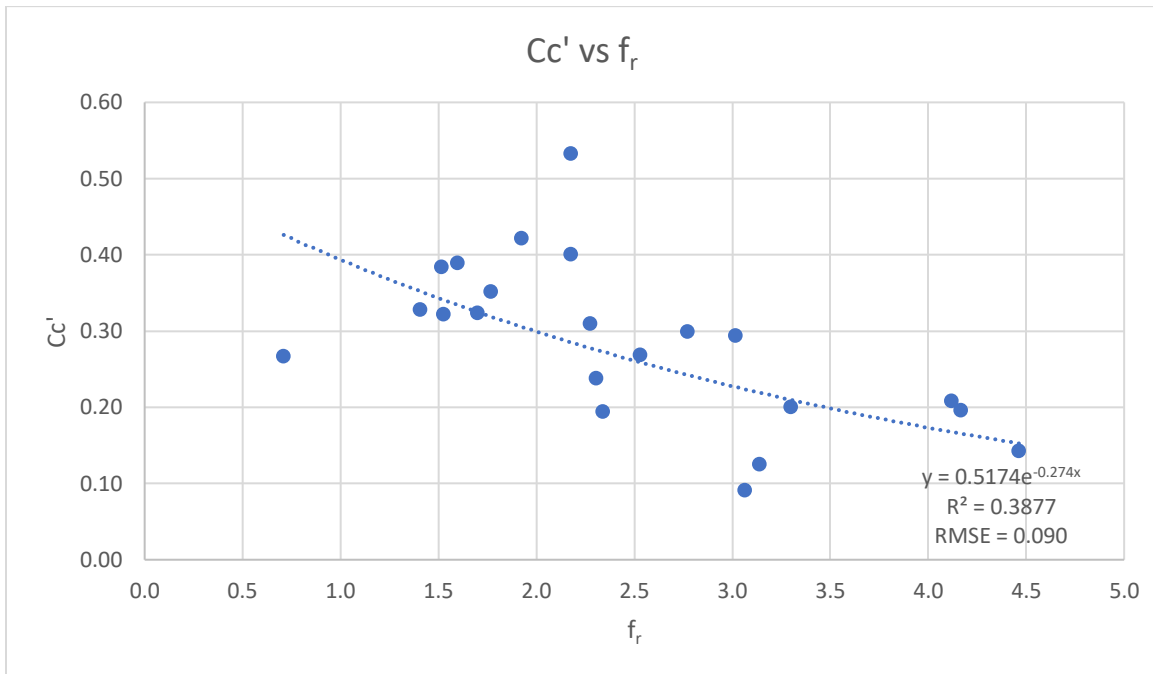


Figure 5-12: Compression Index vs Normalized Friction Ratio, f_r

Table 5-3: Summary of Results, Moisture Content ($w > 40\%$)

Recompression Index	Equation	R²	RMSE
Pore Pressure Ratio	$Cr' = 0.0218(Bq) + 0.0302$	0.058	0.017
Compression Index			
Ratio of Pore Pressure	$Cc' = 0.0289(u_N) + 0.156$	0.559	0.063
Pore Pressure Ratio	$Cc' = 0.3466(Bq) + 0.194$	0.484	0.072
Friction Ratio	$Cc' = -0.0753(Rf) + 0.4469$	0.371	0.082
Normalized Friction Ratio	$Cc' = 0.5174e^{0.274(Fr)}$	0.388	0.090

5.3.2 Recommended Models and Discussion

The previous section displayed all correlations between CPT parameters and compressibility indices. The strongest correlations for Activity and Moisture content are summarized in Table 5-2 and 5-3, respectively. These tables show a strong correlation between compressibility and the cone penetration test's pore pressure and friction ratio parameters. The justification for these correlations were discussed in Chapter 4. This discussion will instead focus on the significant increase in correlation strength due to the application of these filters.

The reliability of pore pressure and friction ratio parameters increased significantly. The percent increase for each category with respect to the correlations from Chapter 4 referred to as the CPT correlations can be found below in Table 5-4. The significant increase in reliability is due to the removal of less clayey materials (soils with high sand percentages or low activity clays) allowing only the soils with more pronounced colloidal properties in the analysis. There was little overlap in the activity and moisture content filter as points with low moisture content do not necessarily have low activity, and vice versa. This little overlap is because sand content greatly impacts moisture content but does not impact the activity. This claim is supported by the positive trend between moisture content and percent finer in Figure 5-13 and the lack of a trend between activity and percent finer in Figure 5-14.

Table 5-4: Model Reliability Increase

Model Type	Friction Ratio		Ratio of Pore Pressures	
	R ²	% Increase	R ²	% Increase
CPT	0.233	0	0.341	0
Activity	0.305	31	0.621	82
Moisture	0.371	59	0.559	64

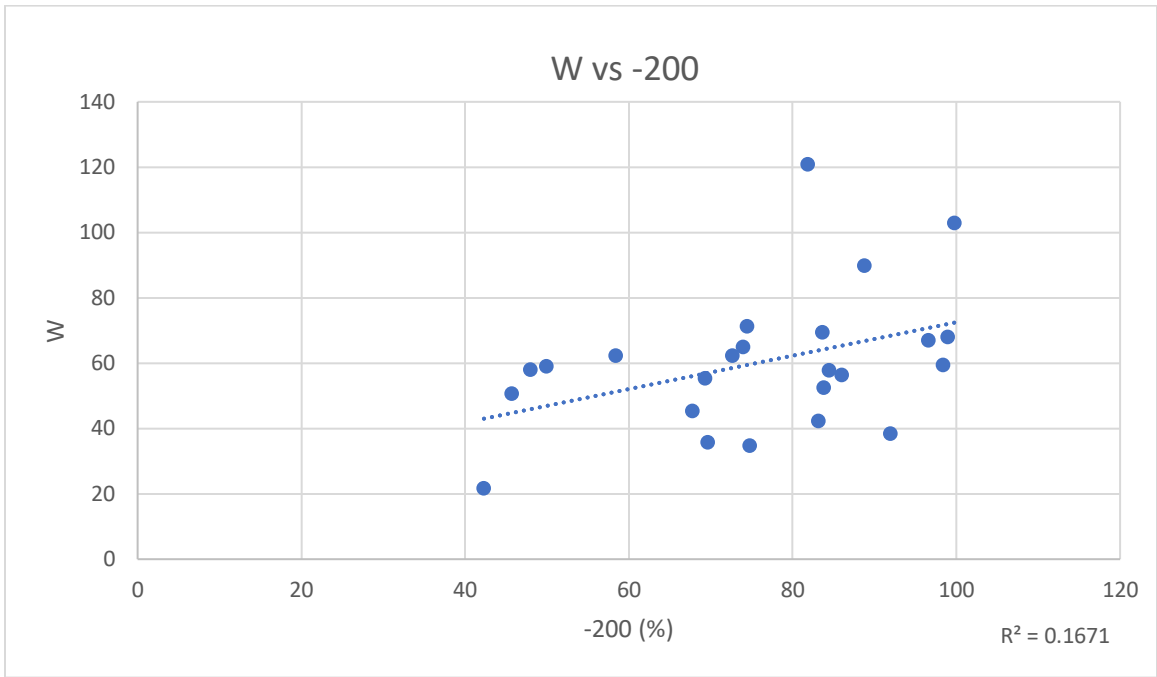


Figure 5-13: Moisture Content vs Percent Finer

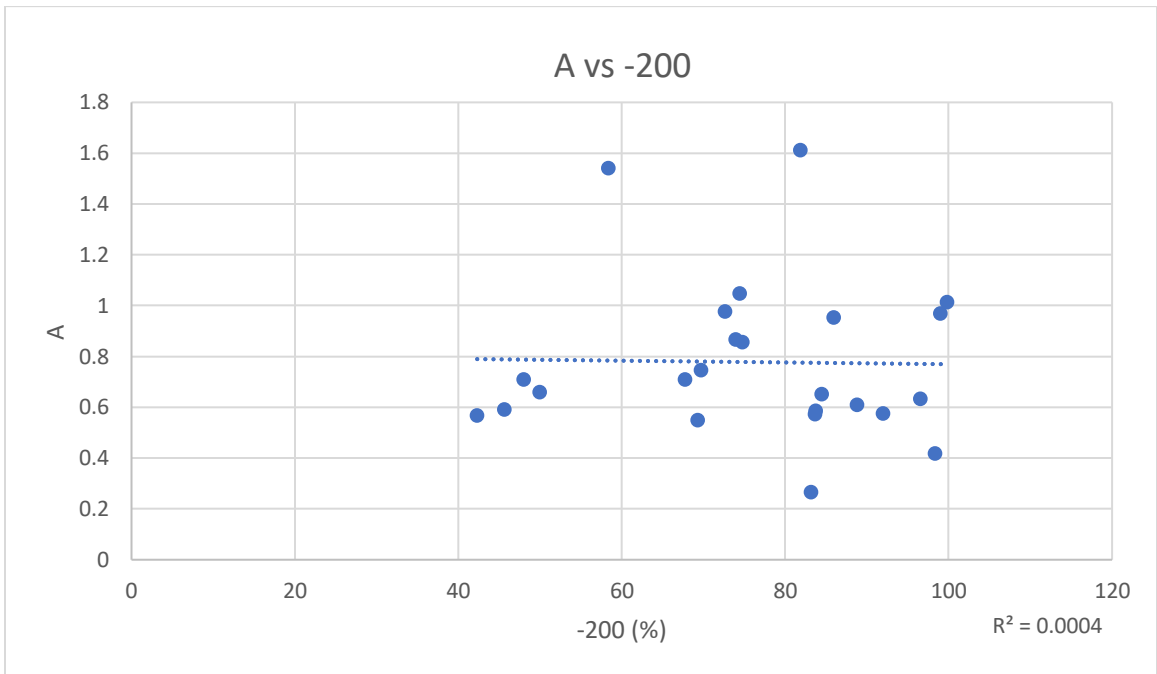


Figure 5-14: Activity vs Percent Finer

Table 5-5: Recommended Model, Activity

Recompression Index	Equation	R ²	RMSE
Compression Index	$Cr' = 1/7 Cc'$	0	0.020
Compression Index			
Ratio of Pore Pressure	$Cc' = 0.0315(u_N) + 0.137$	0.621	0.075

Table 5-6: Recommended Model, Moisture Content

Recompression Index	Equation	R ²	RMSE
Compression Index	$Cr' = 1/7 Cc'$	0	0.017
Compression Index			
Ratio of Pore Pressure	$Cc' = 0.0289(u_N) + 0.156$	0.559	0.063

5.4 Conclusion

The findings of this chapter indicate that the CPT should be utilized to estimate virgin compressibility of fine-grained soils with pronounced colloidal properties. Tables 5-5 and 5-6 summarize the recommended models for high activity and high moisture content soils, respectively. These tables show improved models to compression index, as well as a refined ratio to estimate recompression index. It should be noted that only an activity and moisture content filter was applied, however, it is likely that any index property filter would increase the CPT model's reliability.

This study expanded upon chapter 4 to show that the CPT test can estimate compressibility. These findings should demonstrate the proper methodology and analysis required to relate the CPT to compressibility, however, a larger data base is required to recommend a model for use in practice.

CHAPTER 6 CONCLUSION

6.1 Summary

This paper recommends models to estimate compressibility indices from index properties and Cone Penetration Test parameters. These correlations enable practitioners to accurately estimate compressibility of fine-grained soils in Central Florida from common laboratory and field-testing techniques. It has been found that index properties, specifically moisture content, can estimate the compressibility indices with strong reliability. It was also found that the CPT pore pressure reading can be used to estimate the compression index for all fine-grained soils. This correlation was proven to be more reliable for soils with high moisture contents and/or high activity.

The index property correlations are supported by a strong data base and are recommended with a high degree of confidence. The CPT correlations require further research supported by a larger data base to be reliable. However, the CPT correlations for soils of high activity and moisture content show a strong correlation does exist. This implies it is worth investing the effort to expand the current data base to further examine this relationship. Once a reliable model is proposed, it will be possible to produce a continuous compressibility profile from a practical in-situ field test.

6.2 Recommendations

6.2.1 Compression Index Recommendation

The models recommended to estimate compressibility indices from index properties, CPT parameters, and CPT parameters for soils of high activity and high moisture content have been discussed in chapters 3, 4, and 5, respectively. Table 6-1 summarizes these findings. Chapter 3 analyzed recompression and compression indices (C_r & C_c) in void ratio-stress space. For these correlations to be

practical, a correlation to void ratio was provided and will be shown again in Table 6-2. The analysis for Chapters 4 and 5 were performed in strain–stress space, Cr' and Cc' . These parameters do not require void ratio to be utilized in practice.

Table 6-1: Summary of Recommended Models

Recompression Index	Equation	R²	RMSE
Compression Index	$Cr = 1/8 Cc$	0.507	0.074
Compression Index			
Moisture Content	$Cc = 0.015W - 0.275$	0.679	0.329
Ratio of Pore Pressure	$Cc' = 0.0315(u_N) + 0.137$	0.621	0.075

Table 6-2: Void Ratio Model

Void Ratio	Equation	R-Squared	RMSE
Moisture Content	$e_0 = 0.0271W - 0.0247$	0.953	.188

6.2.2 OCR Recommendation

The purpose of this section is to provide a correlation to the overconsolidation ratio (OCR). The OCR is a ratio of the preconsolidation pressure and current in-situ effective vertical stress. As discussed in the introduction, the preconsolidation pressure must be used in conjunction with the compressibility indices to estimate site settlements (equations 1 through 3). This parameter may be used alone (without the equations) to quickly determine if the site will experience plastic deformations, which will occur if the preconsolidation pressure is exceeded during construction. These plastic deformations are typically responsible for most of the site's settlement.

Mayne and Kemper (1988) proposed a correlation between the overconsolidation ratio, ratio of preconsolidation pressure to current in-situ stress, and the CPT. A brief summary of this study is found in section 2.6. The application of their formula to the Central Florida soils yields the graph seen in Figure 6-1. The line of best fit suggests a K_c of 0.15 is most applicable to these soils. However, this line of best fit

is poor and an improved analysis is required before any model can be recommended. This poor correlation is likely due to the use of Casagrande's visual method to determine preconsolidation pressure as well as the small number of data points.

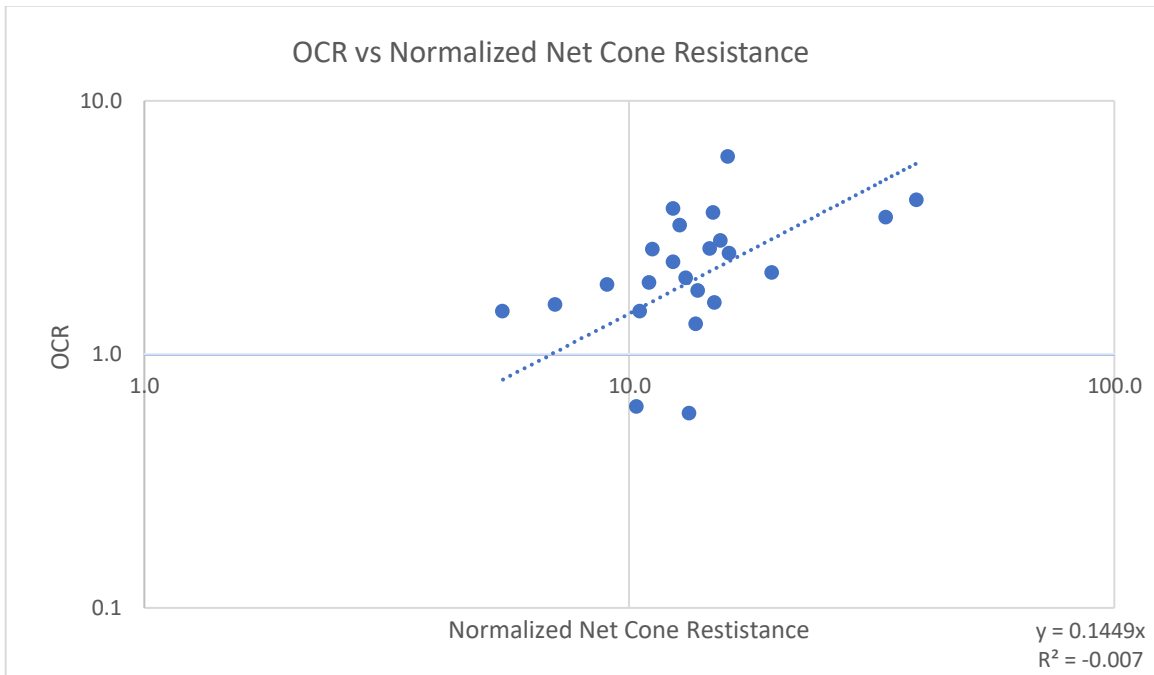


Figure 6-1: Over Consolidation Ratio vs Normalized Net Cone Resistance

6.3 Limitations and Future Works

This study required projects which performed both CPT and Oedometer Testing. The coupled point was then put through a rigorous filtering process which removed approximately 1/3 of all data points. These restrictions increased the quality of data but severely limited the quantity of points for analysis. Due to this limitation the study requires more data points to be utilized in practice. In order to expand this data set it would be necessary to perform, or subcontract, CPT and Oedometer Tests instead of retrieving the data from a 3rd party. This direct testing would not only provide more data but give the researcher complete quality control, which would immensely increase the reliability of this correlation. Another limitation is the uncertainty in selecting the corresponding CPT depth. This variability is the

nature of soil and some uncertainty will always remain; however, it could be minimized by directly overseeing the CPT and Oedometer Testing.

Once a stronger data base is provided, the analysis could improve as well. This would consist of strengthening the current correlations to compressibility indices, as well as performing a similar trial and error regression analysis for the Preconsolidation Pressure (σ_c'). The coefficient of consolidation (C_v) is utilized to estimate the rate of consolidation. This design consideration is equally important as the estimation of the magnitude of consolidation. However, this parameter can be directly measured from the CPT dissipation test. The dissipation test is common, relatively inexpensive, reliable, and relatively time efficient. For this reason, the scope of the future works will remain focused on the magnitude of consolidation.

This report provides a strong correlation between recompression and compression indices and moisture content. The moisture content is the most ideal index property to correlate to as the test is cost and time effective, and there is minimal room for error. The report also provides a strong correlation between CPT pore pressure and compression index. This suggest the CPT can be used to create continuous and repeatable soil compressibility profiles. Future works will consist of improving the CPT correlations to compressibility indices and preconsolidation pressure.

APPENDIX A – INDEX PROPERTY CORRELATIONS

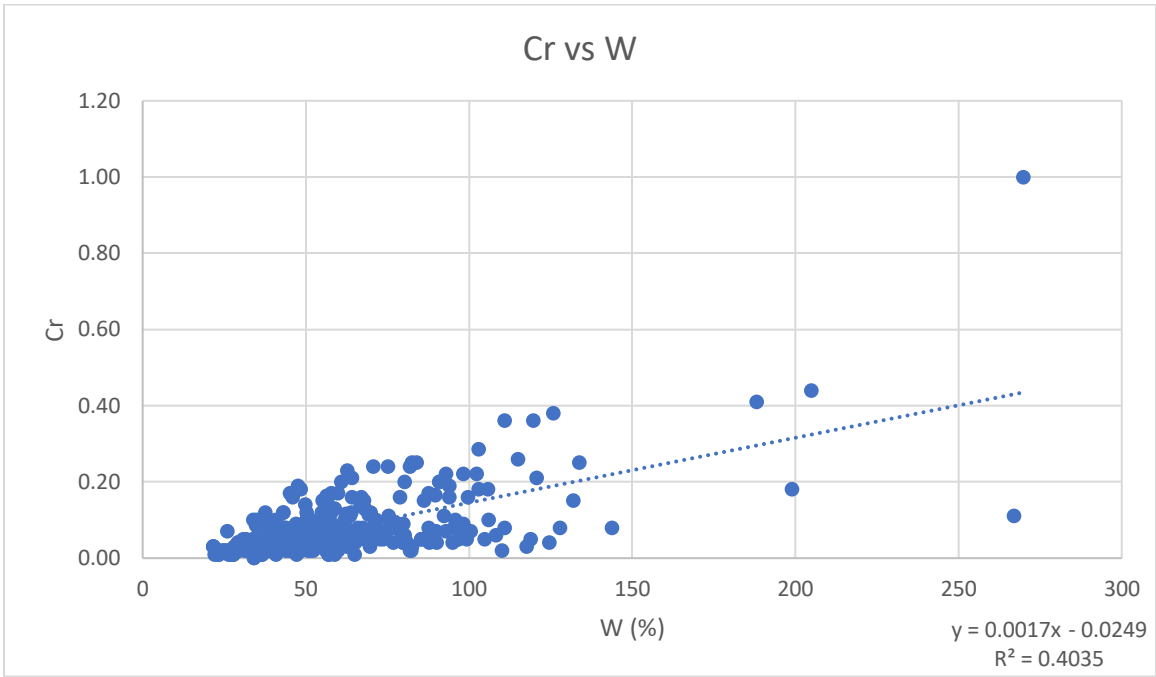


Figure A-1: Recompression Index vs Moisture Content, W

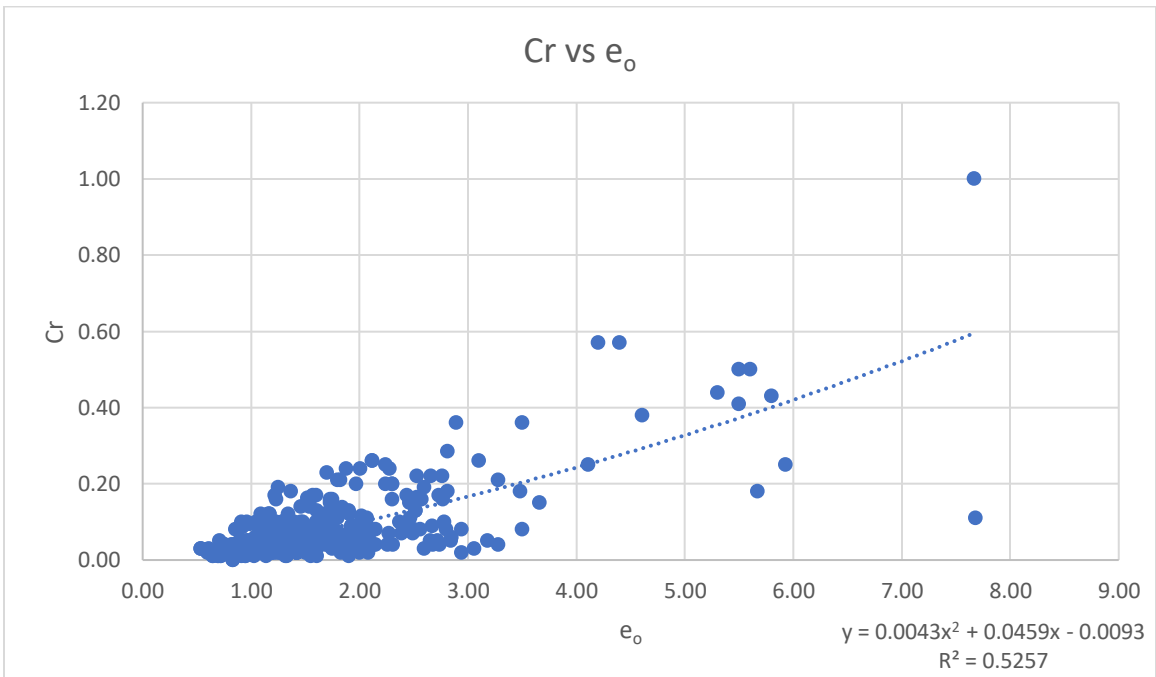


Figure A-2: Recompression Index vs Initial Void Ratio, e_o

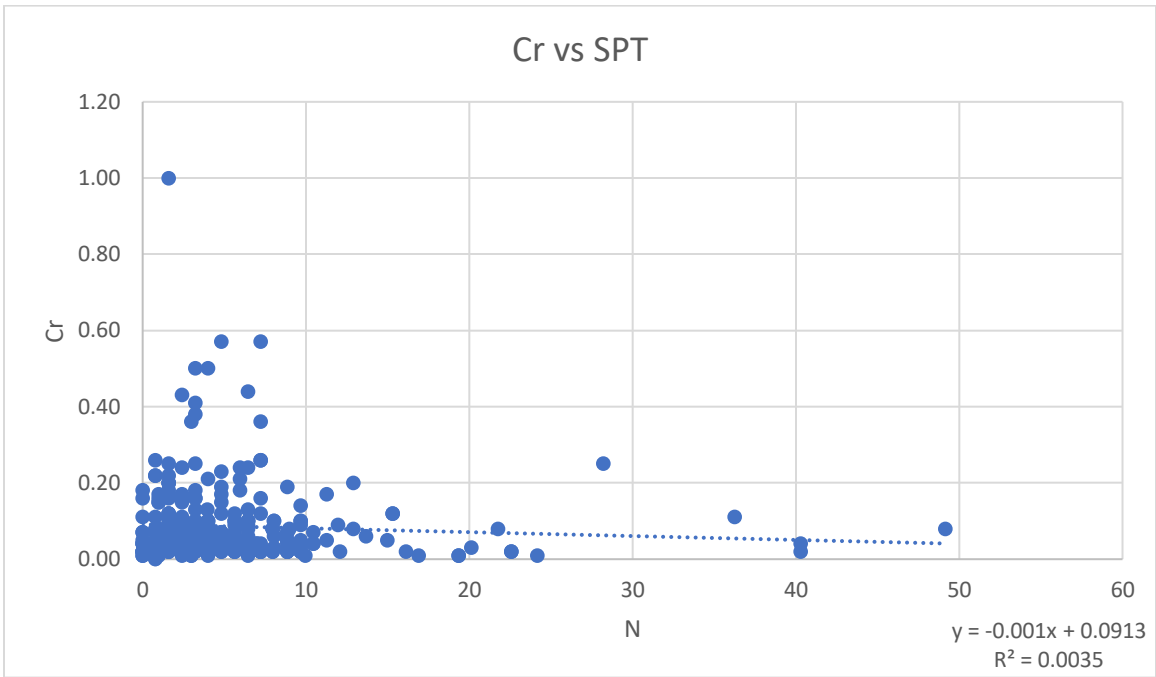


Figure A-3: Recompression Index vs Standard Penetration Test Blow Count, N

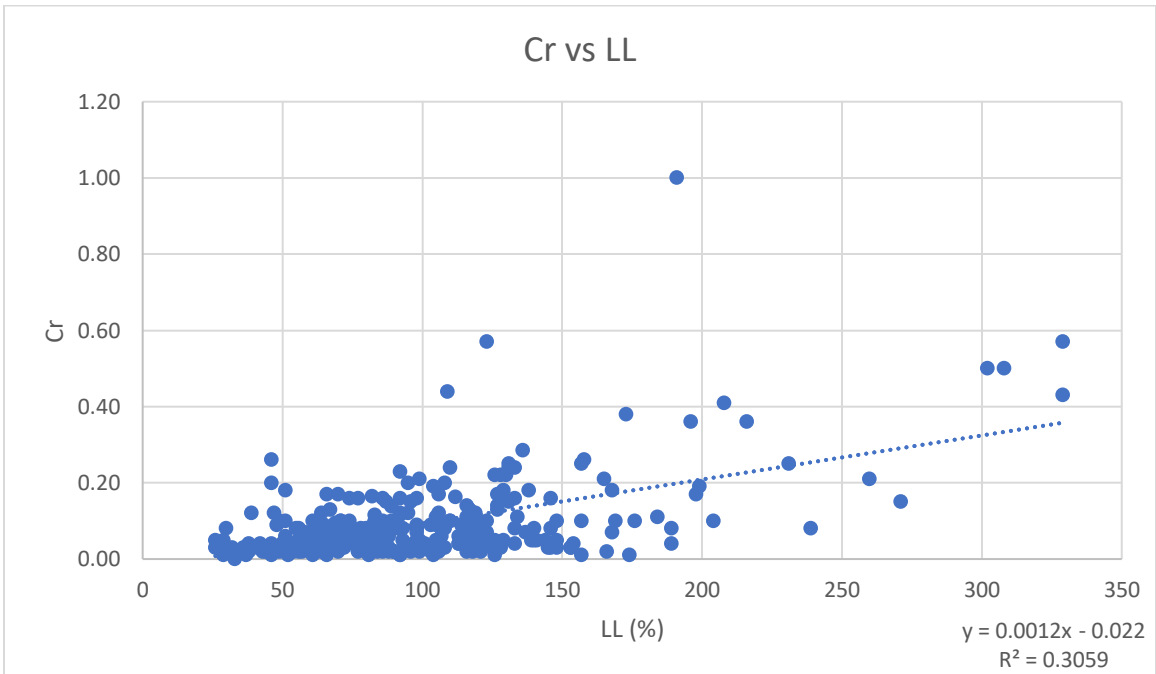


Figure A-4: Recompression Index vs Liquid Limit, LL

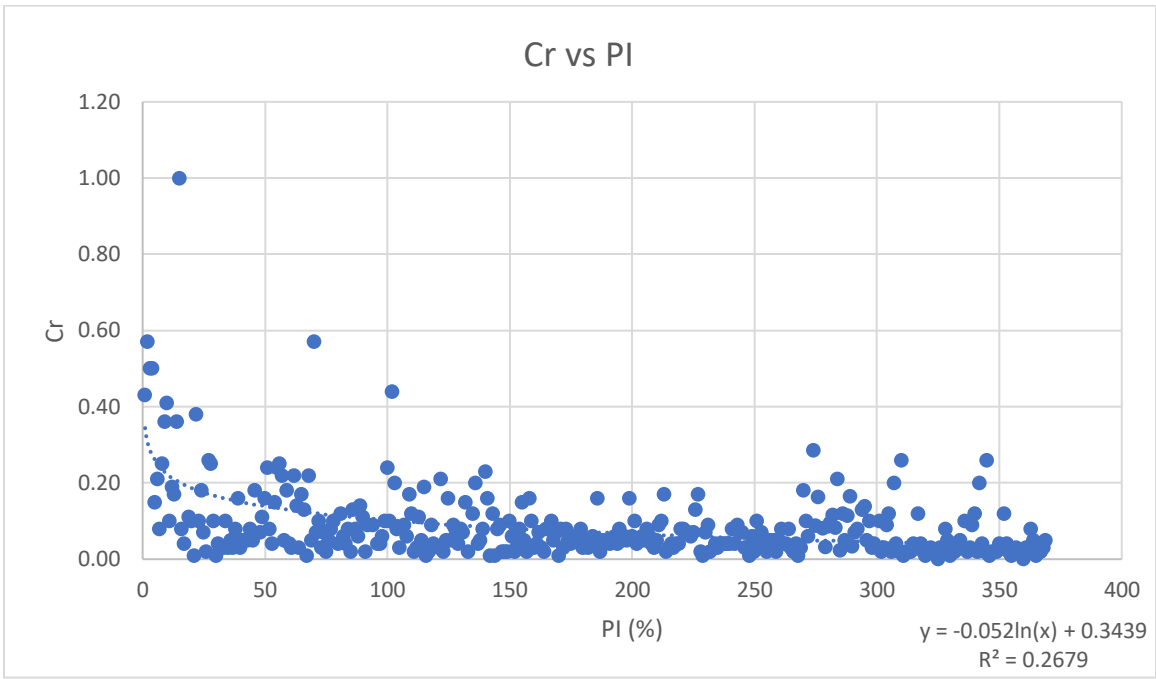


Figure A-5: Recompression Index vs Plasticity Index, PI

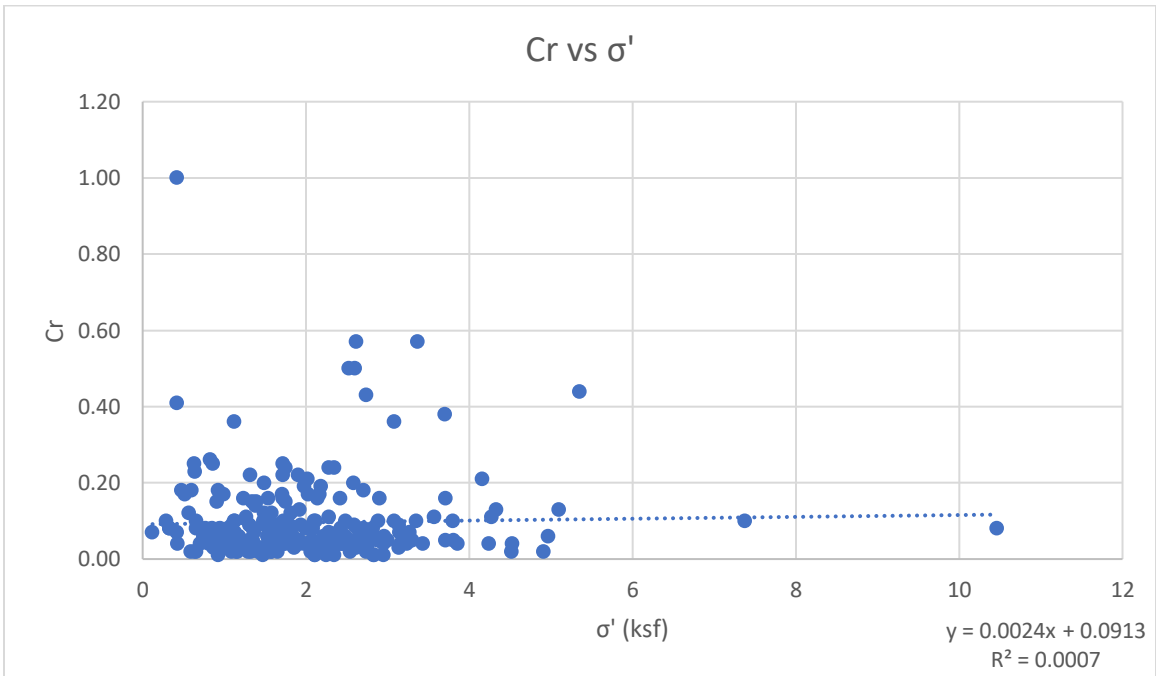


Figure A-6: Recompression Index vs Effective Vertical Stress

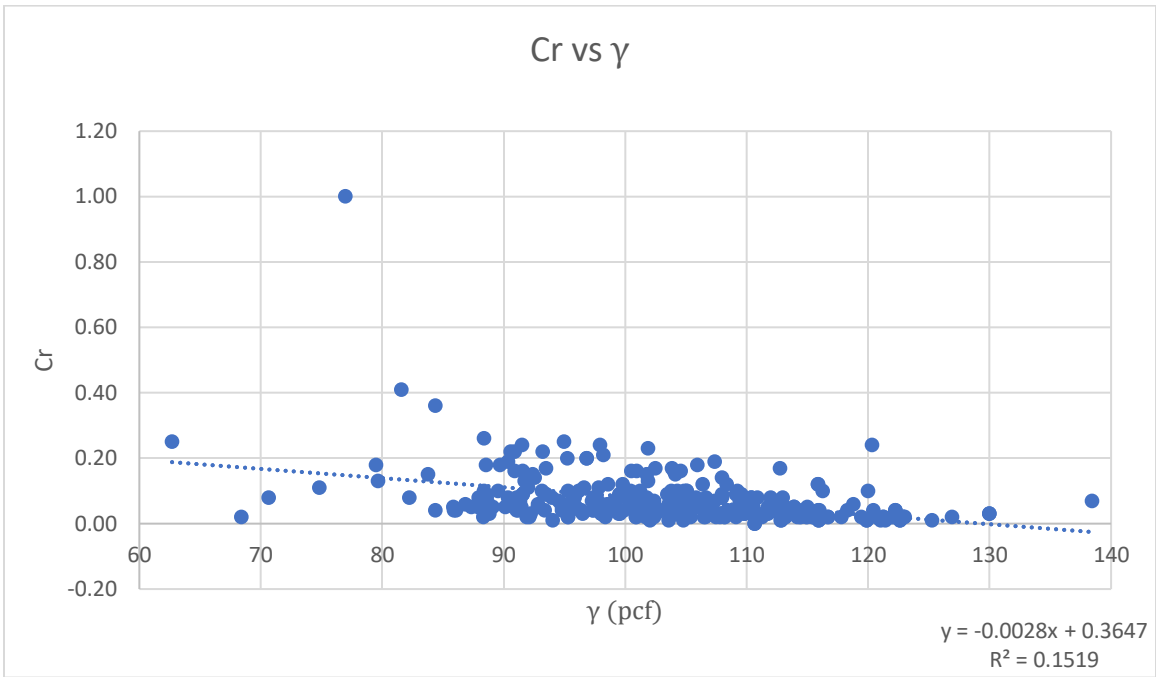


Figure A-7: Recompression Index vs Wet Density, γ

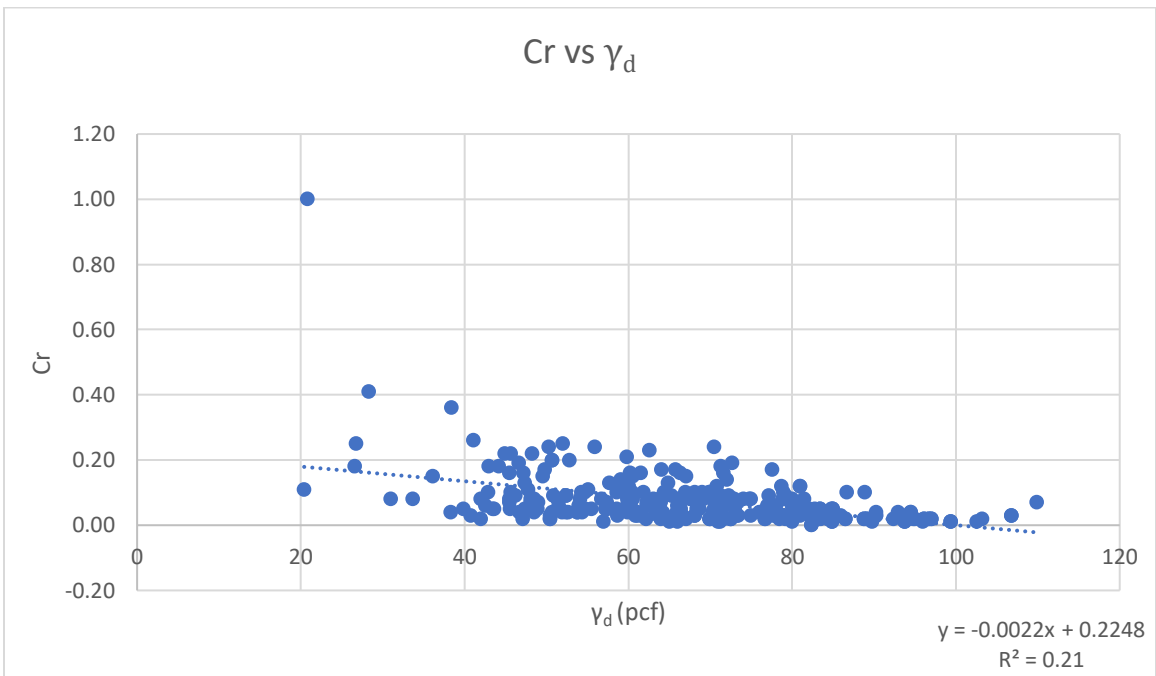


Figure A-8: Recompression Index vs Dry Density, γ_d

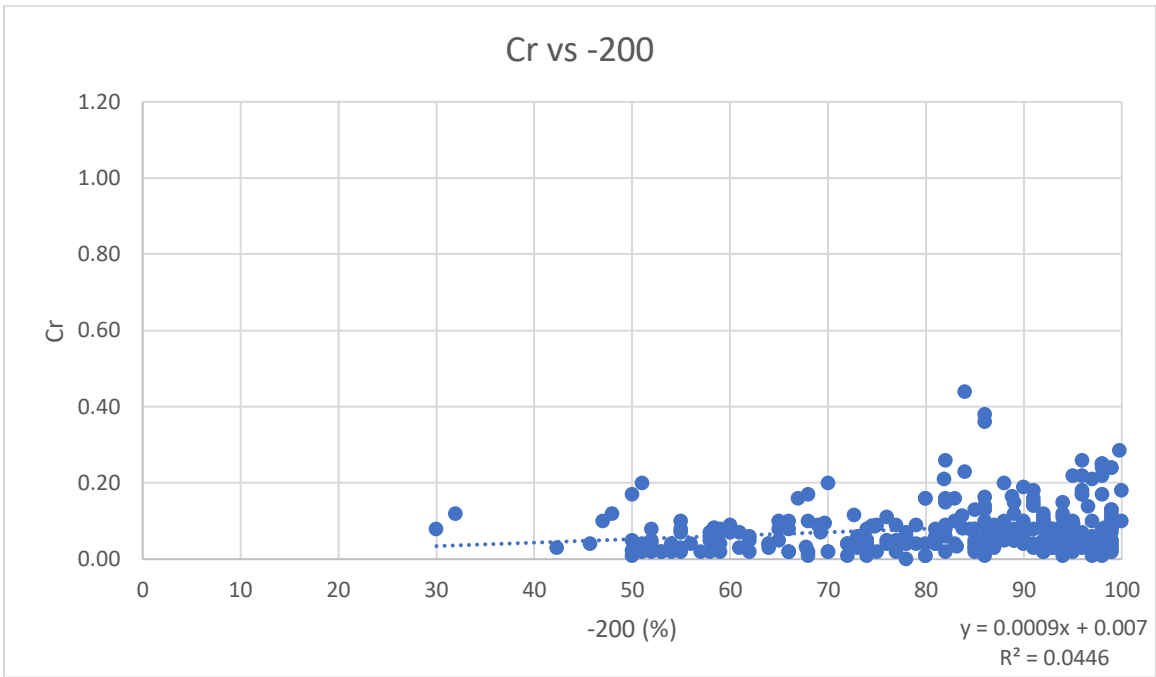


Figure A-9: Recompression Index vs Percent Finer, -200

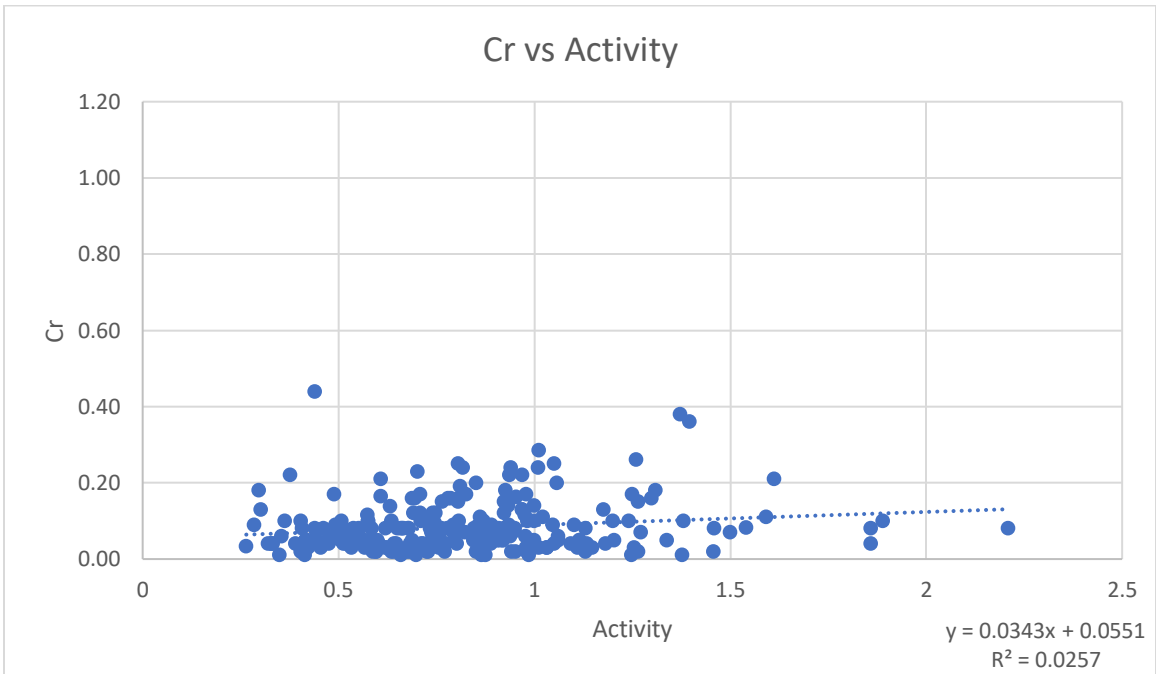


Figure A-10: Recompression Index vs Activity, A

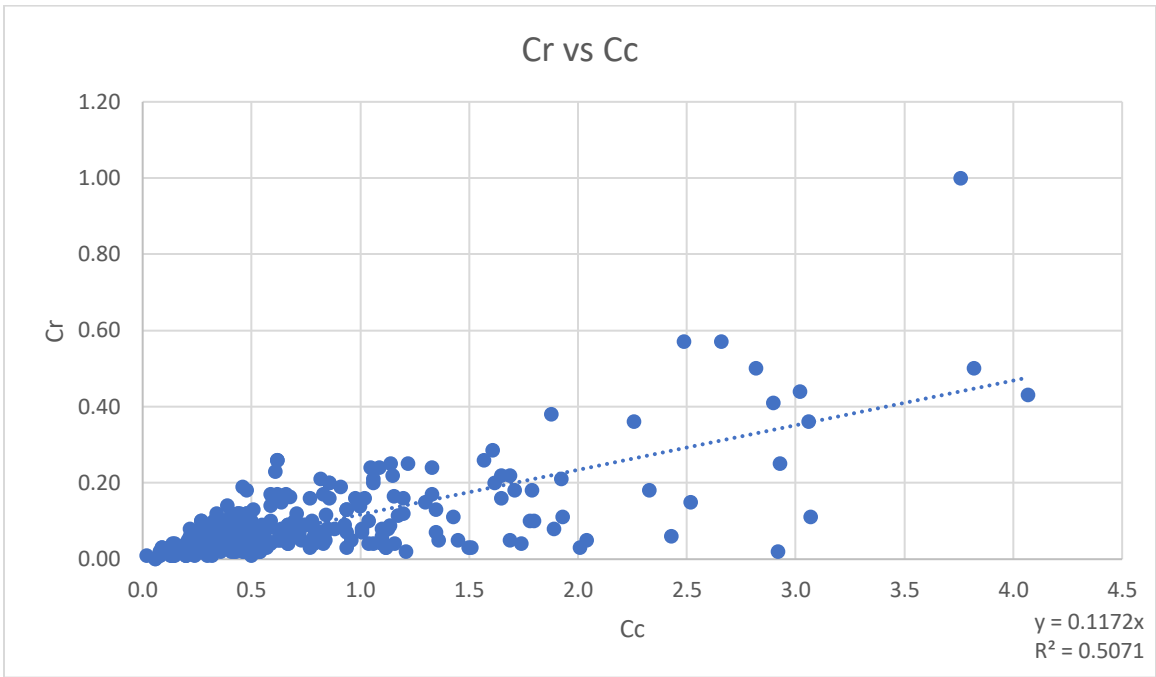


Figure A-11: Recompression Index vs Compression Index

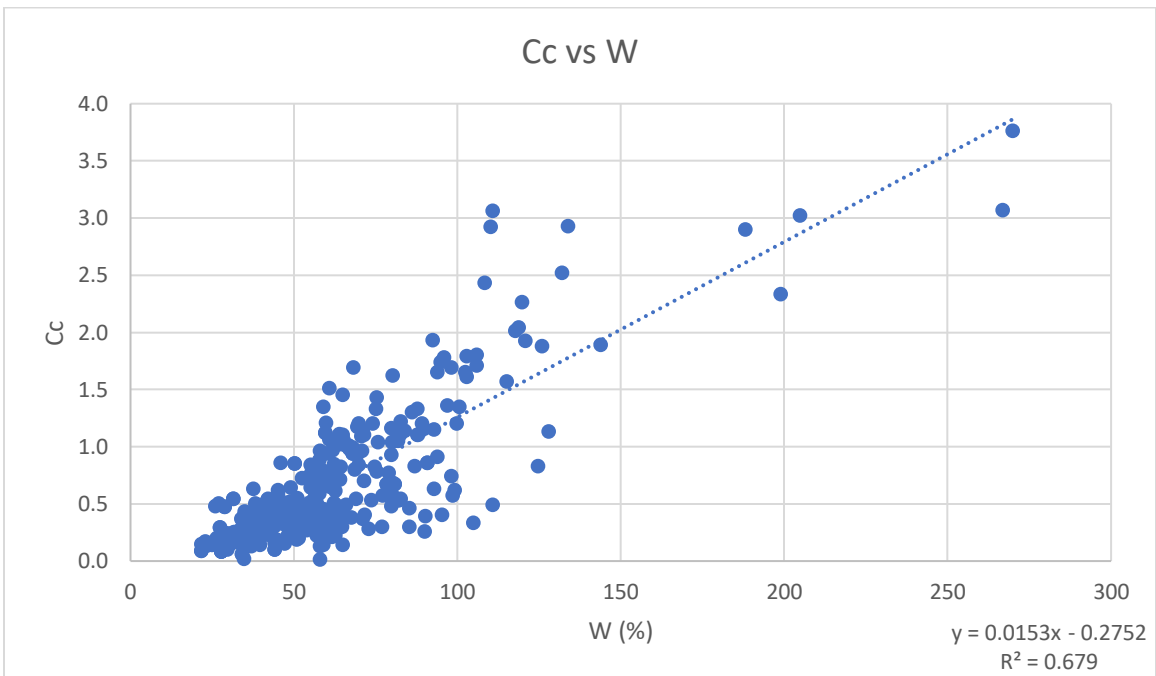


Figure A-12: Compression Index vs Moisture Content, W

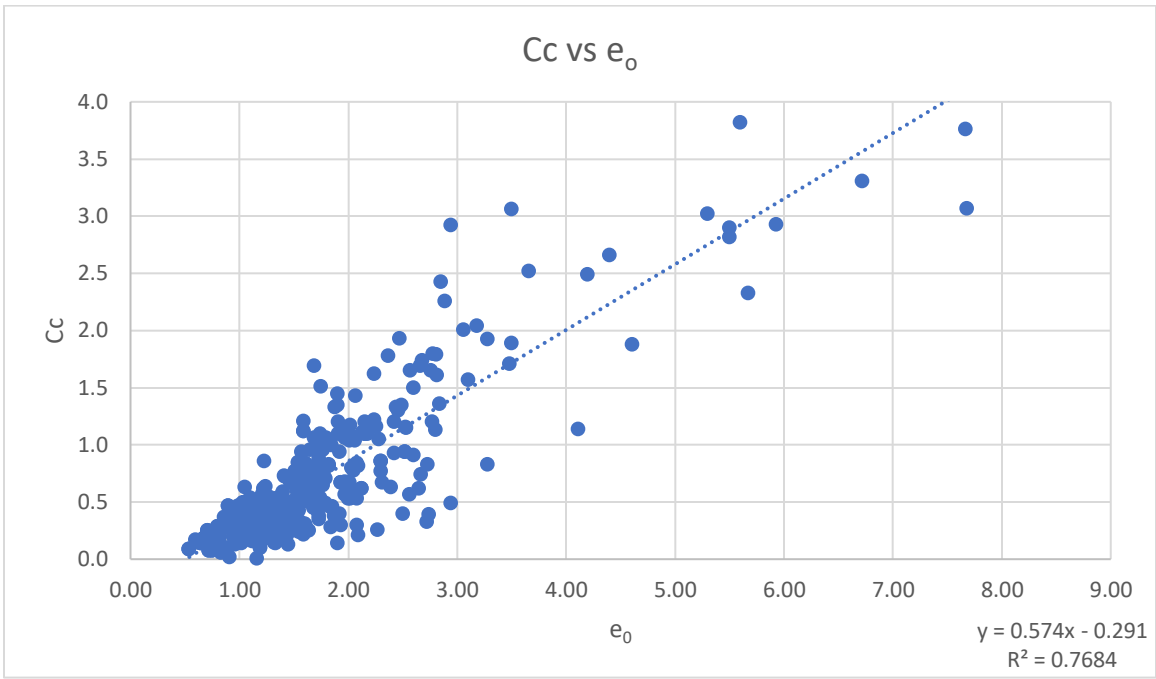


Figure A-13: Compression Index vs Initial Void Ratio, e_o

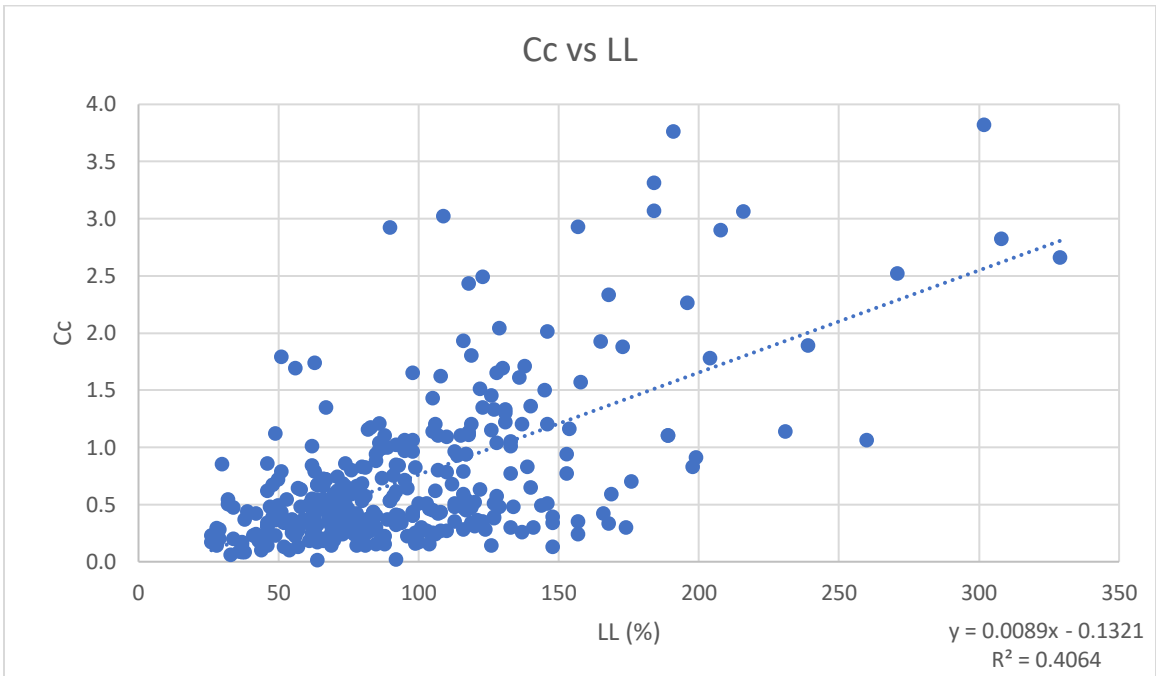


Figure A-14: Compression Index vs Liquid Limit, LL

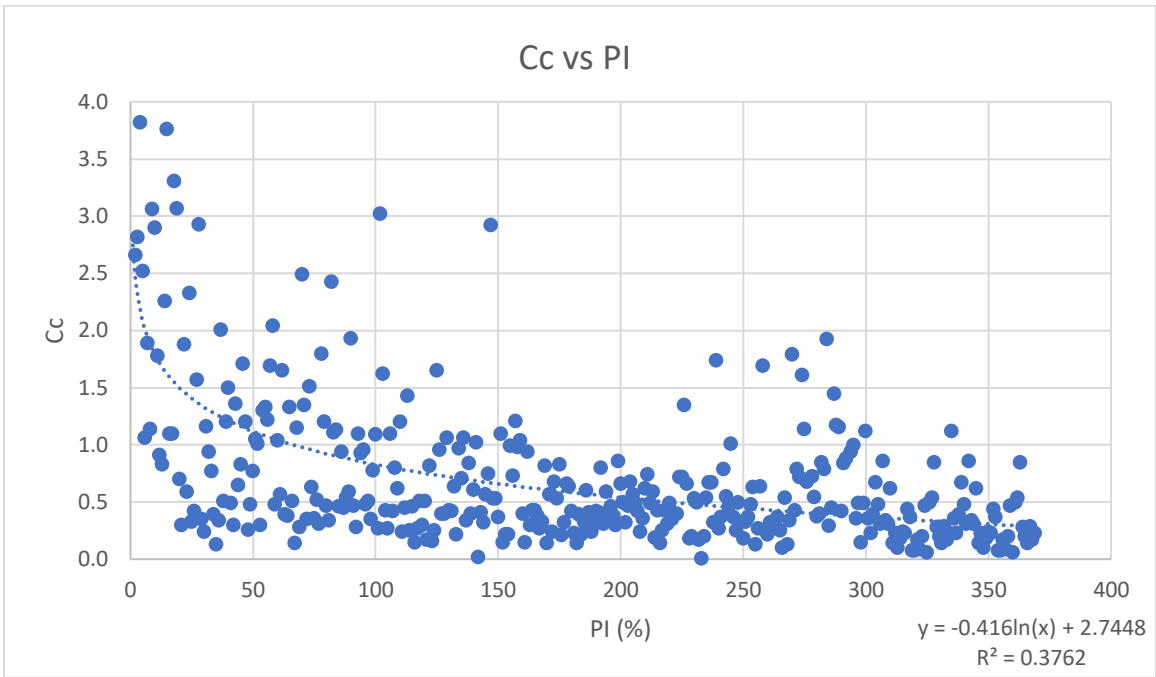


Figure A-15: Compression Index vs Plasticity Index, PI

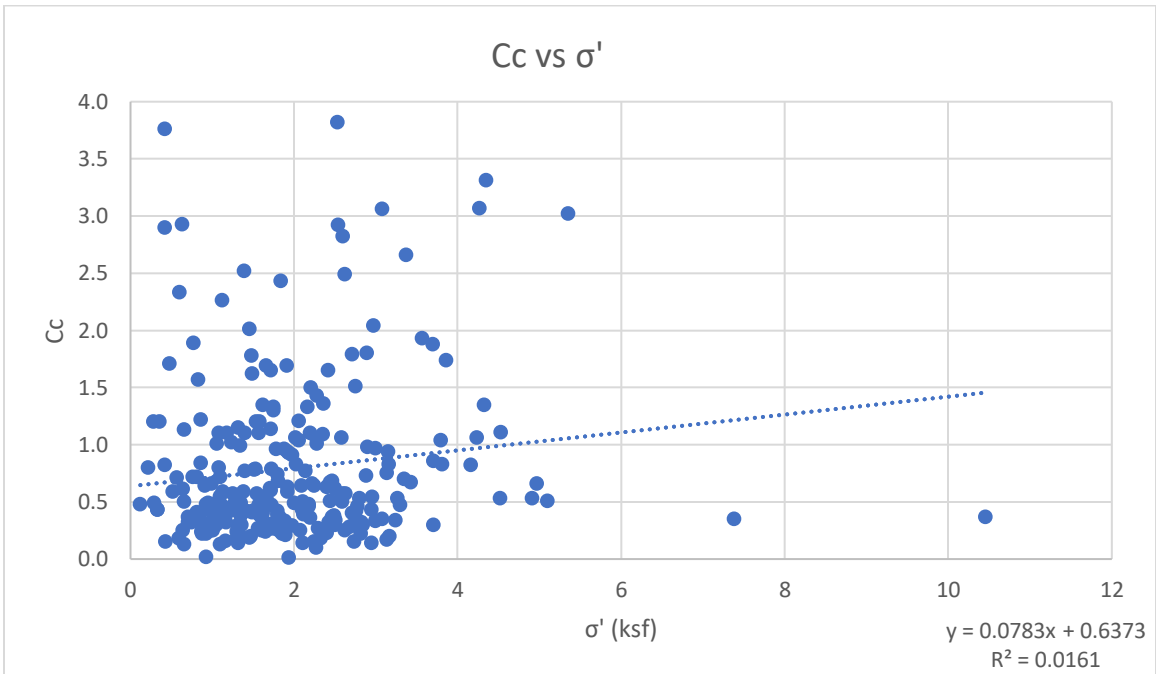


Figure A-16: Compression Index vs Effective Vertical Stress, σ'

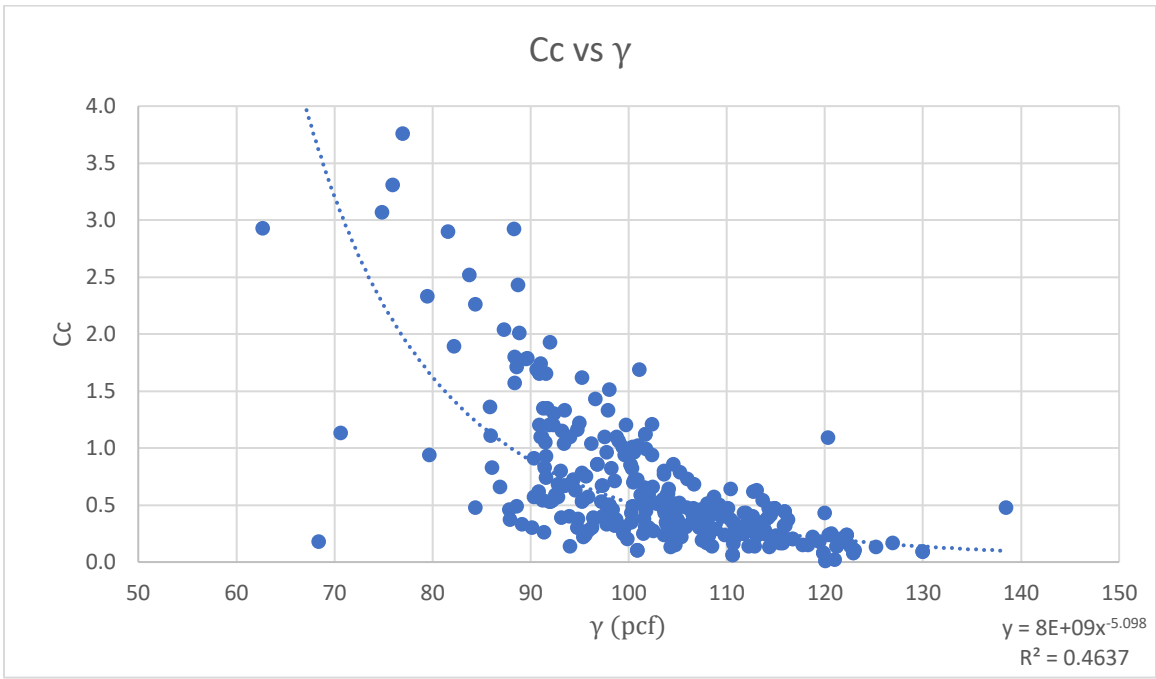


Figure A-17: Compression Index vs Wet Unit Weight, γ

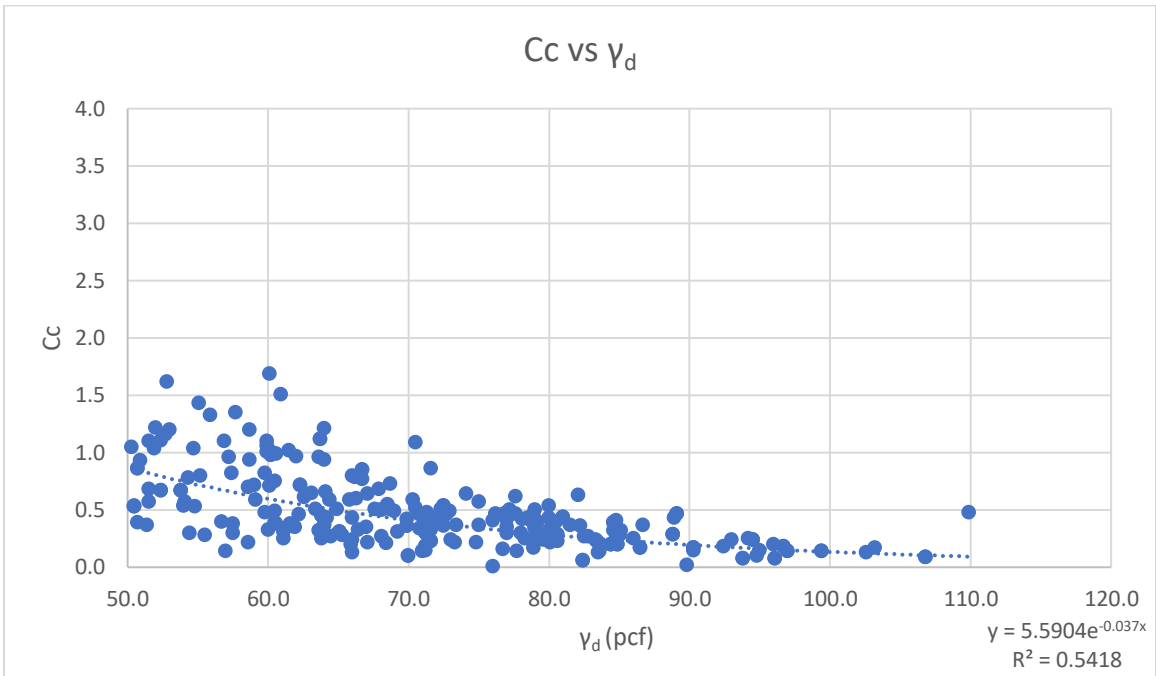


Figure A-18: Compression Index vs Dry Unit Weight, γ_d

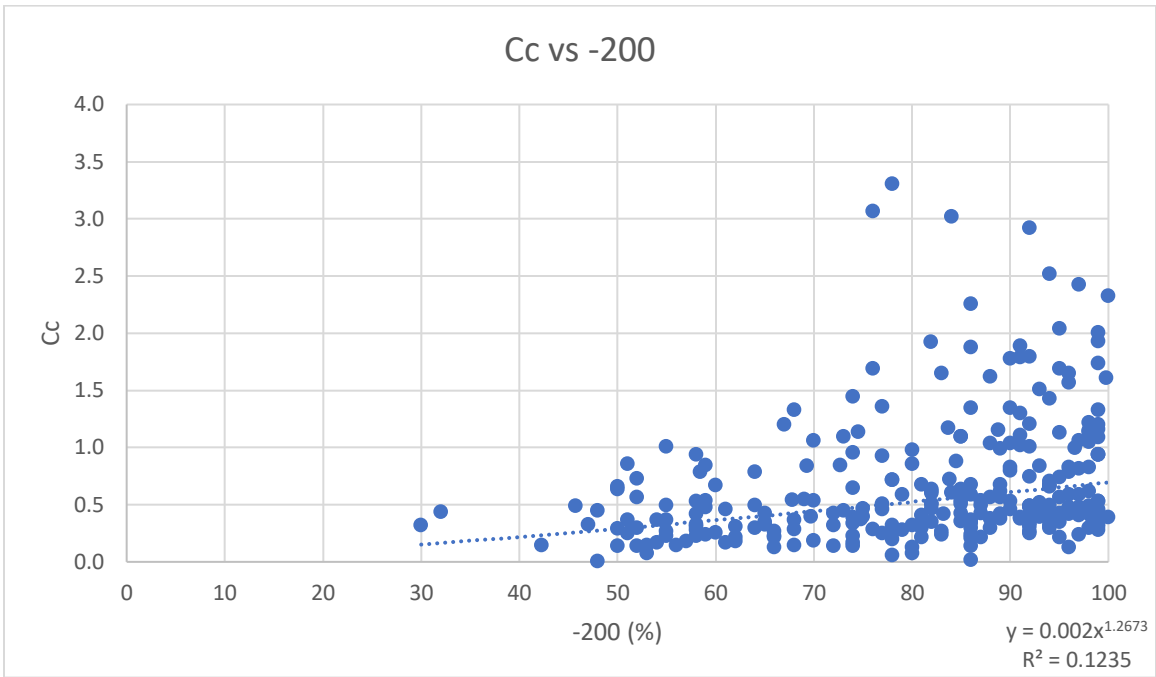


Figure A-19: Compression Index vs Percent Finer

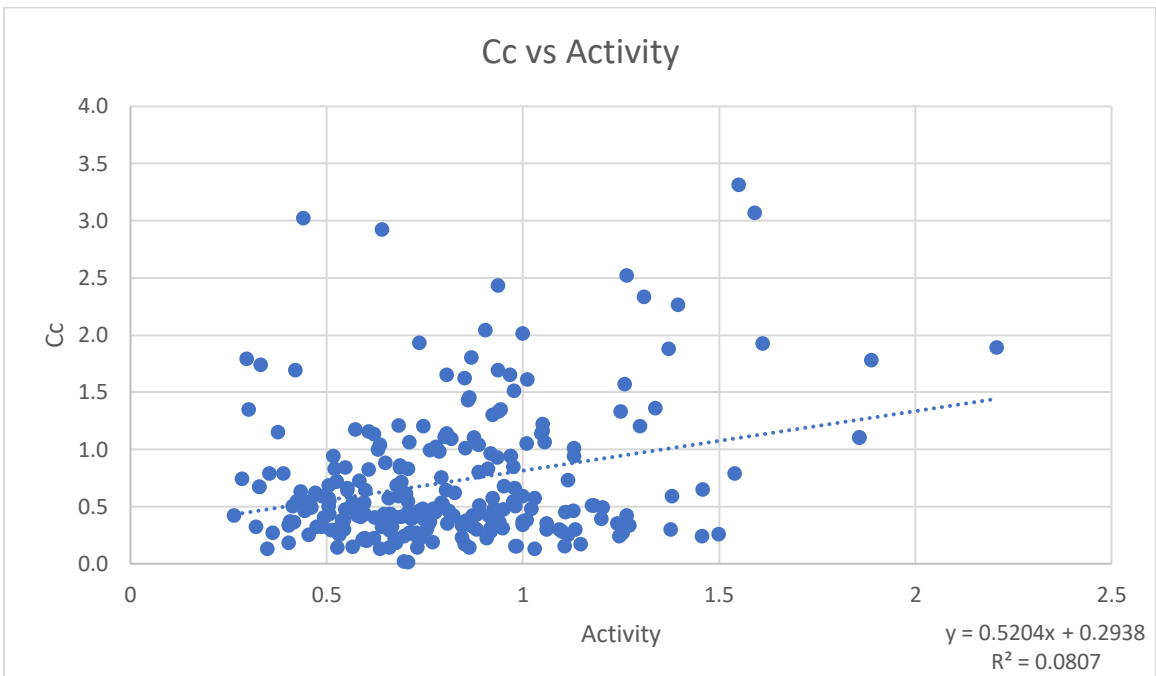


Figure A-20: Compression Index vs Activity, A

APPENDIX B – CONE PENETRATION TEST BASED CORRELATIONS (UNDIVIDED)

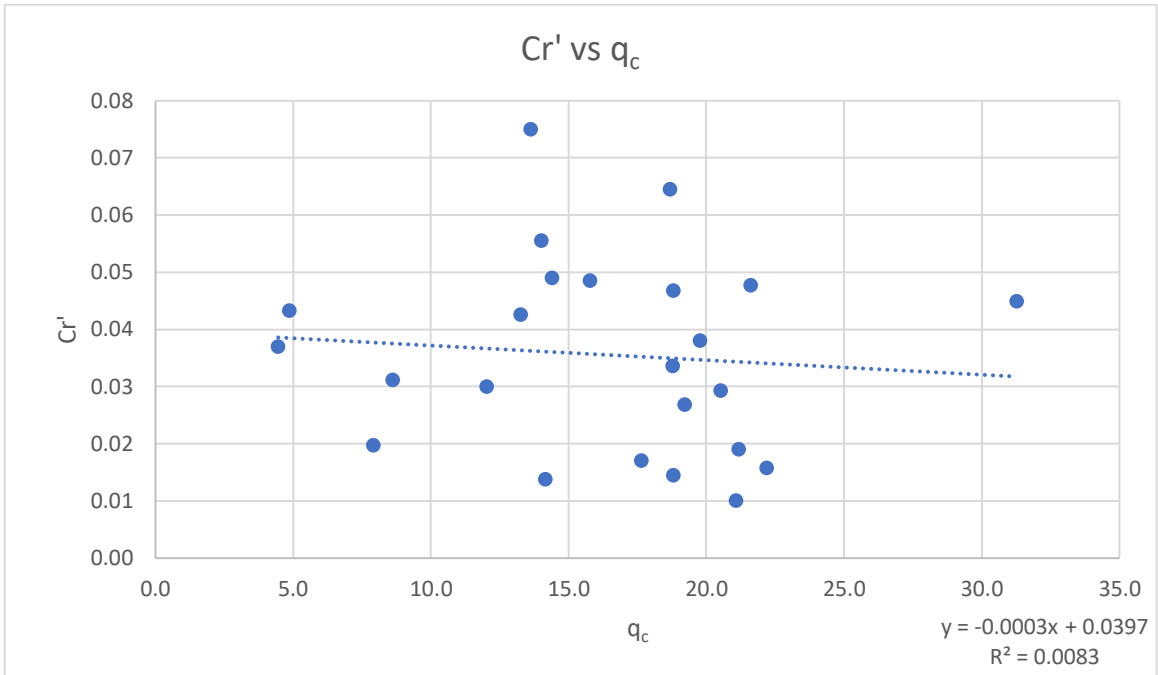


Figure B-1: Recompression Index vs Tip Resistance, q_c

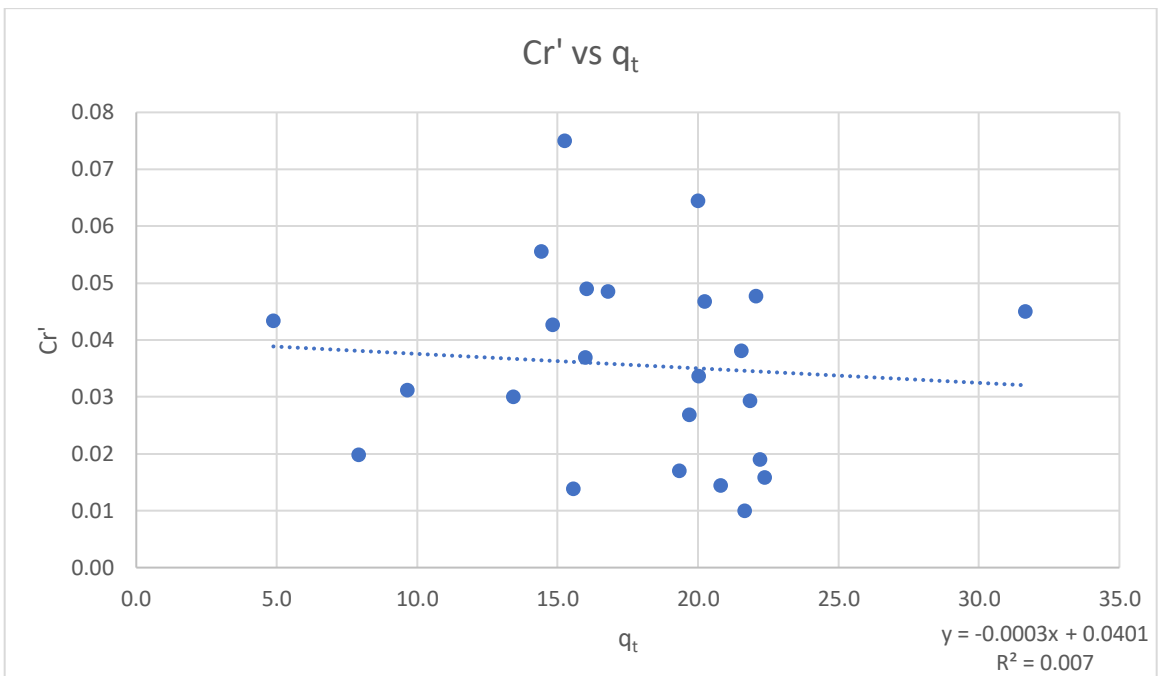


Figure B-2: Recompression Index vs Corrected Tip Resistance, q_t

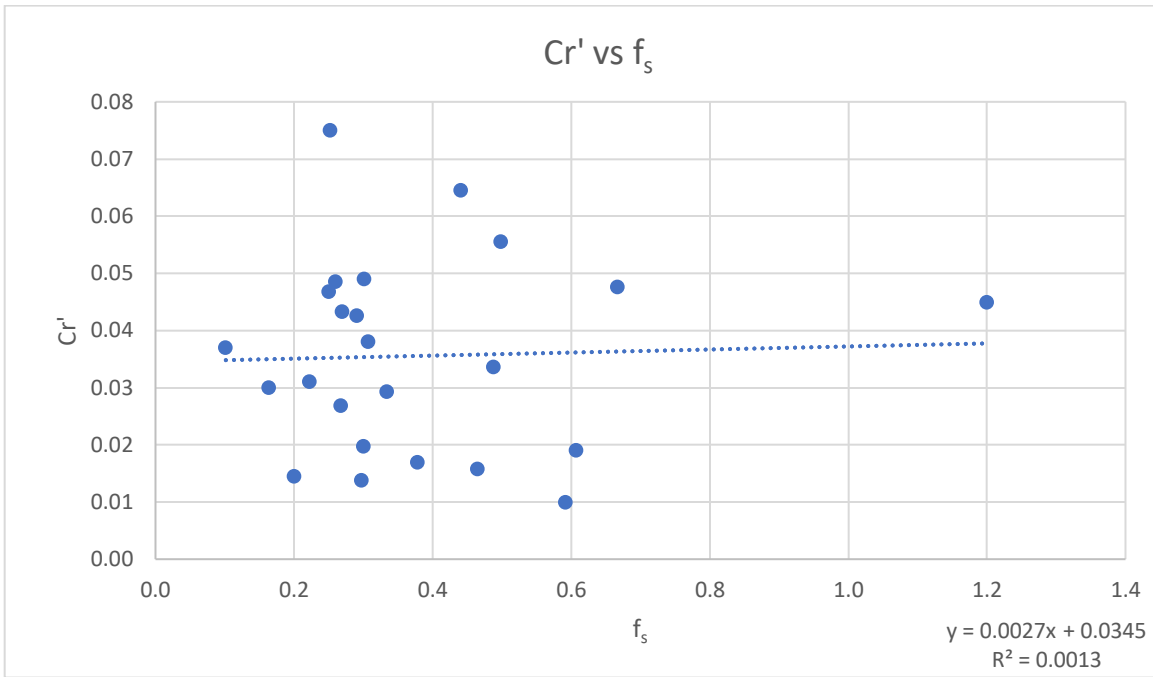


Figure B-3: Recompression Index vs Sleeve Friction, f_s

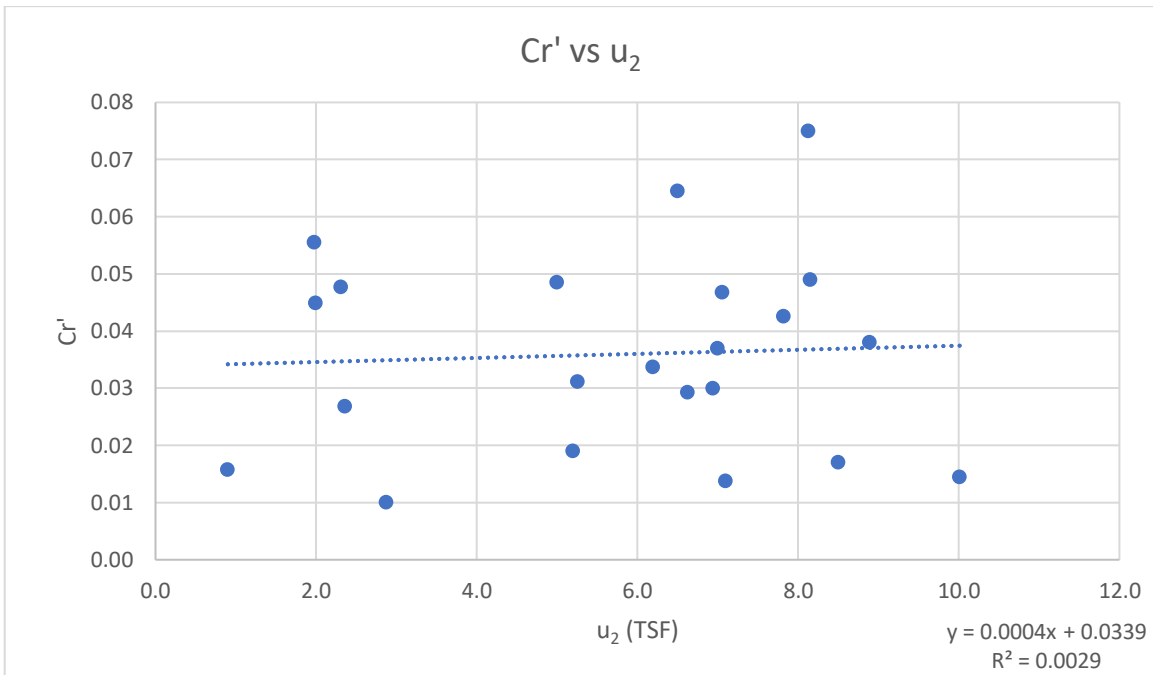


Figure B-4: Recompression Index vs Pore Pressure, u_2

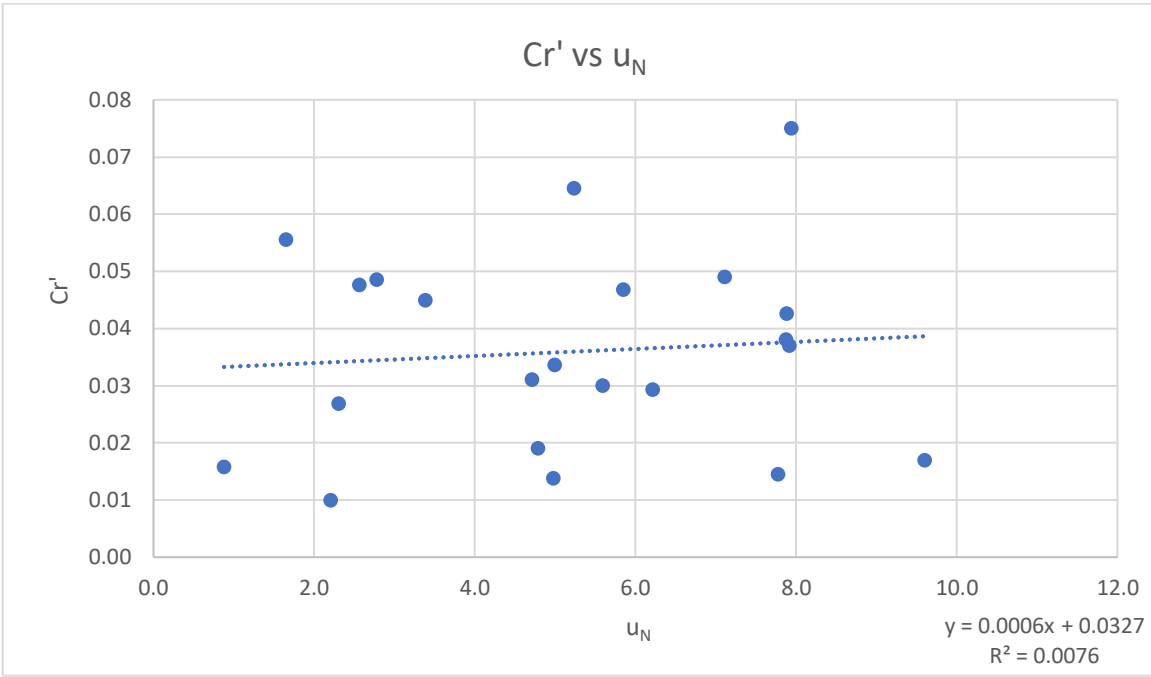


Figure B-5: Recompression Index vs Ratio of Pore Pressures, u_N

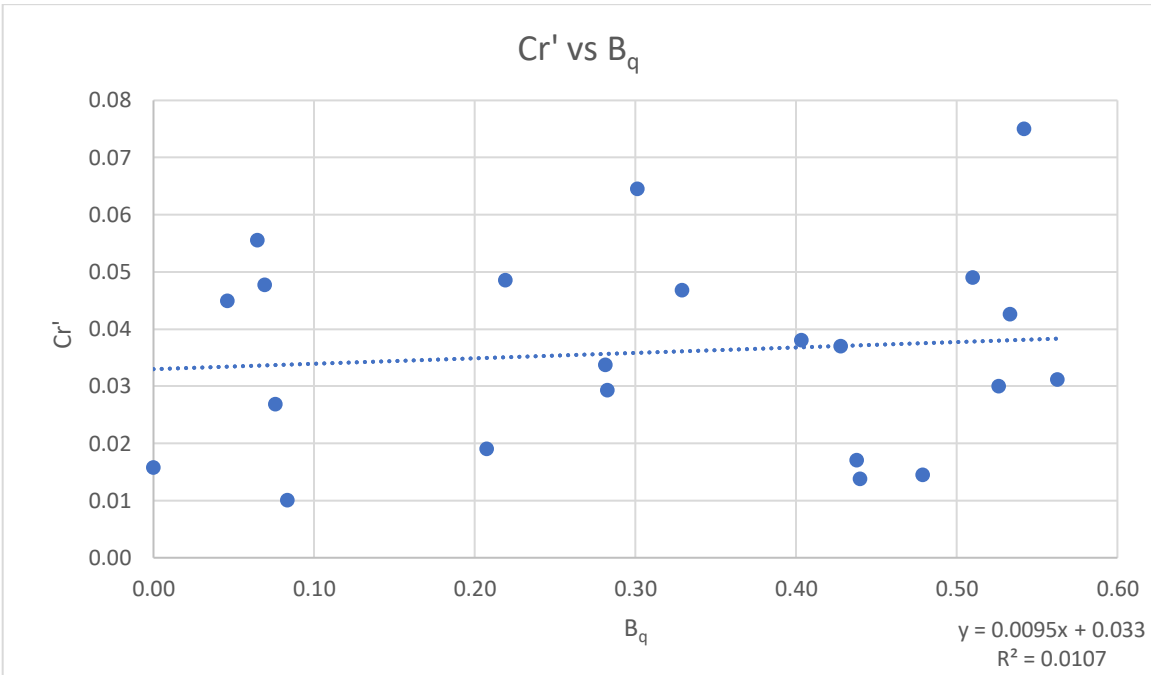


Figure B-6: Recompression Index vs Pore Pressure Ratio, B_q

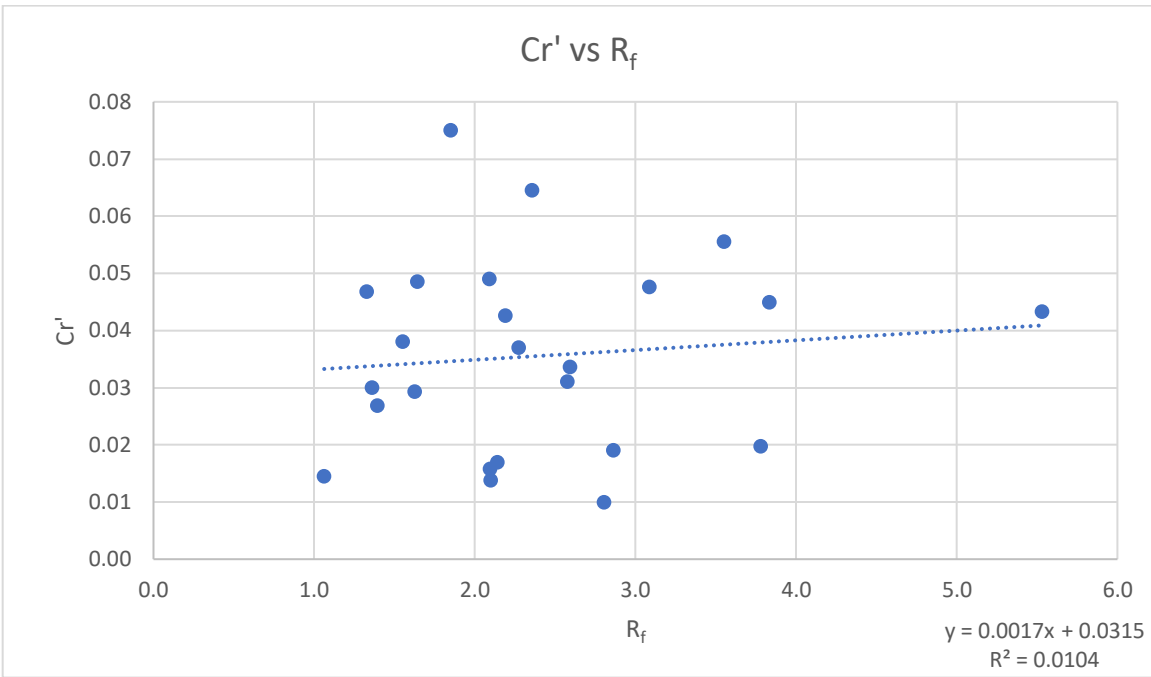


Figure B-7: Recompression Index vs Friction Ratio, R_f

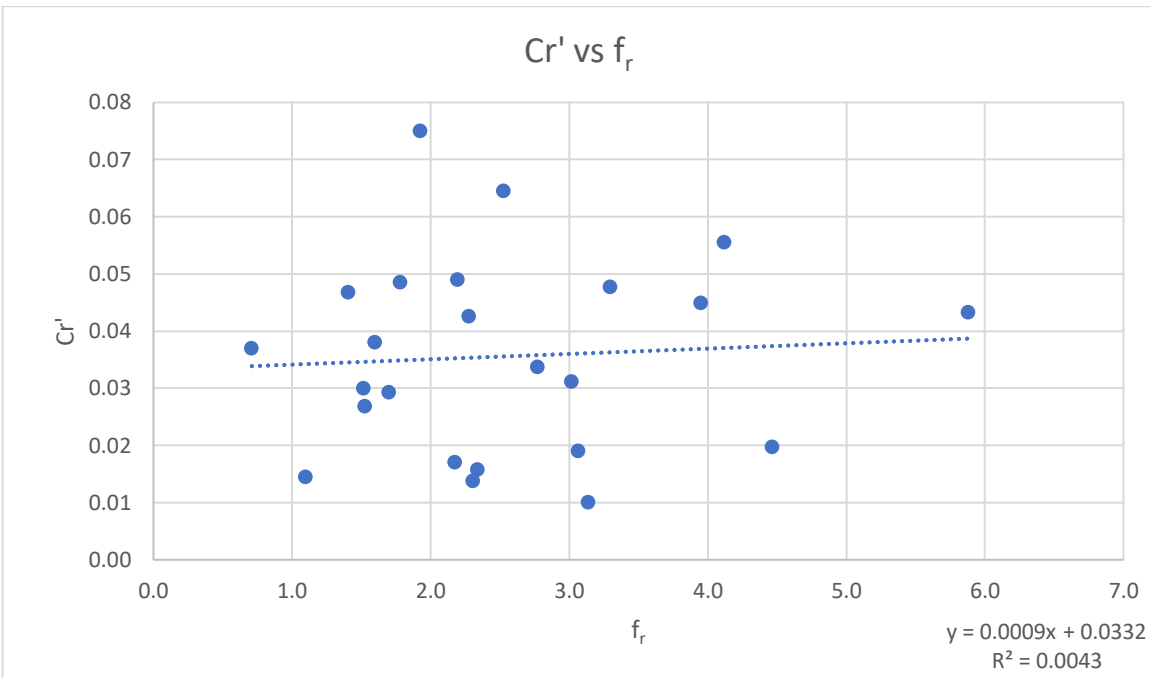


Figure B-8: Recompression Index vs Normalized Friction Ratio, f_r

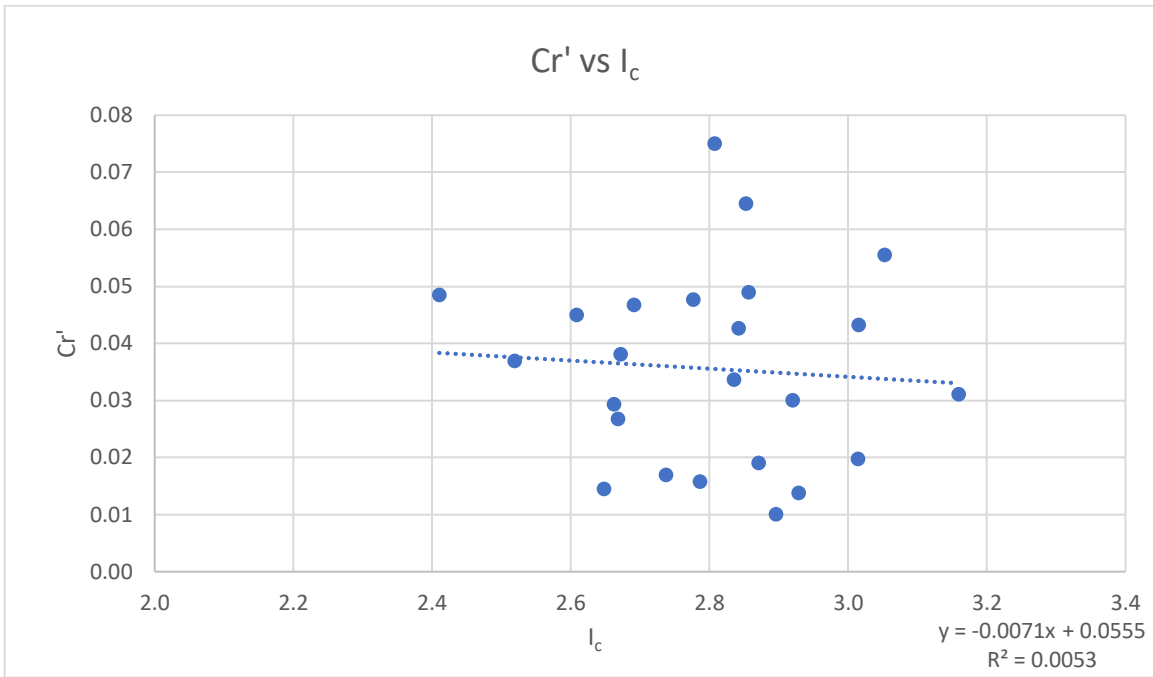


Figure B-9: Recompression Index vs Soil Behavior Type Index, I_c

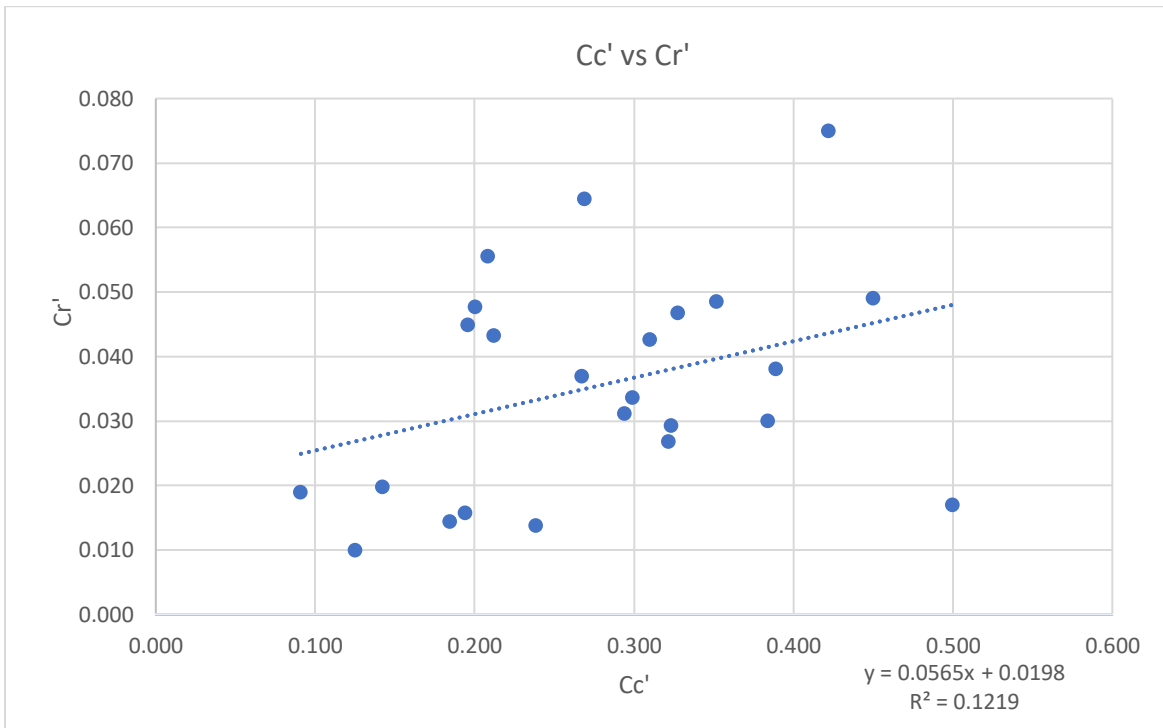


Figure B-10: Compression Index vs Recompression Index

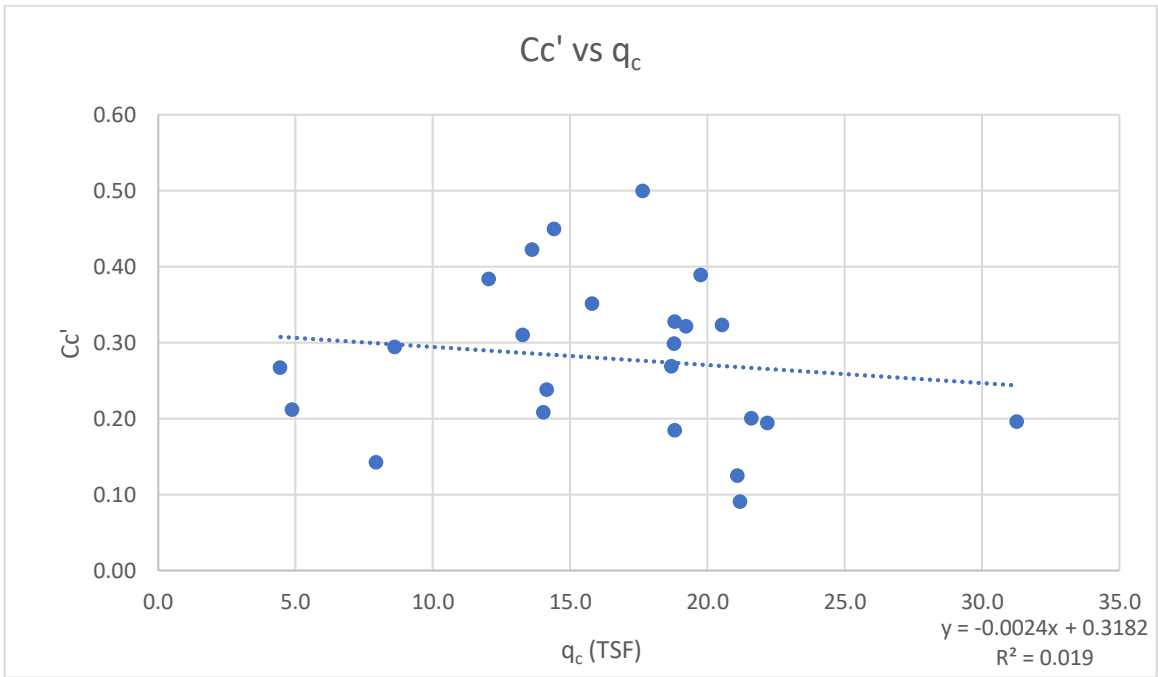


Figure B-11: Compression Index vs Tip Resistance, q_c

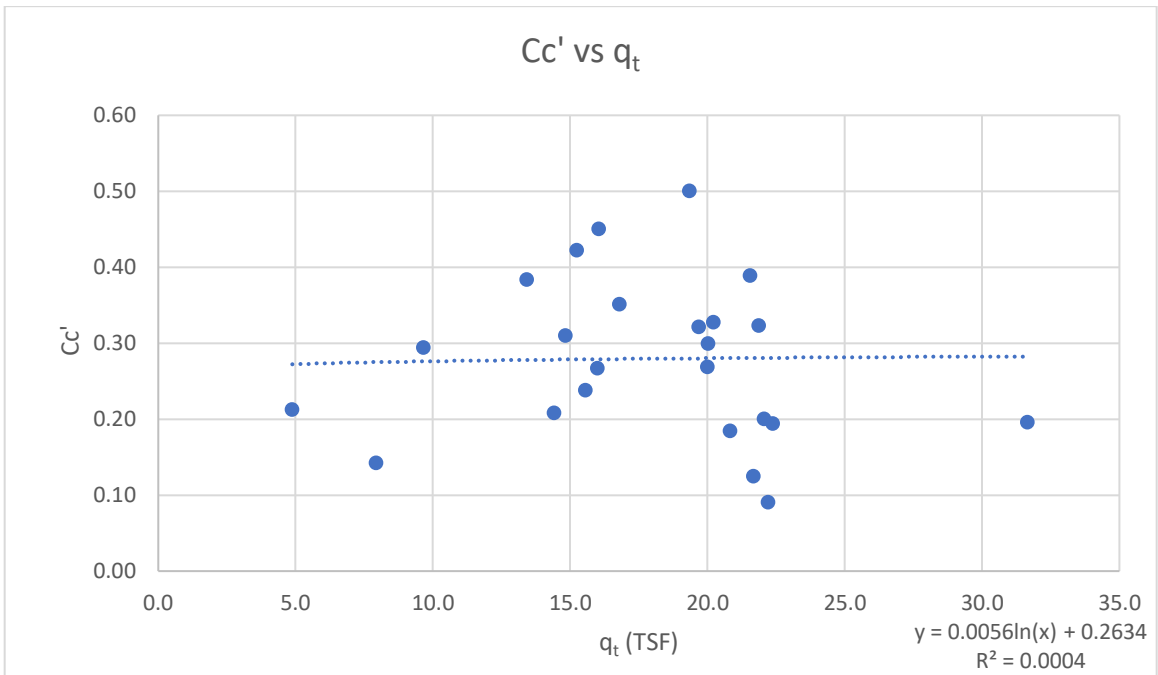


Figure B-12: Compression Index vs Corrected Tip Resistance, q_t

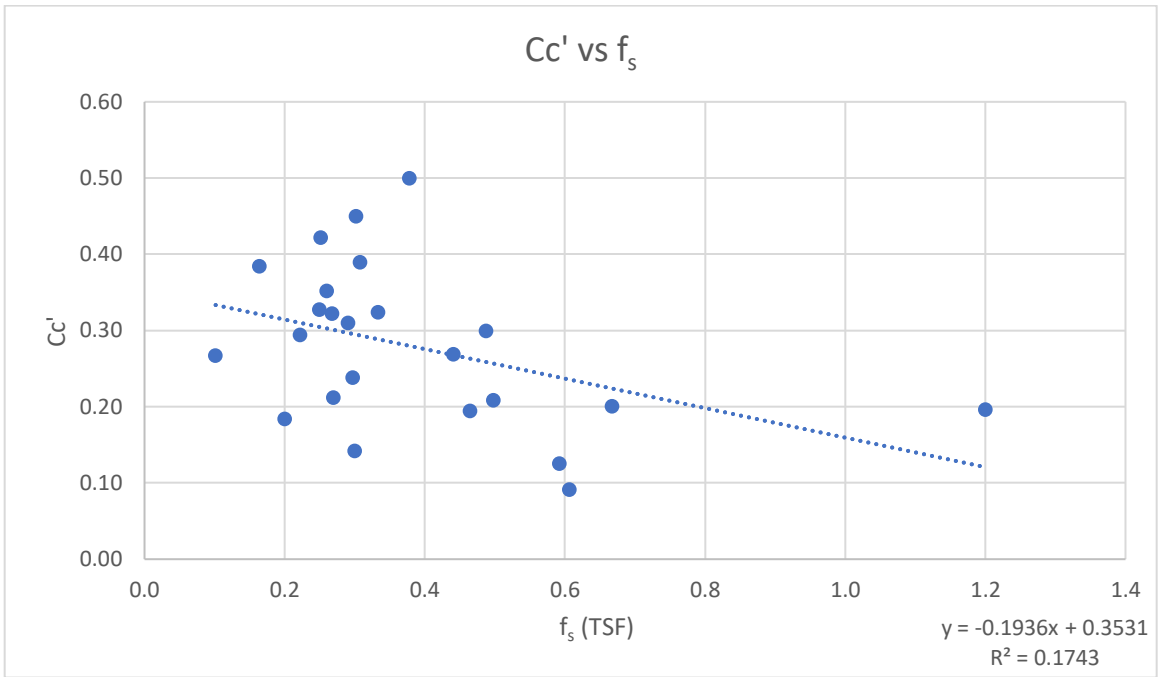


Figure B-13: Compression Index vs Sleeve Friction, f_s

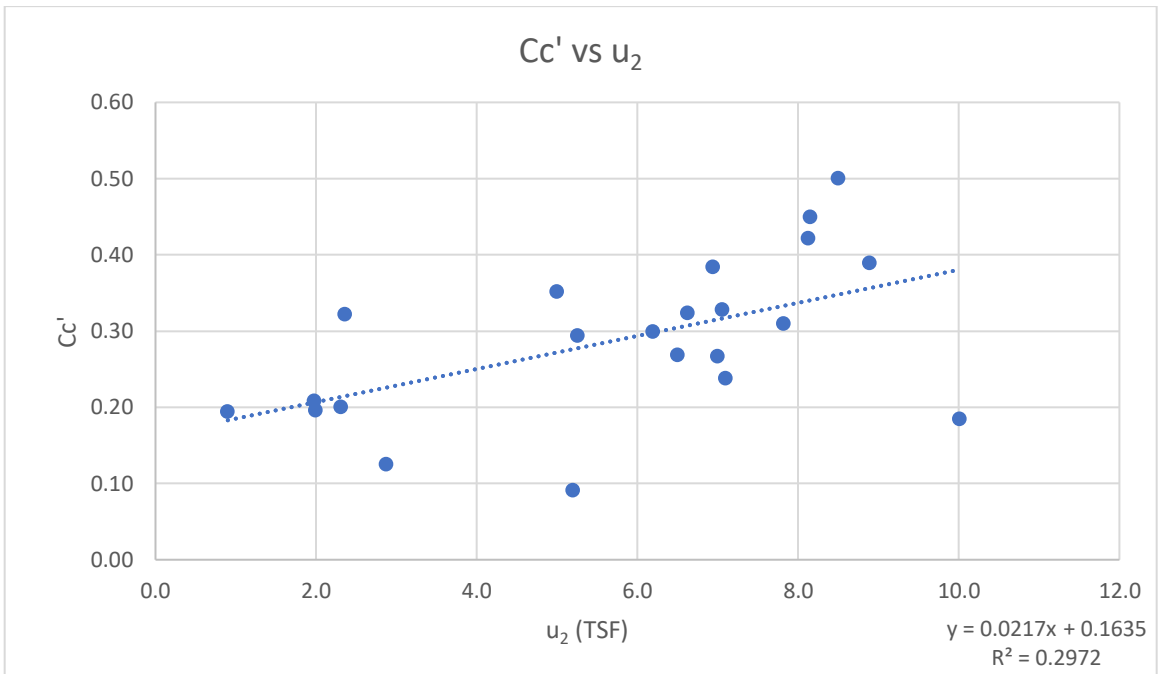


Figure B-14: Compression Index vs Pore Pressure, u_2

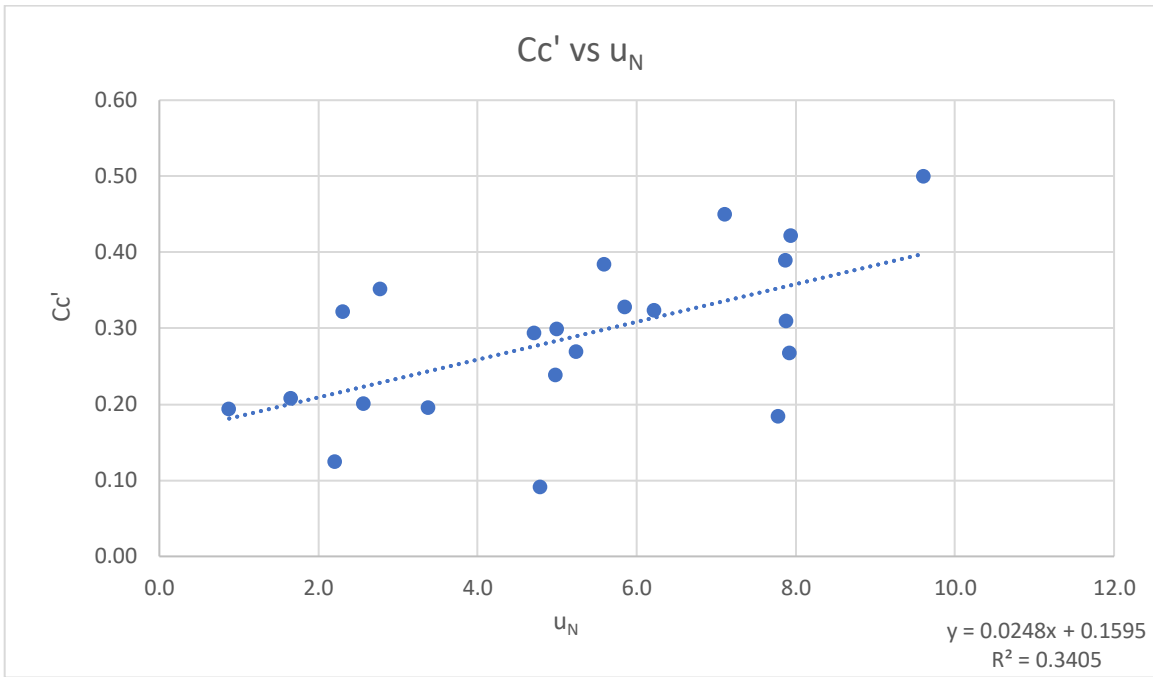


Figure B-15: Compression Index vs Ratio of Pore Pressures, u_N

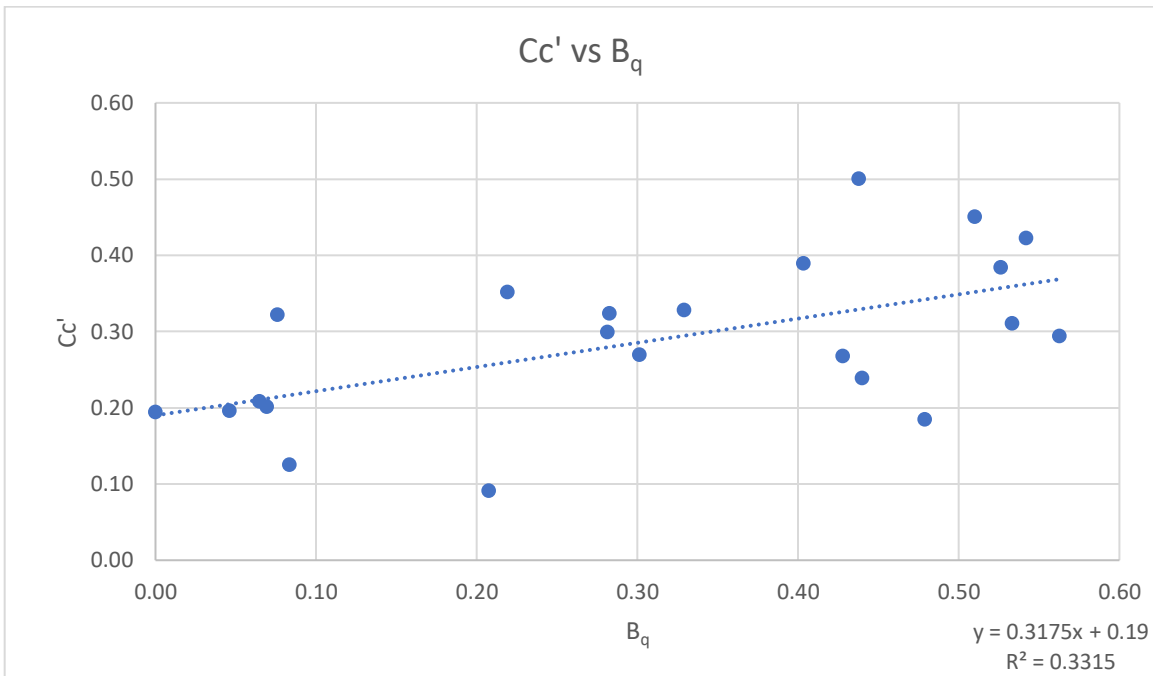


Figure B-16: Compression Index vs Pore Pressure Ratio, B_q

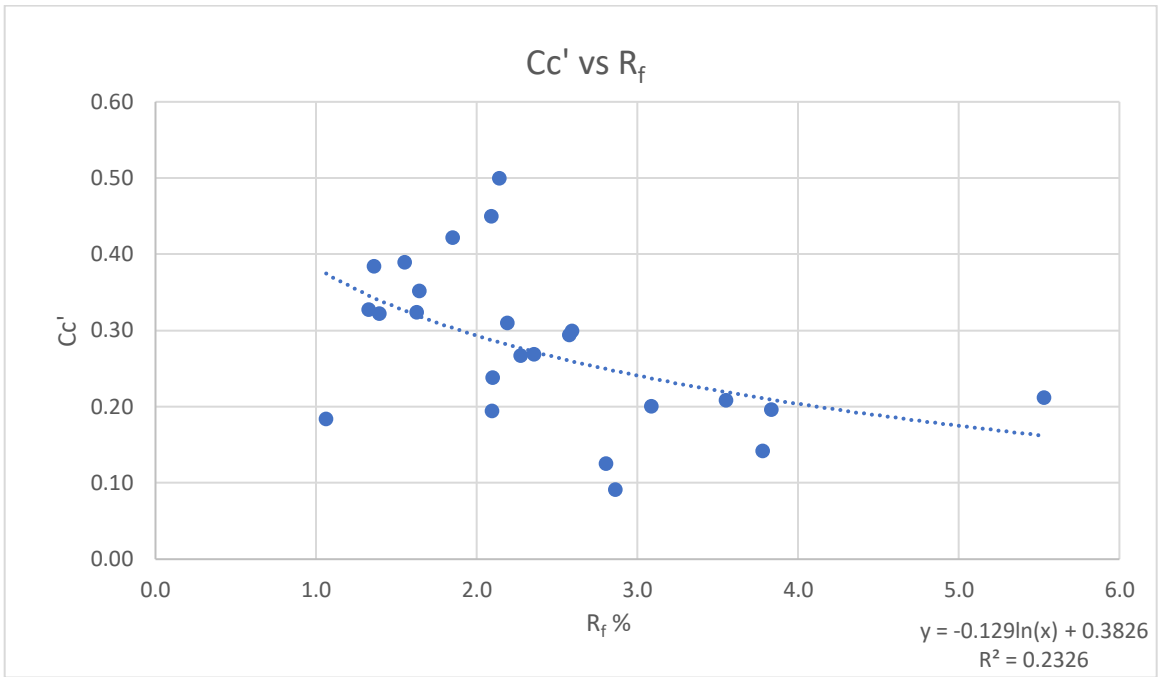


Figure B-17: Compression Index vs Friction Ratio, R_f

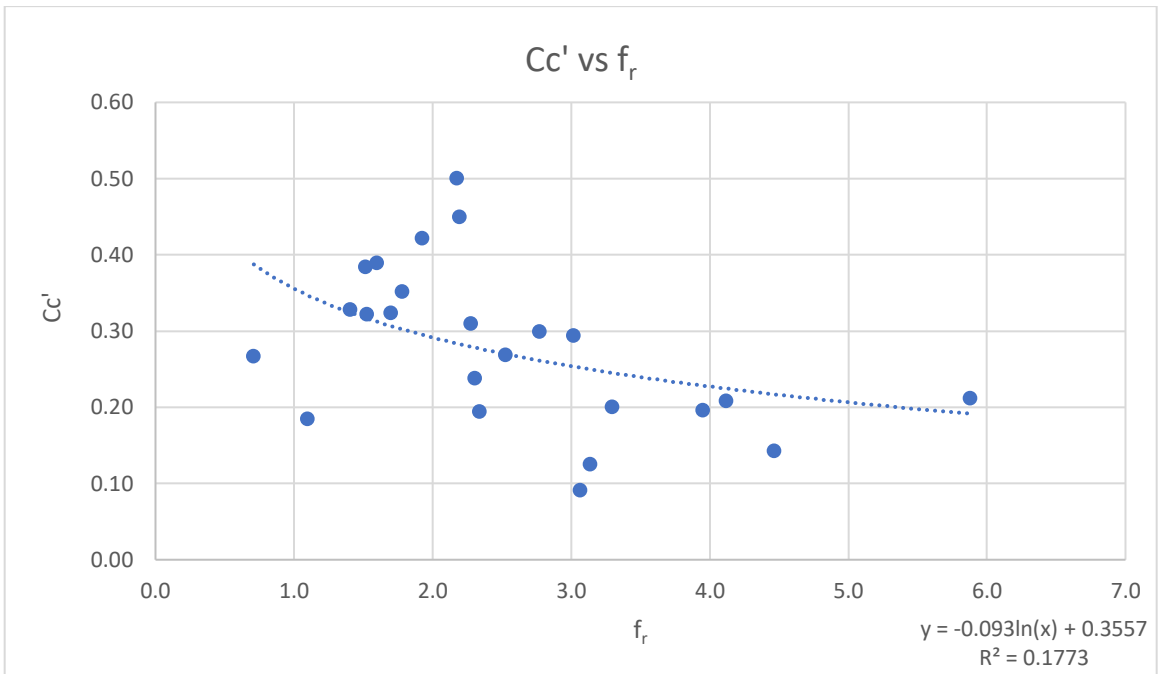


Figure B-18: Compression Index vs Normalized Friction Ratio, f_r

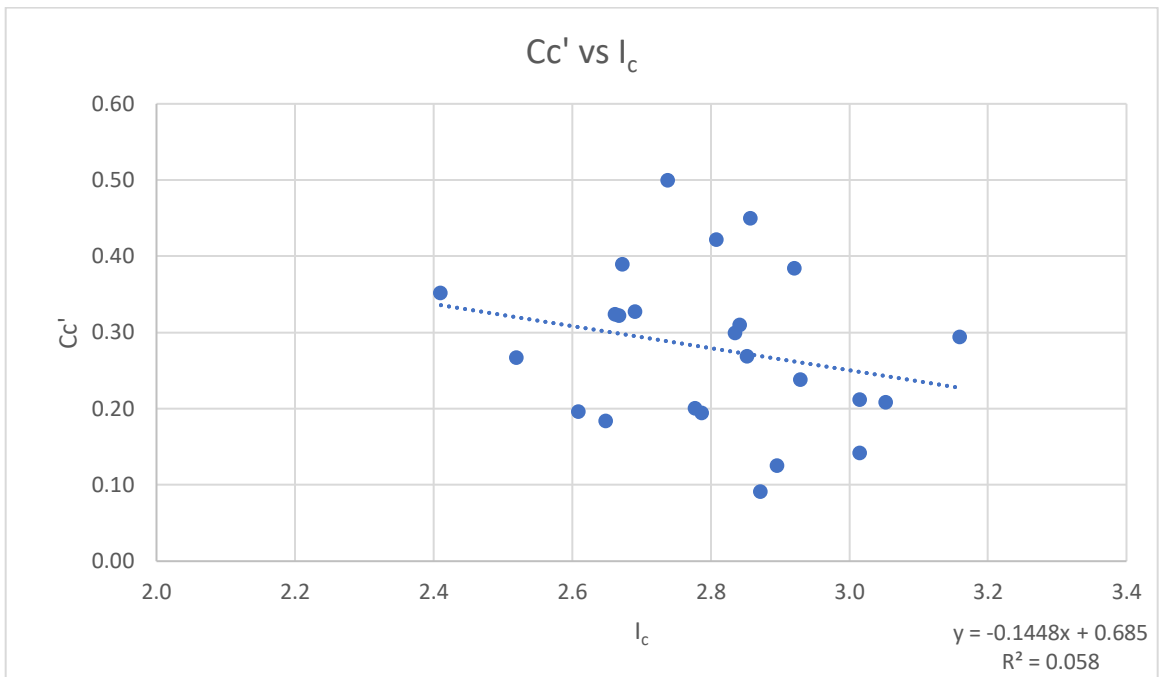


Figure B-19: Compression Index vs Soil Behavior Type Index, I_c

APPENDIX C - CONE PENETRATION TEST BASED CORRELATIONS (DIVIDED)

Divided - Activity

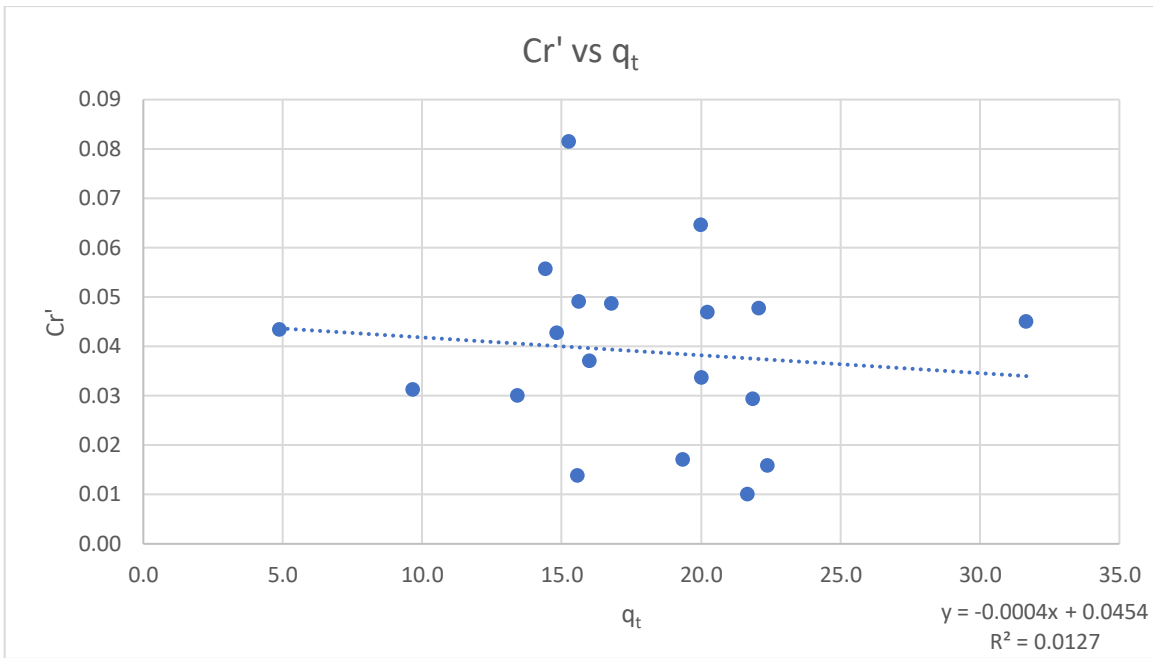


Figure C-1: Recompression Index vs Corrected Tip Resistance, q_t

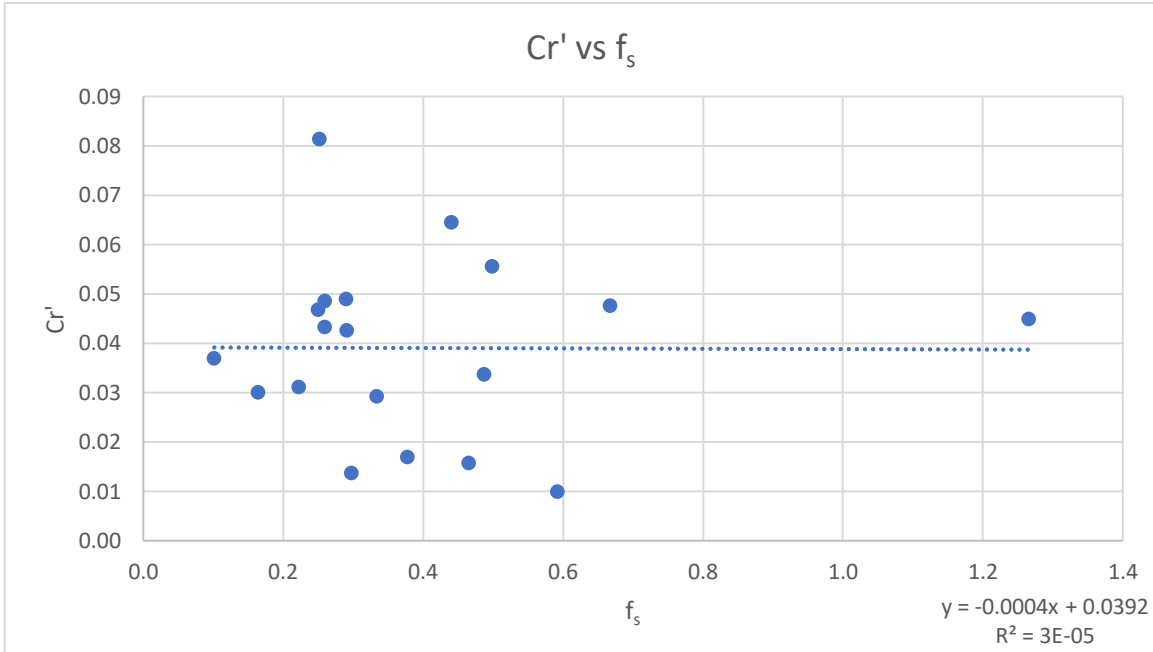


Figure C-2: Recompression Index vs Sleeve Friction, f_s

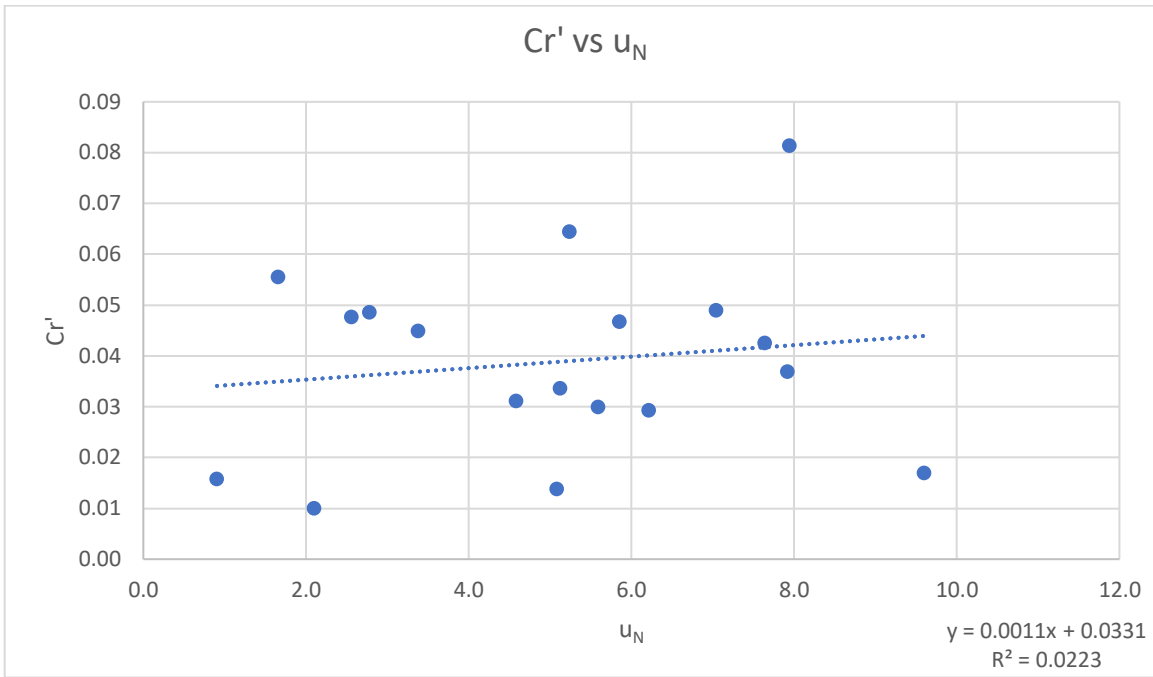


Figure C-3: Recompression Index vs Ratio of Pore Pressures, u_N

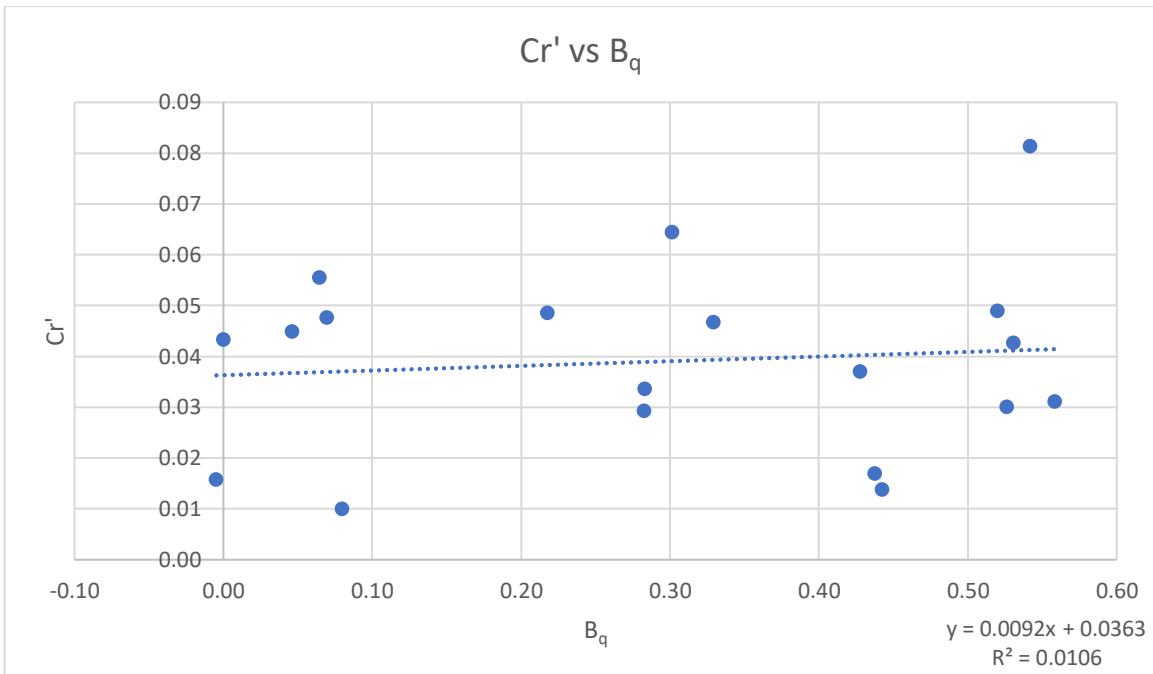


Figure C-4: Recompression Index vs Pore Pressure Ratio, B_q

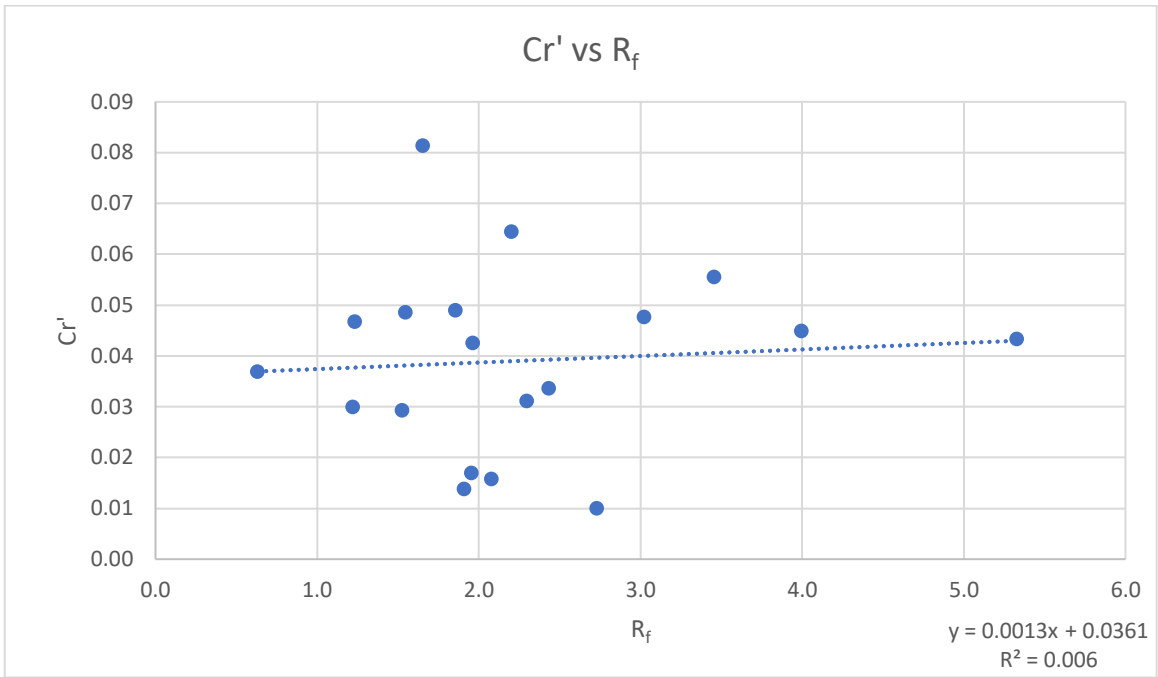


Figure C-5: Recompression Index vs Friction Ratio, R_f

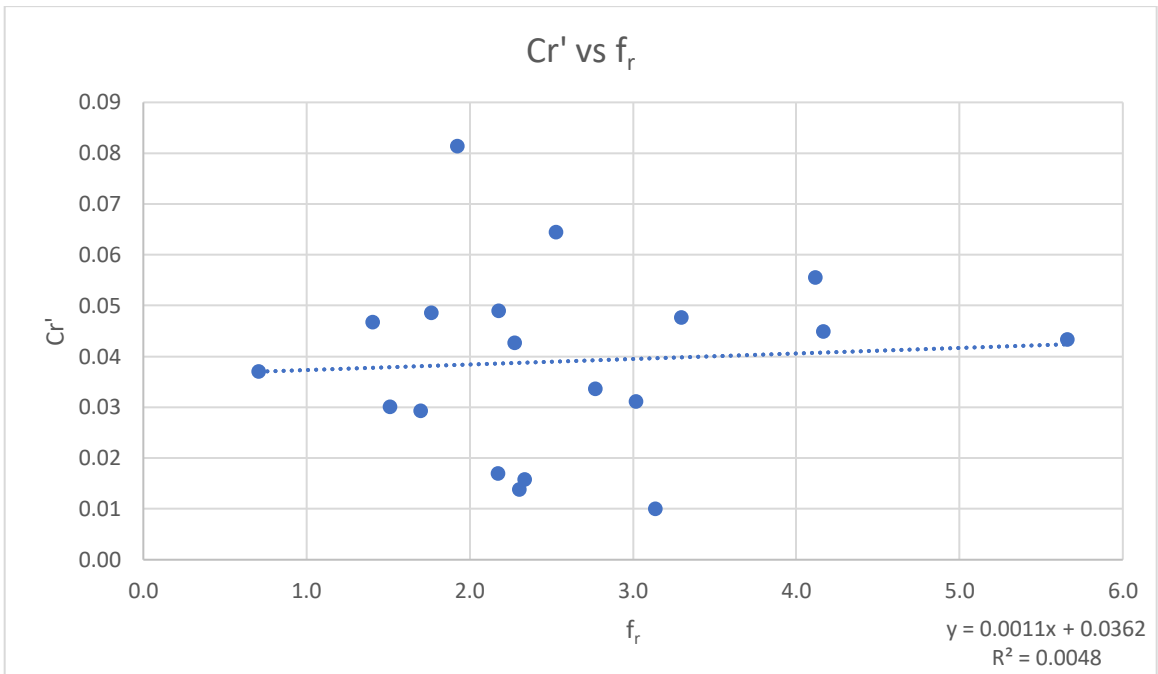


Figure C-6: Recompression Index vs Normalized Friction Ratio, f_r

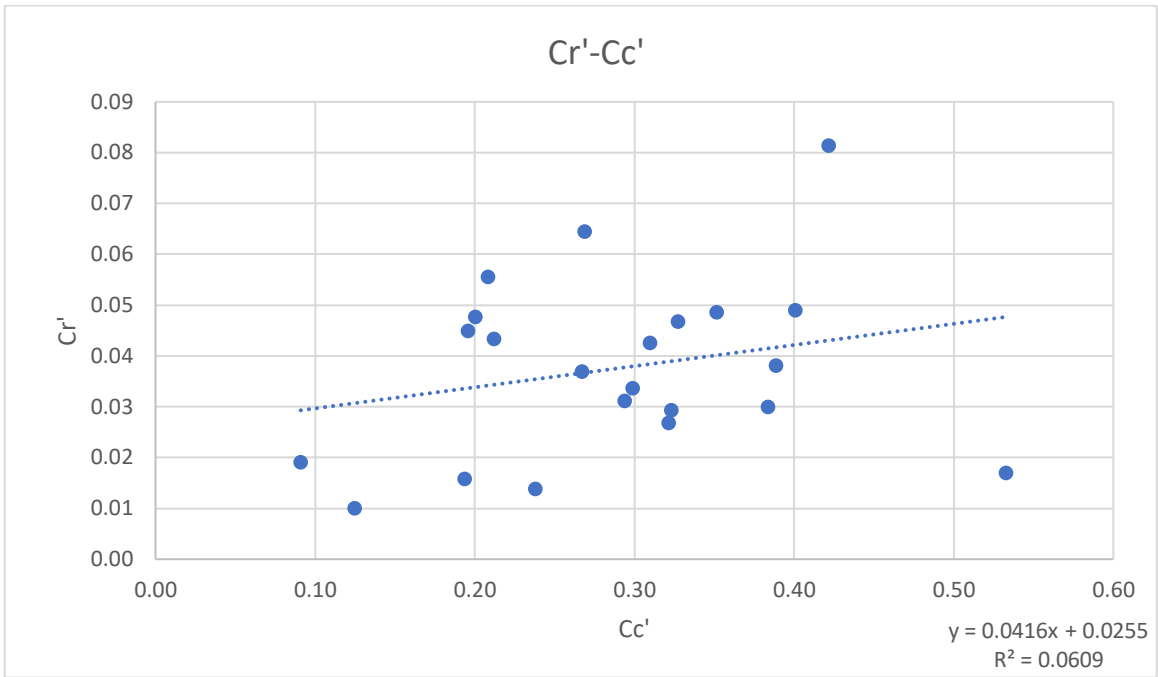


Figure C-7: Recompression Index vs Compression Index

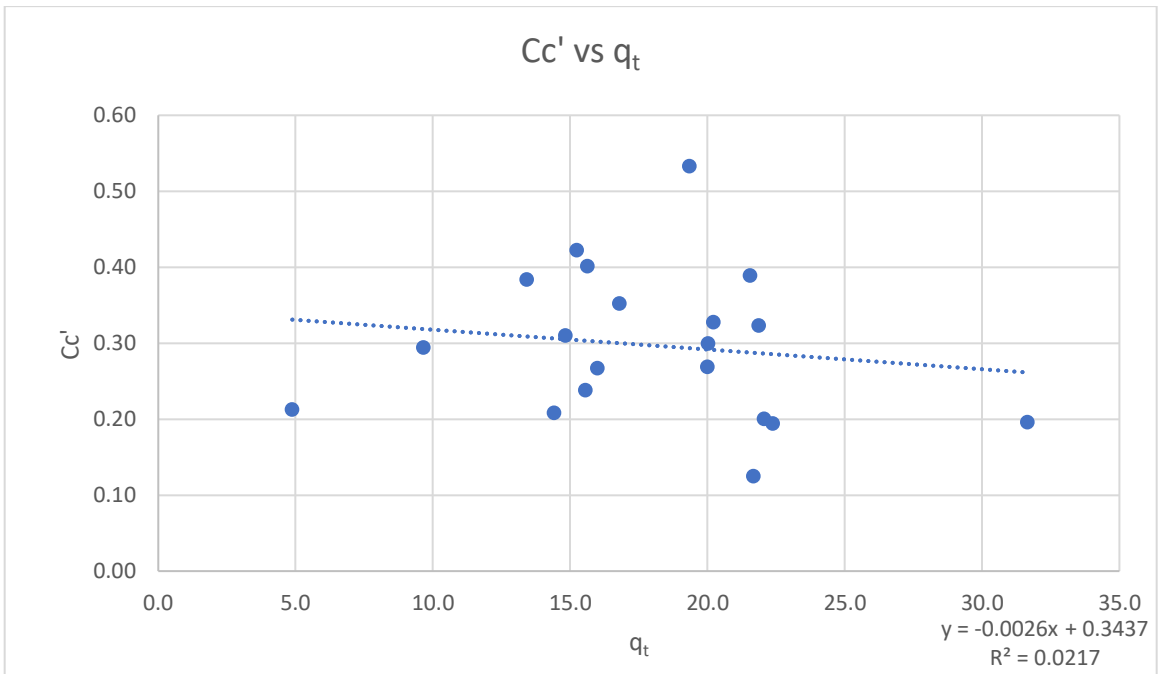


Figure C-8: Compression Index vs Corrected Tip Resistance, q_t

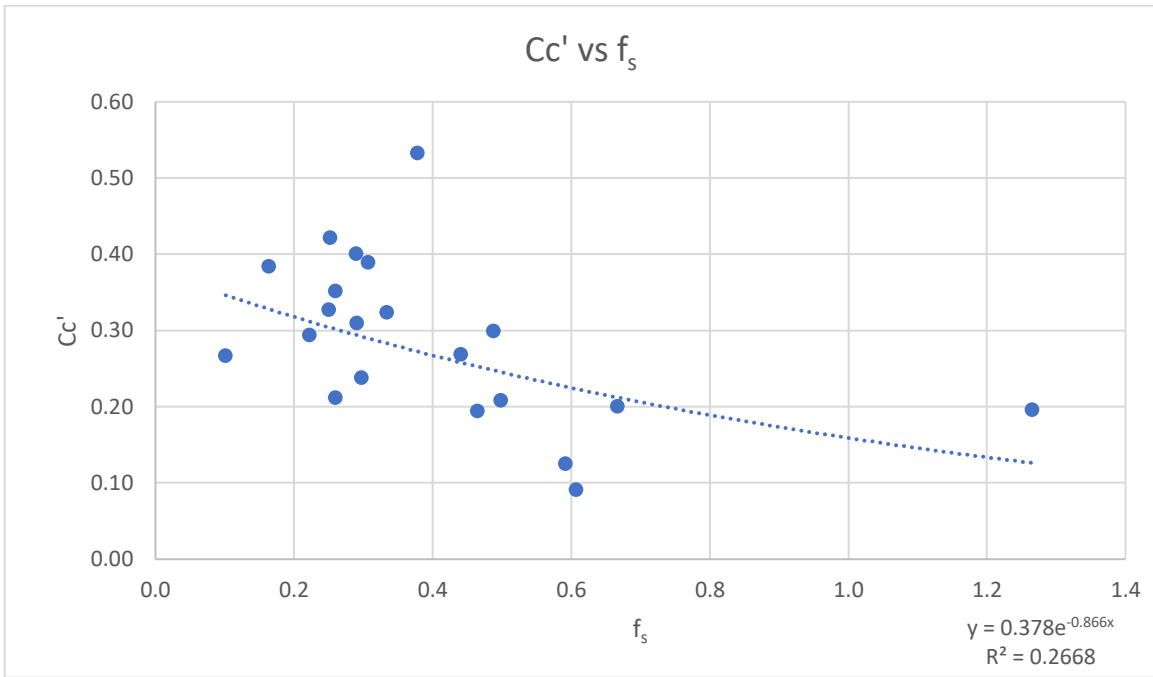


Figure C-9: Compression Index vs Sleeve Friction, f_s

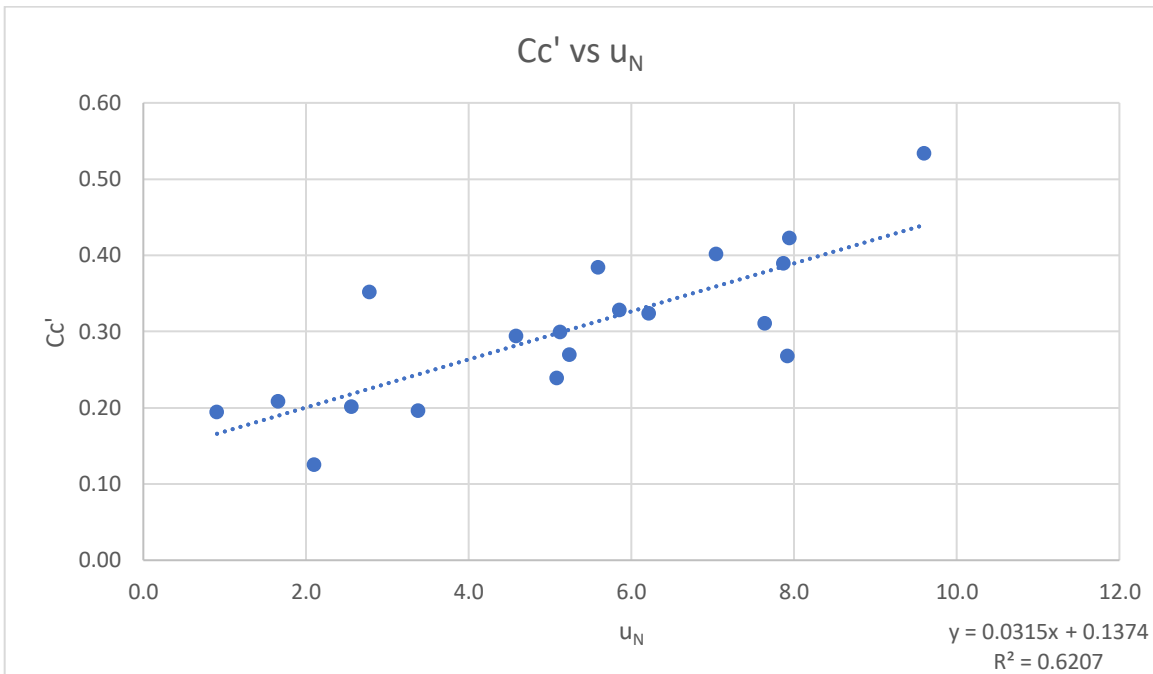


Figure C-10: Compression Index vs Ratio of Pore Pressures, u_N

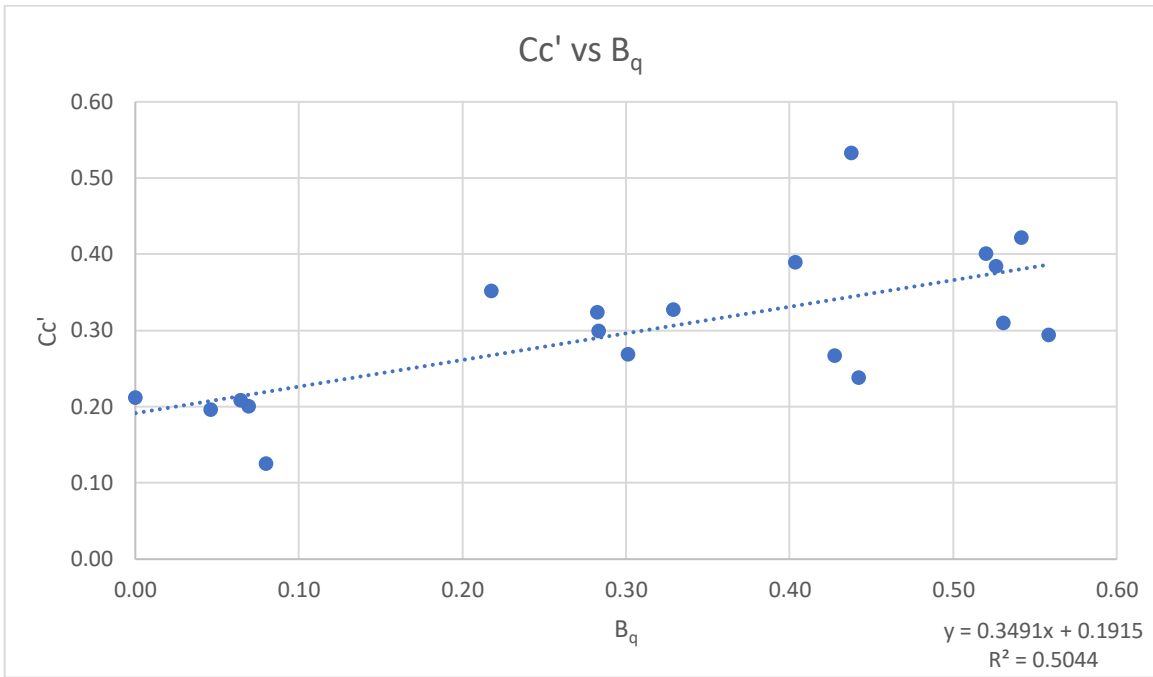


Figure C-11: Compression Index vs Pore Pressure Ratio, B_q

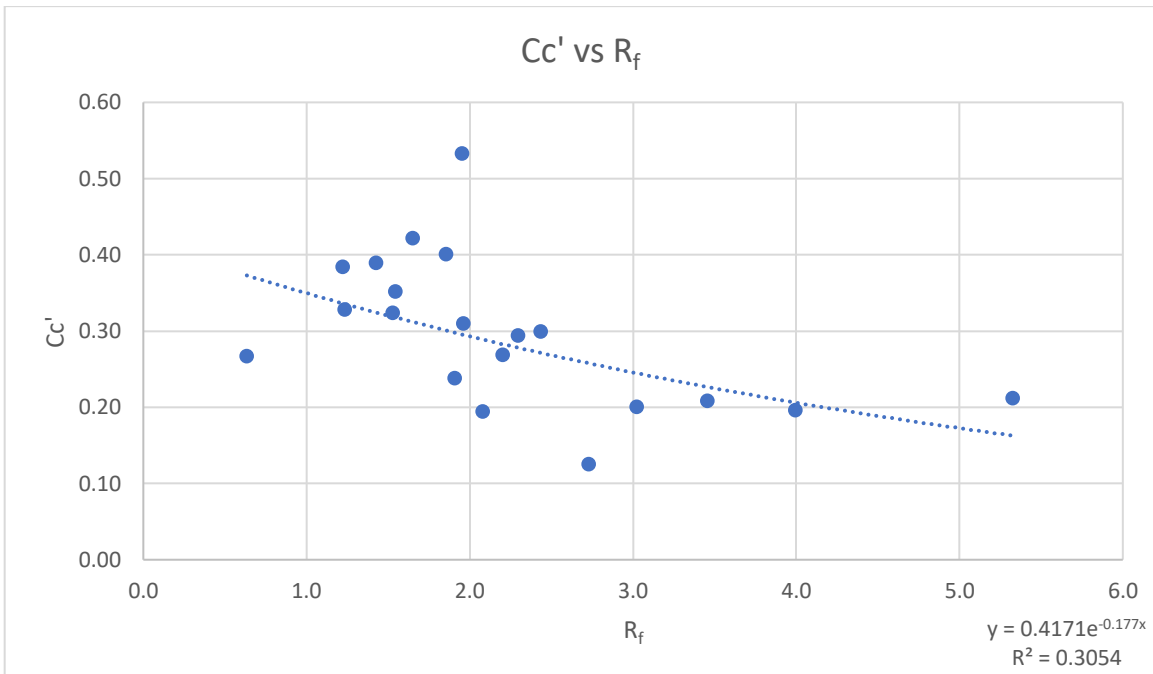


Figure C-12: Compression Index vs Friction Ratio, R_f

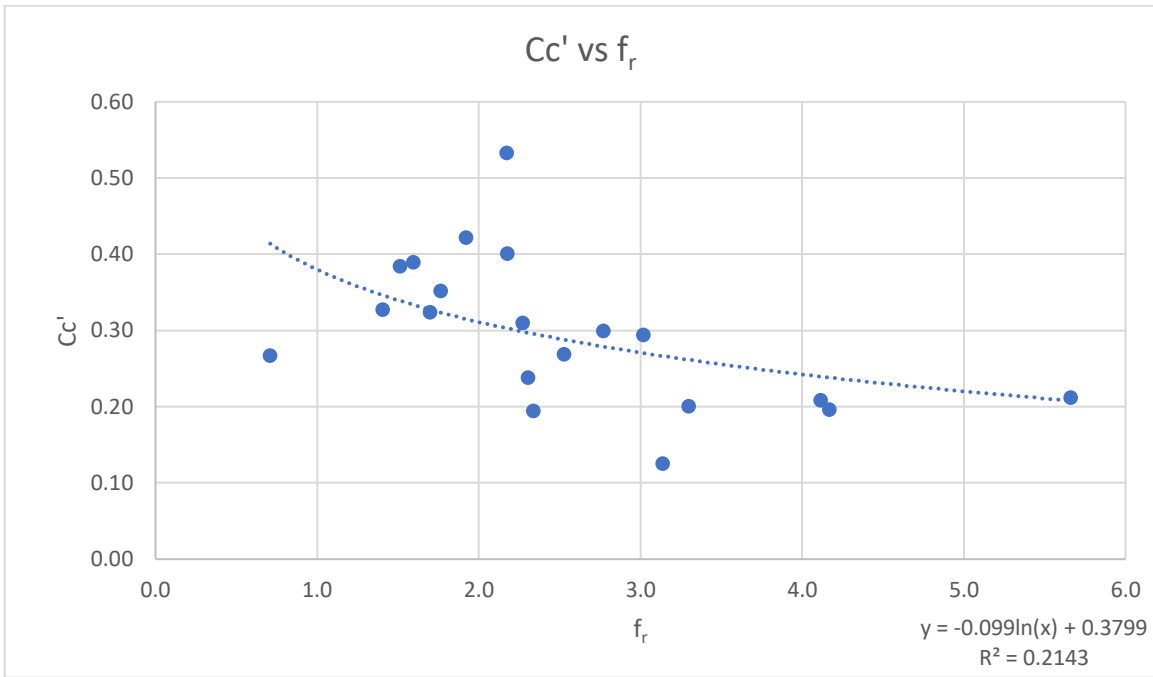


Figure C-13: Compression Index vs Normalized Friction Ratio, f_r

Divided – Moisture Content

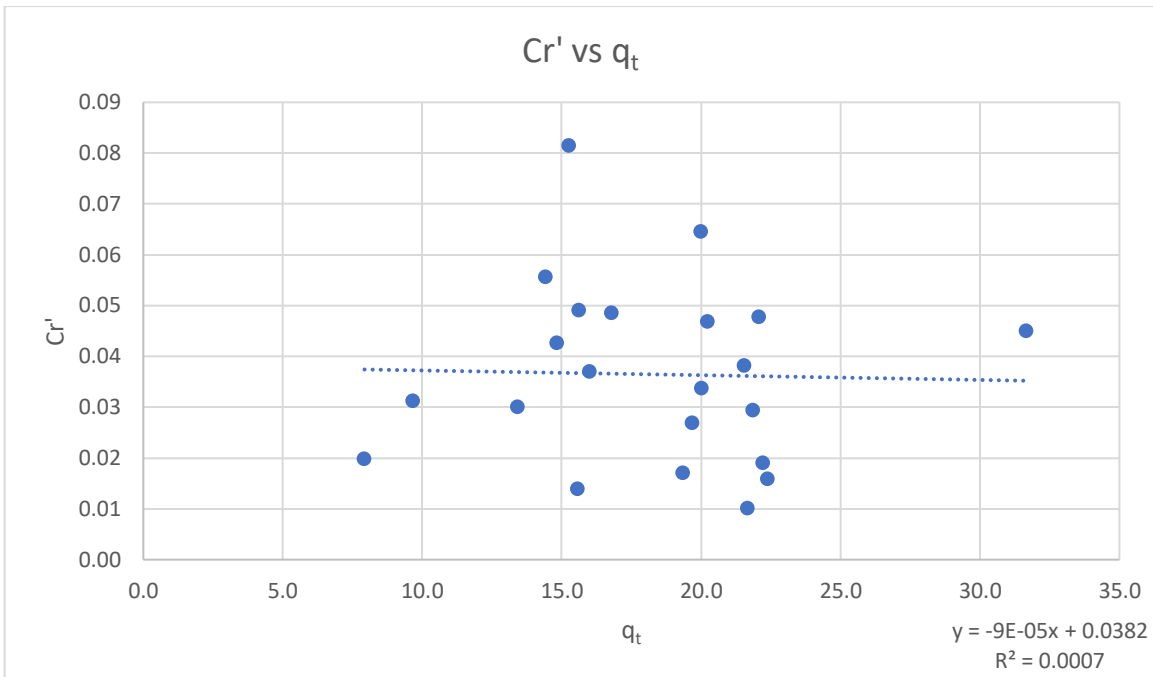


Figure C-14: Recompression Index vs Corrected Tip Resistance, q_t

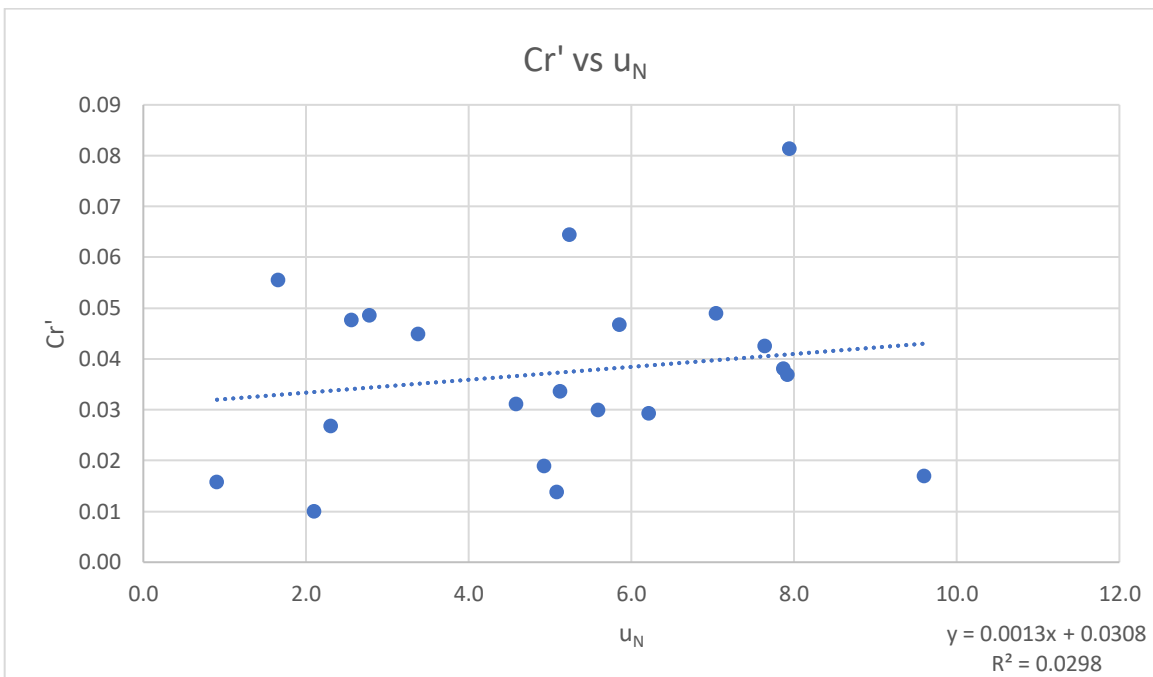


Figure C-15: Recompression Index vs Ratio of Pore Pressures, u_N

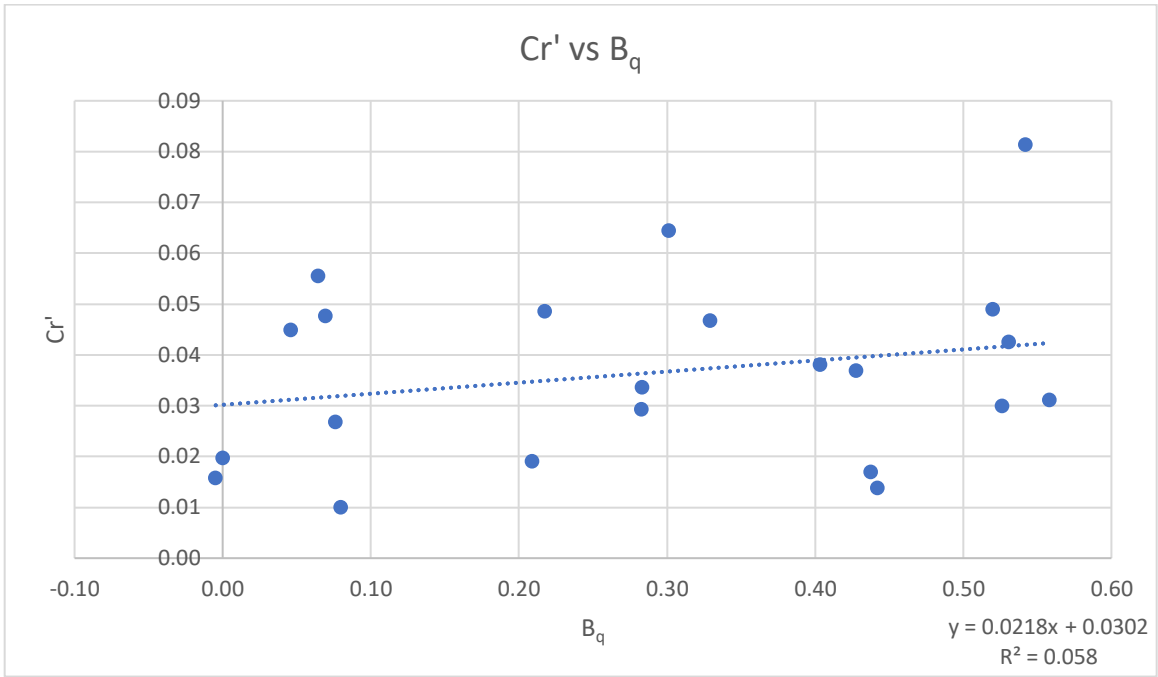


Figure C-16: Recompression Index vs Pore Pressure Ratio, B_q

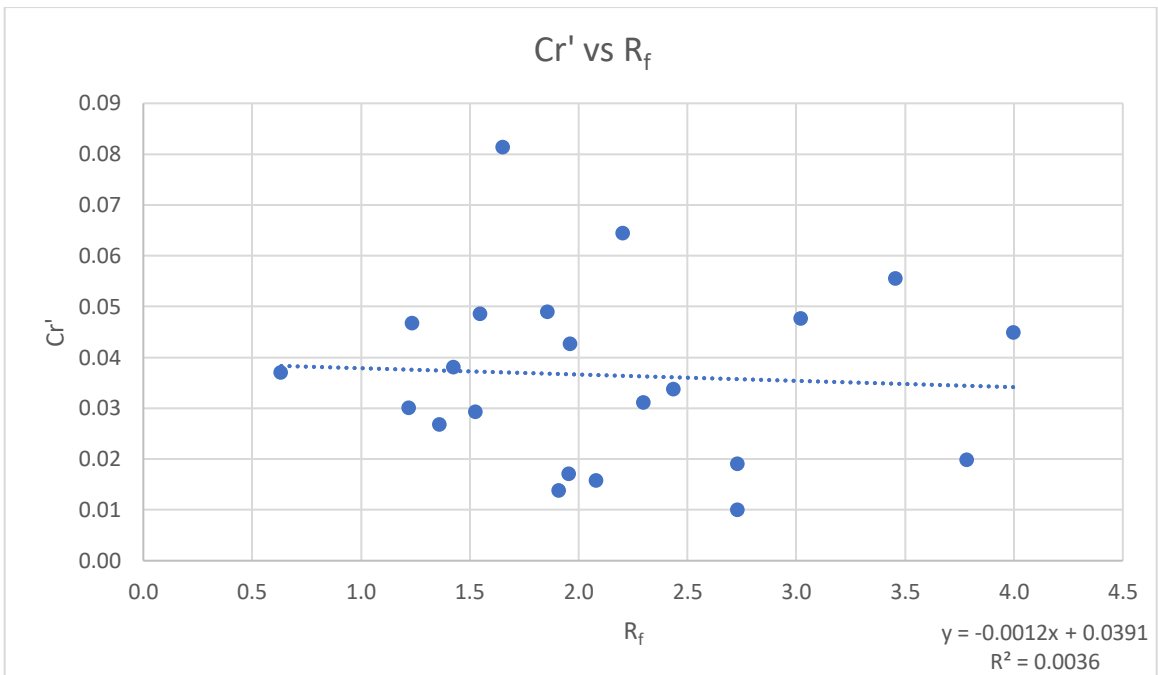


Figure C-17: Recompression Index vs Friction Ratio, R_f

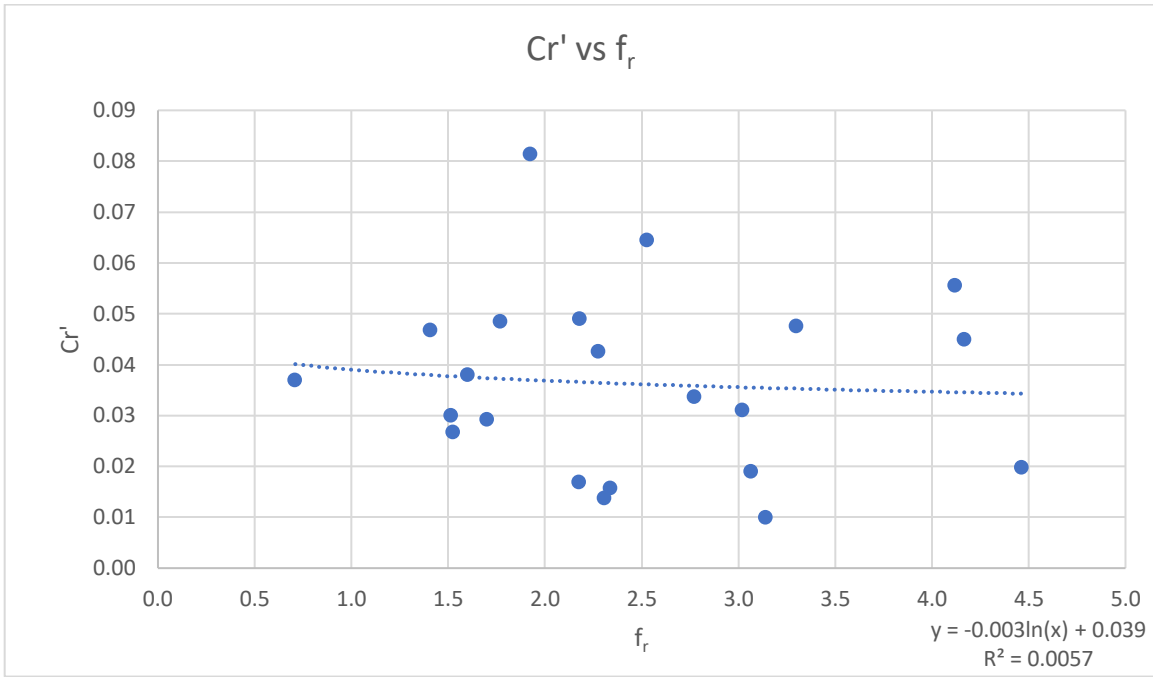


Figure C-18: Recompression Index vs Normalized Friction Ratio, f_r

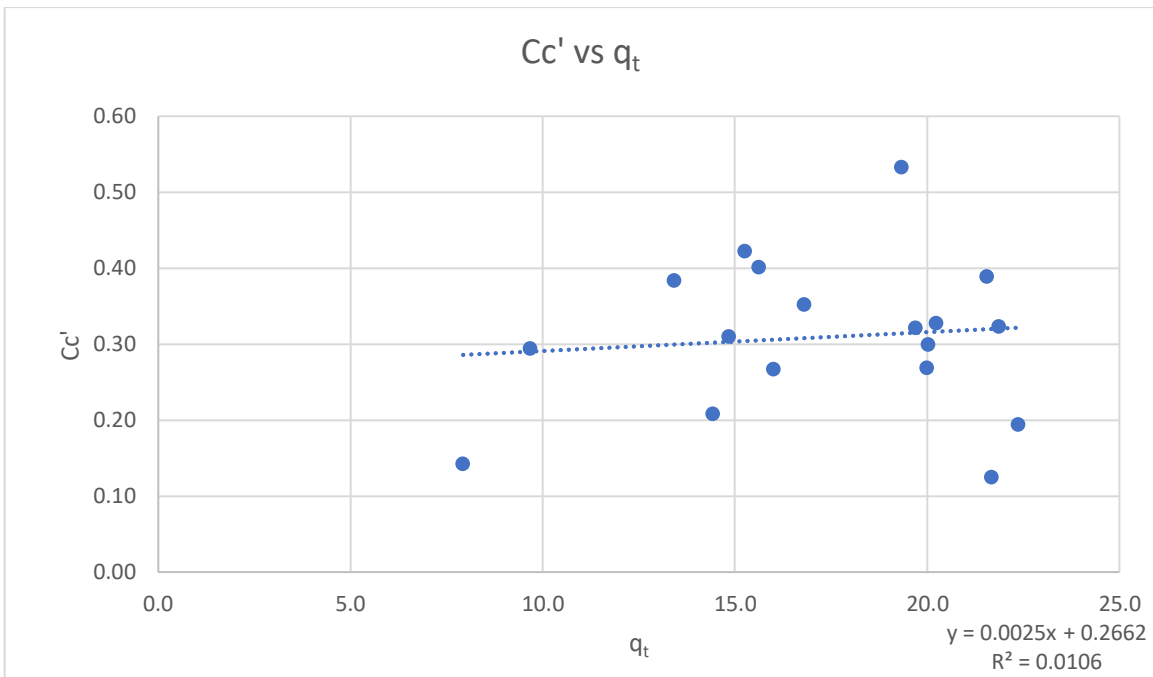


Figure C-19: Compression Index vs Corrected Tip Resistance, q_t

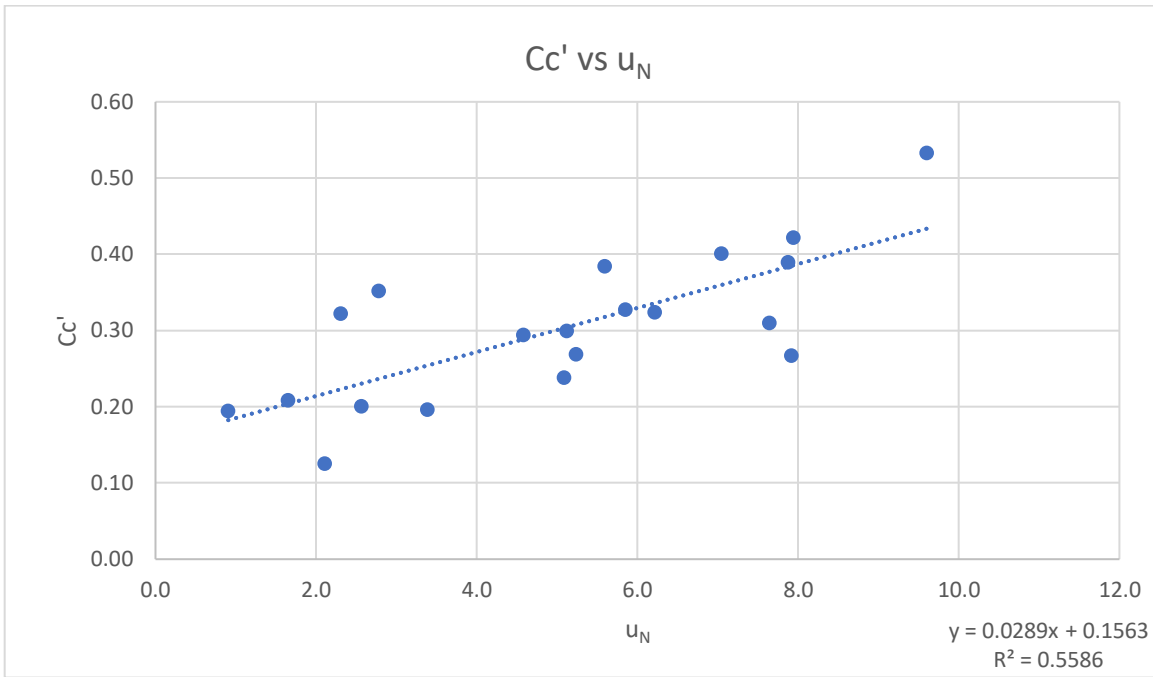


Figure C-20: Compression Index vs Ratio of Pore Pressures, u_N

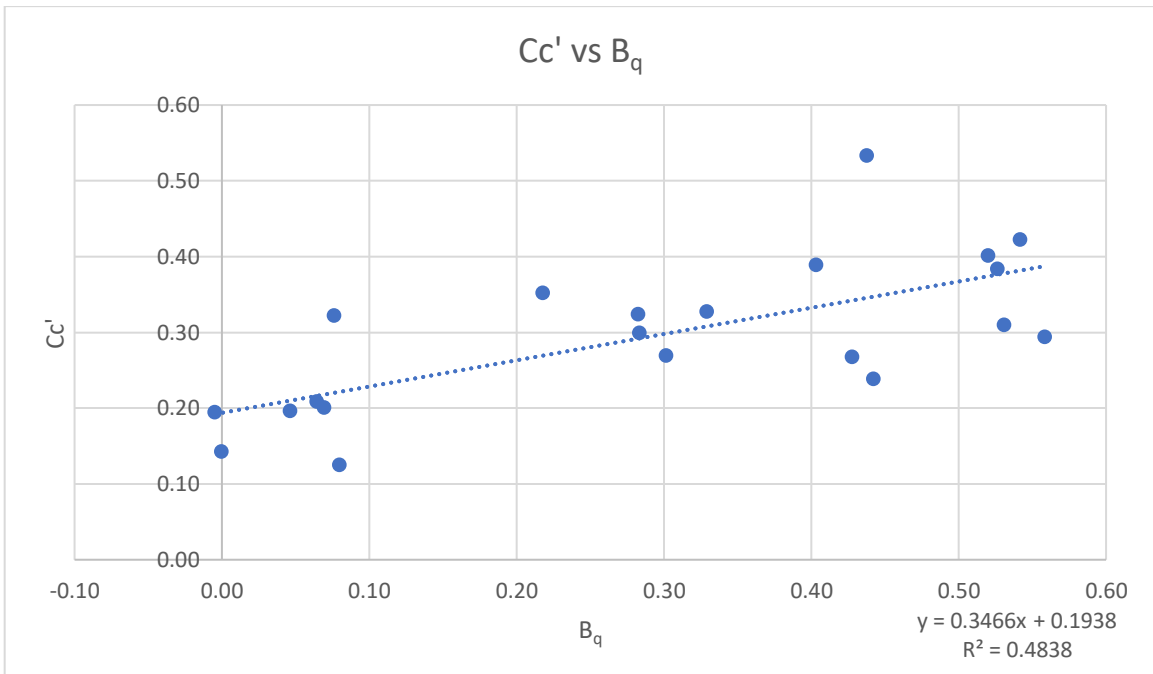


Figure C-21: Compression Index vs Pore Pressure Ratio, B_q

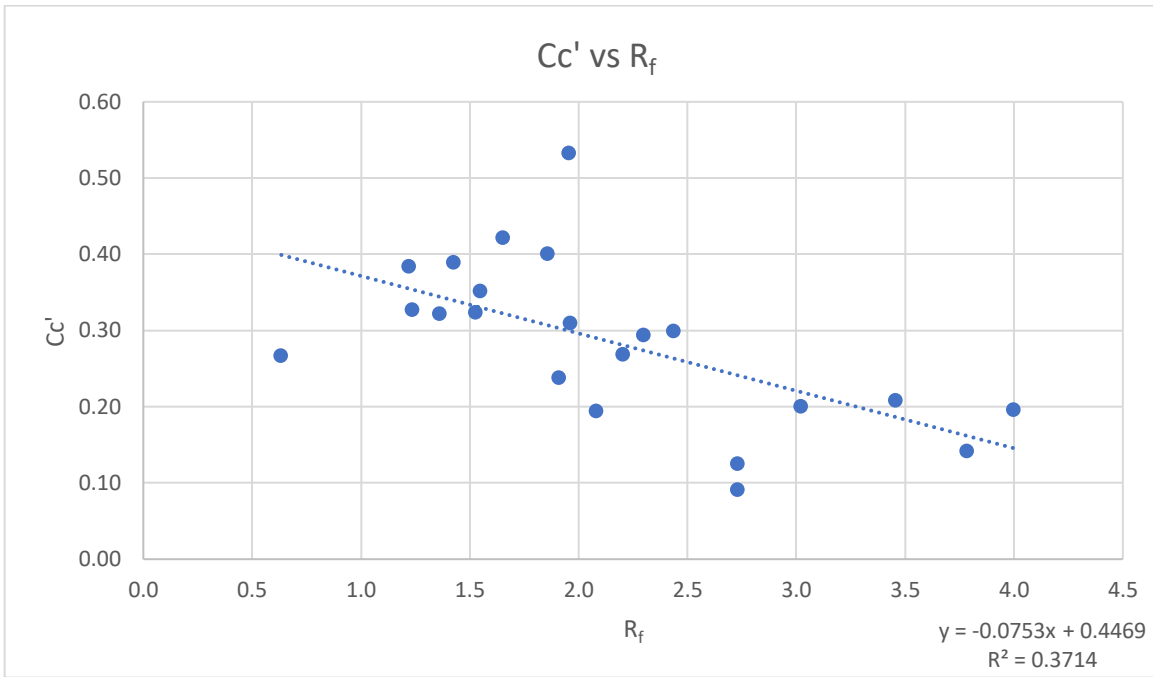


Figure C-22: Compression Index vs Friction Ratio, R_f

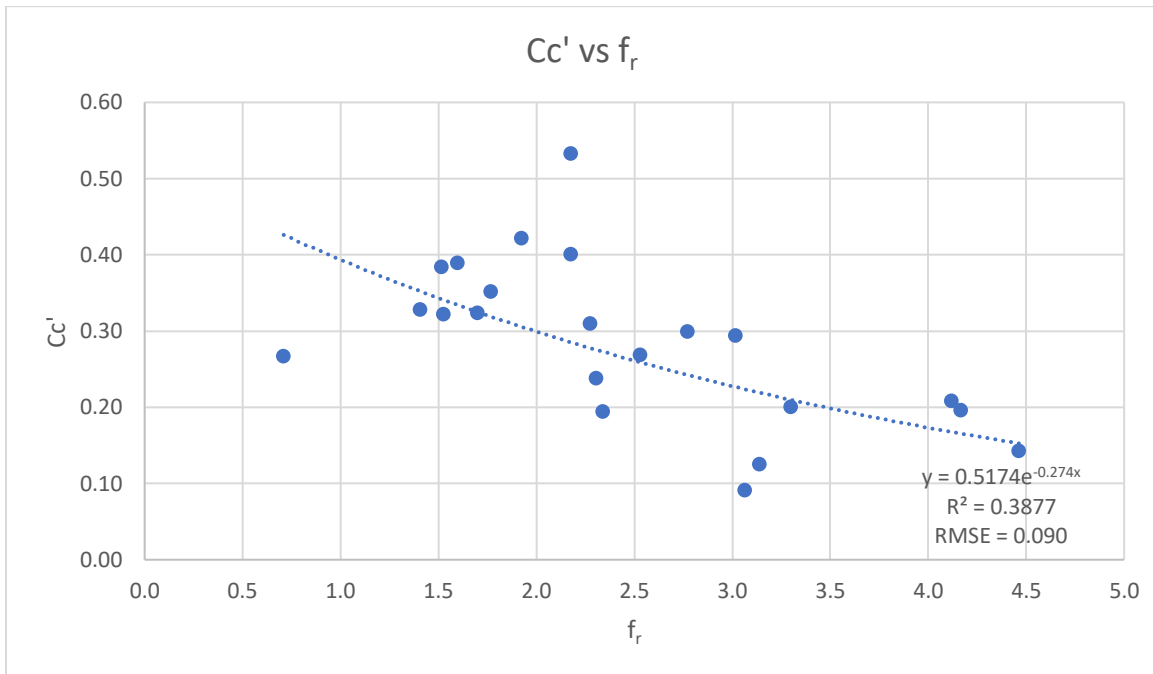


Figure C--23: Compression Index vs Normalized Friction Ratio, f_r

APPENDIX D – SNIPPET OF UCF DATA BASE

FPID	Project Description	Soil Type	Classification (USCS)	Effective Overburden Pressure (ksf)	Wet Density (pcf)	Dry Density (pcf)	w (%)	SPT N	Fines (-200) (%)	LL	OC (%)	PI	LI	eo	Gs	Cc	e-stre	Cr	Activity
200966-1	I-75 and Alico Road Intersection	Fine Graine	CH	1.66	101.09	60.1	68.2	2.42	76	56		32	1.38	1.69	2.59	1.69	0.05	0.42	
208224-4	SR 23 Old Jennings Rd to Kindlewood	Fine Graine	CH	0.64	120.67	94.2	28.1	4.03	51	56	2	37	0.25	0.71	2.58	0.25	0.02	0.73	
2770G (GE	Yankee Lake Pump Station	Fine Graine	CH	1.86	95.4	58.6	62.8	1.61	62	56		37	1.18	1.44	2.29	0.22	0.05	0.60	
258462-1	I-4 and Branch Forbes Rd.	Fine Graine	CH/CL	2.43			47	6.45	30	56		20	0.55	1.15		0.32	0.08	0.67	
242702-2	I-4 St. John's River Bridge Ramp B1	Fine Graine	CH	0.71	115.9	84.6	37	2.42	80	55		38	0.53	1.01	2.73	0.32	0.04	0.48	
407143-5	SR 482 over Shingle Creek	Fine Graine	CH	1.98	108.89	80.6	35.1	5.65	76	55		39	0.49	0.83	2.36	0.29	0.04	0.51	
414959-1	US 192 Indian River Relief Bridges	Fine Graine	CH	1.82	87.95	51.4	71.1	3.23	86	55		35	1.46	1.41	1.99	0.37	0.08	0.41	
75280-140	I-4 and Conroy Road Interchange	Fine Graine	CH	1.01	113.52	86.0	32	5.65	77	55		35	0.34	0.83	2.52	0.25	0.03	0.45	
257051-1	SR 688 at 113th St.	Fine Graine	CH	2.27	123.05	94.8	29.8	40.32		54		27	0.10	0.89	2.87	0.10	0.02		
213323-4	I-95 at I-295 Interchange	Fine Graine	CH	1.62	113.68	80.0	42.1	1	59	53		27	0.60	1.10	2.69	0.54	0.04	0.46	
1770 (Ardan	Ardaman Protected 6	Fine Graine	CH		125.27	102.6	22.1		80	52		28	-0.07	0.70	2.8	0.13	0.01	0.35	
258460-1	Improvements from I-75 to McIntosh	Fine Graine	CH	1.86	110.76	79.0	40.2	9.68		52		32	0.63	1.10	2.66	0.34	0.03		
416649-2	SWFIA Access to I-75	Fine Graine	CH	2.71	89.73	44.2	103	3.23	91	51		27	2.93	2.81	2.7	1.79	0.18	0.30	
213301-2	Hammond Blvd, over I-10	Fine Graine	CH	2.10	120.02	88.9	35	1.61	65	51		33	0.52	0.96	2.79	0.43	0.10	0.51	
242702-1	I-4 St. John's River Bridge and Six Lanin	Fine Graine	CH	1.53	105.26	66.2	59	8.06	96	51		34	1.24	1.67	2.83	0.79	0.06	0.35	
10-139	Community Maritime Park	Fine Graine	CH	0.76	94.4	59.0	60			50		30	1.33	1.70	2.55	0.72			
1116L		Fine Graine	CH	2.09			103		99.8	136		101	0.67	2.81	2.70	1.61	0.29	1.01	
1120R		Fine Graine	CH	2.683			71.2		74.5	105		78	0.57	1.96	2.70	1.14	0.09	1.05	
WB212R		Fine Graine	CH	2.623			56.4		86	112		82	0.32	1.52	2.71	0.68	0.16	0.95	
WB-214R		Fine Graine	CH	2.363			52.6		83.8	66		49	0.73	1.42	2.66	0.72	0.08	0.58	
WB-214R		Fine Graine	CH	2.551			45.4		67.8	66		48	0.57	1.28	2.67	0.54	0.03	0.71	
WB-776L		Fine Graine	CH	1.534			34.8		74.8	82		64	0.26	0.92	2.63	0.38	0.09	0.86	
WB-776L		Fine Graine	CH	2.009			35.8		69.7	69		52	0.36	0.99	2.69	0.40	0.09	0.75	
RW2-435		Fine Graine	CH	2.01			62.3		72.7	92		71	0.58	1.73	2.70	0.85	0.12	0.98	
RW50785		Fine Graine	CH	2.3			62.2		58.4	116		90	0.40	1.67	2.70	0.79	0.08	1.54	
RW6-370		Fine Graine	CH	2.3			120.9		81.9	165		132	0.67	3.28	2.71	1.92	0.21	1.61	
TB-1		Fine Graine	CH	2.748			59		50	77		33	0.45	1.33	2.70	0.29	0.02	0.66	
TB-10		Fine Graine	CH	2.263			58		48	64		34	0.82	1.16	2.70	0.45	0.12	0.71	
TB-12		Fine Graine	CH	2.105			65		74	126		64	0.05	1.90	2.70	1.45	0.05	0.86	
B3		Fine Graine	CH	2.381			69.4		83.7	83		48	0.72	2.02		1.18	0.12	0.57	
B3		Fine Graine	CH	2.504125			89.8		88.8	82		54	1.14	2.53		1.16	0.17	0.61	
B3		Fine Graine	CL	2.635313			42.2		83.2	42		22	1.01	1.28		0.42	0.03	0.26	
B4		Fine Graine	CH	2.2129			55.3		69.3	62		38	0.82	1.61		0.84	0.07	0.55	
B4		Fine Graine	CH	2.2785			57.9		84.5	85		55	0.51	1.73		0.88	0.08	0.65	
SPT1		Fine Graine	CH	1.85			68.1		99	117		96	0.49	2.52	2.67	0.94	0.13	0.97	

APPENDIX E – SNIPPET OF CPT DATA BASE

Sample Identification					CPT											Consolidation										
Test #	Project	Boring	Sample	Soil Type	Depth(ft)	Depth(ft)	qc(tsf)	fs(tsf)	u2(tsf)	Rf	qt(tsf)	uN	lc	Bq	Fr	Cc' (ε-σ)	Cr'	Cc (e-σ)	Cr	Cc/Cr	GWT	σ'p (tsf)	u0 (tsf)	σ' (tsf)	σ (tsf)	OCR
1	Wekiva 8	1116L	US-1	CH	37.5-38.5	38.0	13.6	0.25	8.1	1.8	15.3	7.9	2.8	0.5	1.9	0.42	0.08	1.61	0.29	0.2	5	2.0	1.0	1.0	2.2	1.9
2	Wekiva 8	1120R	US-1	sandy clay	44.5-45.5	45.0	12.0	0.16	6.9	1.4	13.4	5.6	2.9	0.5	1.5	0.38	0.03	1.14	0.09	0.1	5	2.1	1.2	1.3	2.6	1.6
3	I-4 Section	WB212R	US-8	CH w/ sand	44.5-46	45.0	18.7	0.44	6.5	2.4	20.0	5.2	2.9	0.3	2.5	0.27	0.06	0.68	0.16	0.2	5	4.9	1.2	1.3	2.6	3.7
4	I-4 Section	WB-850L	US-5	Clayey FS	38.5-40	39.0	21.2	0.61	5.2	2.9	22.2	4.8	2.9	0.2	3.1	0.09	0.02	0.15	0.03	0.2	4	1.8	1.1	1.4	2.4	1.3
8	I-4 Section	WB-214R	US-9	CH	43.5-45	44.0	18.8	0.49	6.2	2.6	20.0	5.0	2.8	0.3	2.8	0.30	0.03	0.72	0.08	0.1	4	2.1	1.2	1.2	2.4	1.8
9	I-4 Section	WB-214R	US-10	sandy CH	49.5-51	50.0	14.2	0.30	7.1	2.1	15.6	5.0	2.9	0.4	2.3	0.24	0.01	0.54	0.03	0.1	4	2.4	1.4	1.3	2.7	1.9
10	I-4 Section	WB-776L	US-3	sandy CH	23.5-25	24.0	31.3	1.20	2.0	3.8	31.7	3.4	2.6	0.0	4.0	0.20	0.04	0.38	0.09	0.2	5	3.1	0.6	0.8	1.3	4.0
11	I-4 Section	WB-776L	US-4	sandy CH	33.5-35	34.0	21.6	0.67	2.3	3.1	22.1	2.6	2.8	0.1	3.3	0.20	0.05	0.40	0.09	0.2	5	2.1	0.9	1.0	1.8	2.1
13	SR528/436	RW2-435	----	CH w/ sand	37.5-39	38.0	13.3	0.29	7.8	2.2	14.8	7.9	2.8	0.5	2.3	0.31	0.04	0.85	0.12	0.1	6	2.6	1.0	1.0	2.0	2.6
14	SR528/436	RW50785	----	Sandy CH	41.5-43	42.0	8.6	0.22	5.3	2.6	9.7	4.7	3.2	0.6	3.0	0.29	0.03	0.79	0.08	0.1	6	1.7	1.1	1.2	2.3	1.5
15	SR528/436	RW6-370	----	CH w/ sand	41.5-43	42.0	14.4	0.30	8.2	2.1	16.0	7.1	2.9	0.5	2.2	0.45	0.05	1.92	0.21	0.1	5	1.7	1.1	1.2	2.3	1.5
16	SR46	TB-1	----	Clay w/pho	50.5-51.5	49.0	21.1	0.59	2.9	2.8	21.7	2.2	2.9	0.1	3.1	0.13	0.01	0.29	0.02	0.1	7	0.8	1.3	1.4	2.8	0.6
17	SR46	TB-10	----	sandy clay	42.5-44.5	43.5	14.0	0.50	2.0	3.6	14.4	1.7	3.1	0.1	4.1	0.21	0.06	0.45	0.12	0.3	5	0.7	1.2	1.1	2.3	0.6
18	SR46	TB-12	----	sandy clay	32.5-34.5	33.5	17.6	0.38	8.5	2.1	19.3	9.6	2.7	0.4	2.2	0.50	0.02	1.45	0.05	0.0	5	3.8	0.9	1.1	2.0	3.6
24	UCF	B3	Consol Graph		40-42.5	41.4	19.8	0.31	8.9	1.6	21.6	7.9	2.7	0.4	1.6	0.39	0.04	1.18	0.12	0.1	5	3.1	1.1	1.2	2.3	2.6
25	UCF	B3	Consol Graph		42.5-45	43.9	18.8	0.25	7.1	1.3	20.2	5.9	2.7	0.3	1.4	0.33	0.05	1.16	0.17	0.1	5	2.5	1.2	1.3	2.5	2.0
26	UCF	B3	Consol Graph		45-47.5	46.5	18.8	0.20	10.0	1.1	20.8	7.8	2.6	0.5	1.1	0.18	0.01	0.42	0.03	0.1	5	3.0	1.3	1.3	2.6	2.3
27	UCF	B4	Consol Graph		37.5-38.7	38.1	19.2	0.27	2.4	1.4	19.7	2.3	2.7	0.1	1.5	0.32	0.03	0.84	0.07	0.1	5	3.1	1.0	1.1	2.1	2.8
28	UCF	B4	Consol Graph		38.75-40	39.4	20.5	0.33	6.6	1.6	21.9	6.2	2.7	0.3	1.7	0.32	0.03	0.88	0.08	0.1	5	2.8	1.1	1.1	2.2	2.5
29	Lake Nona	B-3	ST-1	SC	41-43	42.1	22.2	0.47	0.9	2.1	22.4	0.9	2.8	0.0	2.3	0.19	0.02	0.49	0.04	0.1	9	2.1	1.0	1.3	2.5	1.6
31	SR100A	SPT1		CH	30-32	30.5	4.5	0.10	7.0	2.3	16.0	7.9	2.5	0.4	0.7	0.27	0.04	0.94	0.13	0.1	2	6.0	0.9	0.9	1.7	6.5
33	I4ult_Tierra	B201-2		CH	40-42	63.0	15.8	0.26	5.0	1.6	16.8	2.8	2.4	0.2	1.8	0.35	0.05	1.00	0.14	0.1	5	3.5	1.8	0.4	2.2	3.5
35	SR 44 Depr	TH-1		Fat Clay w/OH	20-22	27.0	7.9	0.30	----	3.8	7.9	----	3.0	----	4.5	0.14	0.02	0.36	0.05	0.1	5	1.7	0.7	0.5	1.2	3.2
36	SR415	TB-6		Clay	5 TO 6	5.5	4.9	0.27	----	5.5	4.9	----	3.0	----	5.9	0.21	0.04	0.49	0.10	0.2	5	1.0	0.0	0.3	0.3	6.0

LIST OF REFERENCES

- Bishop, C.M. (2006) Pattern recognition and machine learning. Springer, New York
- Boussinesq, J., Applications des potentiels à l'étude de l'équilibre et mouvement des solides élastiques, Gauthier-Villard, Paris, 1885
- Das, B. M. (2002). Principles of geotechnical engineering, Thomson Learning, Urbana, IL.
- Hine, Albert C. *Geology of Florida*. Brooks/Cole, 2009,
www.cengage.com/custom/enrichment_modules/bak/data/1426628390_Florida-LowRes_watermarked.pdf
- Kirts, S., Nam, B. H., Panagopoulos, O., Xanthopoulos, P., "Settlement prediction using support vector machine (SVM)-based compressibility models: a case study," *International Journal of Civil Engineering*, Vol. 17, Issue 10, pp 1547-1557
- Kirts, S., Nam, B. H., Panagopoulos, O., Xanthopoulos, P., "Soil-Compressibility Prediction Models Using Machine Learning." *Journal of Computing in Civil Engineering*"
- Mayne, P. W., & Kemper, J. B. (1988). Profiling OCR in stiff clays by CPT and SPT. *Geotechnical Testing Journal*, 11(2), 139–147.
- Robertson, P. K., & Robertson, K. L. (2006). *Guide to cone penetration testing and its application to geotechnical engineering*. Signal Hill, CA: Gregg Drilling & Testing, Inc.
- Robertson, P. K. (2009). Interpretation of cone penetration tests - a unified approach. *Can. Geotechnical*, 26, 1337–1352.
- Sanglerat, G. (1972). The Static Penetrometer and the Prediction of Settlements. *The Penetrometer and Soil Exploration*, 337–405.
- Skempton, A. W. "The Colloidal 'Activity' of Clays." *Selected Papers On Soil Mechanics*, 1984.
- Teh, C. I., & Houlsby, G. T. (1992). An analytical study of the cone penetration test in clay. *Géotechnique*, 41(1), 17–34.